The cellular biology of tendon grafting
And graft integration

A thesis submitted for the degree of Doctor of Medicine

Faculty of Medicine and Human Sciences

University of Manchester

2011

Nawsheen Alam

School of Medicine

Table of Contents

List of Figures

Chapter One

Chapter two

Chapter three

List of Tables

Chapter One

Chapter Two

Chapter 3

Declaration A

No part of this thesis has been submitted in support of an application for any degree or qualification of the University of Manchester or any other University or Institute of Learning**.**

Declaration B

Data from this thesis were presented in posters and presentations listed in page 183

Contributions

The cell based tendon construct was developed by Zoher Kapacee. The PCL construct was developed and SEM done by Lucy Bosworth.

Copyright notice

i. The author of this thesis (including any appendices and/or schedules to this thesis) owns any copyright in it (the "Copyright") and he has given The University of Manchester the right to use such Copyright for any administrative, promotional, educational and/or teaching purposes.

ii. Copies of this thesis, either in full or in extracts, may be made only in accordance with the regulations of the John Rylands University Library of Manchester. Details of these regulations may be obtained from the Librarian. This page must form part of any such copies made.

iii. The ownership of any patents, designs, trademarks and any and all other intellectual property rights except for the Copyright (the "Intellectual Property Rights") and any reproductions of copyright works, for example graphs and tables ("Reproductions"), which may be described in this thesis, may not be owned by the author and may be owned by third parties. Such Intellectual Property Rights and Reproductions cannot and must not be made available for use without the prior written permission of the owner(s) of the relevant Intellectual Property Rights and/or Reproductions.

iv. Further information on the conditions under which disclosure, publication and exploitation of this thesis, the Copyright and any Intellectual Property Rights and/or Reproductions described in it may take place is available from the Dean of the Faculty of Medical and Human Sciences.

Acknowledgements

My deepest thanks and gratitude to Professor Gus McGrouther and Mr Jason K Wong for their support and guidance throughout the project. Special thanks go to Professor Karl Kadler for his advice and directions. Many thanks to Professor Mark Ferguson for his support in the commencement of this study.

Many thanks to the staff in the incubator building, in particular Muhammad Babur and Ian Townsend for their assistance in animal husbandry specially over the use of transgenic mice in this project.

I would also like to thank all members of the Ferguson Corridor, Blond McIndoe Laboratories and Dermatological Sciences for their support, advice and friendship over the years. Special thanks go to Dr Rachel Watson, Lindsay Cottrell, Dr Sue Shawcross and Susan Cooper for all their help and kindness.

I would also like to thank my Colleagues Sarah AlYouha, Etienne O' Brien, Lucy Bosworth and Zoher Kapacee for their help and advice in various matters.

Many thanks to Robert Fernandez for his patience in teaching me advanced imaging techniques.

I gratefully acknowledge the generous financial support of the Royal College of Surgeons of England and the British Society for Surgery of the Hands that made this study possible.

Last but not least I would like to thank my family who have supported me throughout the last years to realise my academic ambitions.

Abstract

Background

Prolonged recovery after tendon injury has given rise to the need for innovative therapy including tendon engineering and cell based therapies. The role of cells in grafted or engineered tendon is poorly understood. Clarifying the persistence of grafted tissue is fundamentally important to ensure that tissue engineering strategies are fit for clinical application. We have devised a murine model for tendon grafting that allows for cell tracking and the assessment of tendon integration and engineered construct integration.

Materials and methods

We studied the macroscopic and microscopic architecture of the mouse Achilles tendon to investigate its properties as a study model. Using microsurgical techniques, transgenic tendon grafting procedures were then carried out between C57B/L6 wild type and GFP (Green Fluorescent Protein) mice Achilles tendon. The temporal and spatial fate of the cells in the graft was assessed using quantitative serial histology and immunohistochemistry with Three Dimensional reconstruction. Markers for proliferation, collagen synthesis, cell death and inflammatory infiltrate were used. The Achilles tendon model was also applied to test its applicability to investigate tissue engineered tendon constructs developed *in vitro*.

Results

GFP positive graft cells were seen at Day 3 and Day 21 but disappeared by Day 90. At Day 21both graft cells and the cells of the recipient tendon showed intense collagen synthetic activity. At the same time both graft and host tendon cells began to show

signs of apoptosis which continued till Day 90. Subcutaneous tissue and paratenon maintained a much higher level of cellularity, cell proliferation, collagen synthesis and apoptosis at all time. The interplay between cell activity and cell death appear to play central role in the integration of the tendon graft.

The persistence of tissue engineered tendon constructs was far less than syngenic or autografts. The Achilles tendon model proved to be a robust and economically viable model for testing of biomaterials particularly at the early stage of their development.

Conclusion

The cells of tendon grafts persist only for a finite time before being repopulated by host cells. Tissue engineered cell-based constructs do not provide sufficient persistence to substitute in place of syngenic or autologous graft options. Future designs of engineered tendon should facilitate tendon integration and aim to persist for longer periods of time in order to participate in the healing process.

Chapter One

Literature Review

1.1 Background- Tendon Injury and disease

With increase in the popularity of sporting activities, sport and activity related tendon injuries are increasing rapidly (Hess, 2010; Nyyssonen et al., 2008). A survey conducted across UK found that around 22 million sports injuries were sustained each year and 42% of these were tendon/ligament injuries (Barclays Space for sport 2005 survey data http://www.personal.barclays.co.uk). In 2008-2009, 9.3% of all A&E attendances involved tendon injuries (Hospital Episode Statistics- http://www.hesonline.nhs.uk) which show the common involvement of these structures in accident and injuries. The tendons commonly involved in injuries are the tendons of the digits, Achilles tendon of the ankle, the Rotator cuff of the shoulder, the tendons in the elbow and wrist. Flexor and extensor tendons of the limbs are prone to accidental cuts and lacerations.

Tendons can also be affected by systemic disease like Rheumatoid Arthritis (Ertel, 1989; Sivakumar et al., 2008), Diabetes Mellitus (Grant et al., 1997) and various autoimmune diseases (e.g. SLE, scleroderma) (Furie and Chartash, 1988; Hanly and Urowitz, 1986), leading to severe disability.

Tendon injury is also common in athletic animals. 43% of National Hunt horses show evidence of tendon disease (Pickersgill et al., 2001) and 14.8% of all horses in flat racing in Japan in 1999 suffered injury to the digital flexor tendons (Takahashi et al., 2004).

The treatment of tendon injury may involves direct repair (Strickland, 1983) of the defect or a more conservative approach of non-operative treatment with or without physiotherapy (Seida et al., 2010) may be adapted. The incidence of tendon surgery in the NHS is gradually increasing (Figure 1.1). Outcome of tendon surgery is unpredictable due to adhesion formation, re-rupture and inadequate functional recovery (Taras et al., 1994). During recovery there is restriction in acts of daily living and there is likely to be a long period of time off work.

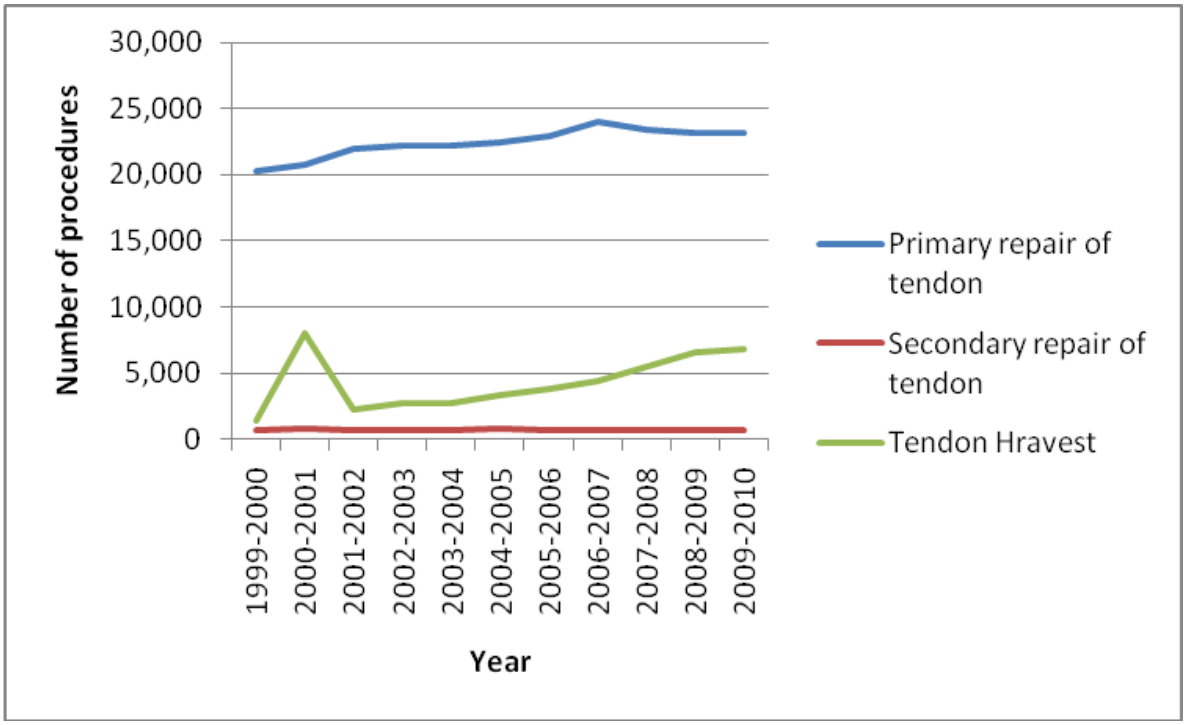

Figure 1.1- Graphical representation of trend in tendon surgery in the NHS (HES) showing gradual increase in primary tendon repair (Blue) and number of tendon harvested (Green) each year between 1999 and 2005.The number of secondary repair of tendon remain low. Of note is the higher number tendon harvest compared to secondary tendon repair indicating the use of tendon graft for other clinical indications.

When the tendon injury is more severe, leading to loss of a segment of tendon, more complex surgery may be required. The defect may occasionally need to be reconstructed with a free segment of tendon known as a tendon graft. Often tendons can rupture or undergo segmental degeneration. Tendon grafts can be used to bridge these defects in tendons or ligaments. Potential sources of tendon grafts are autograft (Patient's own tendon such as the Palmaris Longus in the wrist, Plantaris in the leg, Patellar tendon in the knee) (Figure-1.2), allograft (taken from another member of the same species, i.e.- cadaveric grafts) and xenograft (harvested from a different species such as bovine, porcine etc.). Autograft harvest may leave patients with additional scars and residual donor site weakness (Comley and Krishnan, 1999; Mastrokalos et al., 2005) while allograft carry risk of disease transmission (Kealey, 1997). Both allograft and xenograft carry immunogenic implications and can only be transplanted from either an immunocompatible donor or after donor graft has received special treatment to render it acellular.

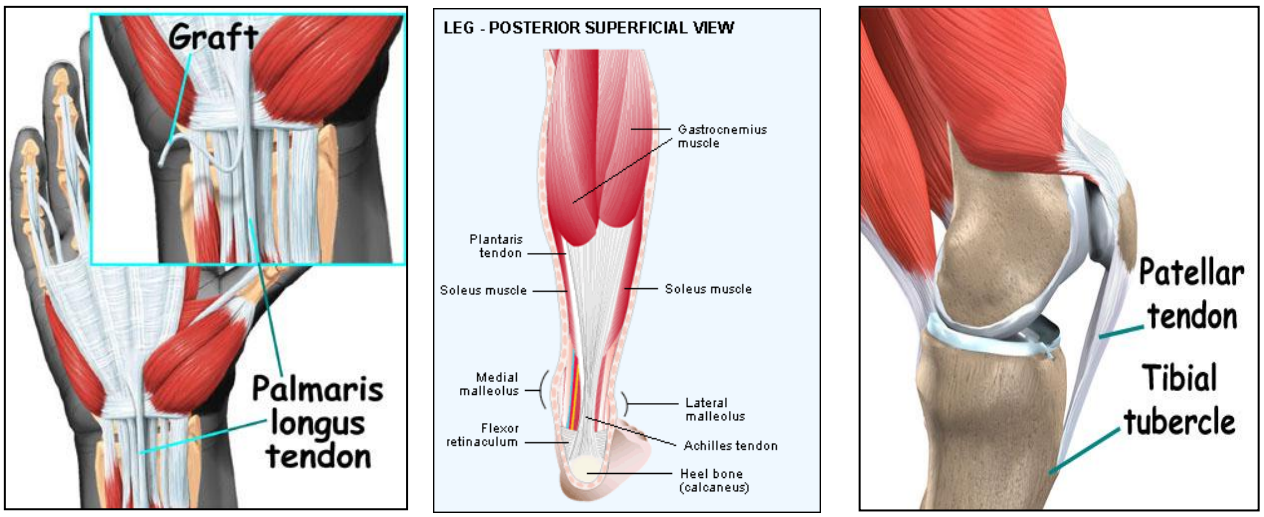

Figure 1.2- Tendons that can be used as autografts- (i) Palmaris Longus at the wrist, (ii) Plantaris at the back of the leg and (iii) Patellar tendon at the knee joint

1.2 Tendon architecture

1.2.1 Microscopic structure

Tendon is a highly organised structure from the molecular level to gross architecture (Figure 1.3), a property which allows it to withstand high tensile forces. The hierarchical organisation of tendon has been demonstrated at light microscopic, ultrastructural and molecular level (Birk and Trelstad, 1986; Oryan and Shoushtari, 2008; Rowe, 1985).

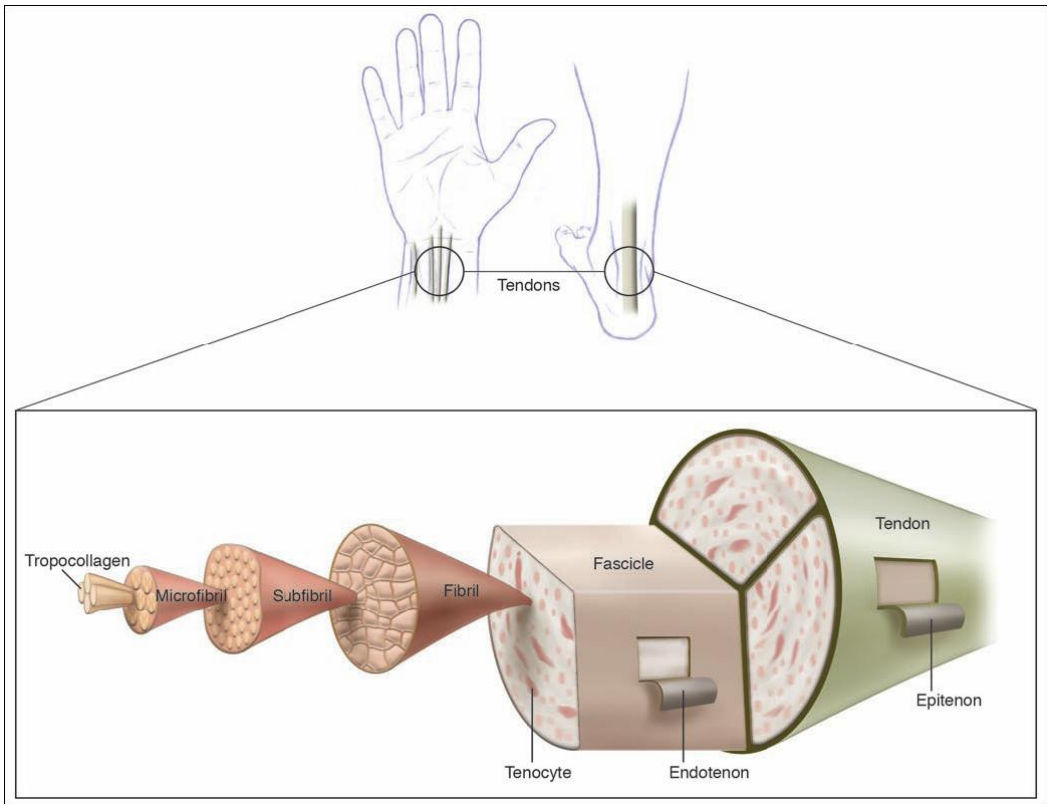

Figure 1.3 - The organization of tendon structure from collagen molecules to the entire tendon (Towler and Gelberman, 2006)- Three polypeptide chains combine together to form a helical tropocollagen molecule, five tropocollagens constitute a microfibril, and microfibrils aggregate together to form fibrils. Fibrils are then grouped into fibres, fibres into fibre bundles and fibre bundles into fascicles. A thin film of loose connective tissue ('endotenon') is present between fascicles and/or fibre bundles. The endotenon is continuous with a further sheet of connective tissue (epitenon) that surrounds the tendon as a whole.

The organised architecture of the tendon makes it an ideal structure to investigate complex biological events such as grafting and allows for study of cellular trafficking. The cells are distributed in parallel rows in between longitudinal fibers and the homogeneity allows cellular reorganisation to be studied relatively easily compared to heterogeneous structures like skin.

1.2.2 Cells of tendon

The majority of cells of adult tendons display a thin layer of cytoplasm around a large heterochromatic nucleus and have been named as "tenocytes" or "tendon fibroblasts". The more active cells, found in immature (Ippolito et al., 1980) or healing tendons containing prominent nucleoli, rough endoplasmic reticulum and golgi apparatus which produce collagen, have been called "tenoblasts" . Several studies have shown that immature developing tendon is hypercellular and cellularity gradually reduces through ageing (Holmes, 1971; Moore and De Beaux, 1987; Oryan and Shoushtari, 2008) indicating a relatively quiescent metabolic state of a mature tendon in comparison to developing tendon. During healing, tendon cells of a more active phenotype are found.

Using cytoplasmic staining McNeilly et al. (McNeilly et al., 1996) demonstrated that tenocytes form a three-dimensional network of cells in contact between collagen bundles by their long cytoplasmic processes. Immunolabelling for connexin 43 showed presence of gap junctions on the cytoplasmic processes which suggests that they may be involved in load sensing and coordination of response to load.

A morphological and functional difference between surface cells and internal cells described in earlier histological experiment has been re-established through immunohistochemical studies. Khan (Khan et al., 1996) described tendon cell populations as an outer layer of specialised fibroblasts and macrophages, (often termed epitenon although this term is confusing as it has different meaning in different publications). The tendon core has a different population of fibroblasts.

Each cell has a unique response to injury. Banes described tendon cells as synovial fibroblast and internal fibroblasts on the basis of sequential enzymatic digestion (Banes et al., 1988). More recently a stem cell population has also been identified in the tendon, though its role is yet to be characterised. Bi et al. performed *invitro* studies (Cell culture, RT-PCR, FACS, transplant studies, immunocytochemistry) and isolated a cell population from both human and mouse tendons that showed increased adherence, could be pushed towards several lineages, expressed both tendon specific and stem cell specific markers and were named tendon stem/progenitor cells (TSPCs) (Bi et al., 2007).This group of cells constituted 6% of the cell population in culture and the authors demonstrated a similar percentage of slow cycling BrdU labeled cells *in vivo* which they considered homologous to the TSPCs identified in culture experiments.

1.2.3 Extracellular Matrix

Tendon matrix is composed of collagens and proteoglycans (Kjaer 2004). Collagen accounts for 65-80% and elastin approximately 1-2% of the dry mass of the tendon (Kannus, 2000). Type I collagen is the dominant collagen found in tendon through immunofluorescent localization (Williams et al., 1984), electron microscopy (Birk and Mayne, 1997), RT-PCR (Heinemeier et al., 2007) and in culture conditions (Gungormus and Kolankaya, 2008) but other collagens (e.g. II, III, V, VI, IX, XI) are also present (Fukuta et al. 1998; Ottani et al. 2002; Kjaer, 2004). Collagen is responsible for the tensile strength of the tendon while proteoglycans provide the viscoelastic properties of tendons (Puxkandl et al. 2002; Robinson et al. 2004).Histological, immunohistochemical and ultrastructural studies have shown that injured tendons heals by fibrillogenesis (Gigante et al., 1996) and the deposition of new collagen can be labelled by HSP47, a molecular chaperone to procollagen synthesis (Hu et al., 1995).

Tendons are of two major types based on the presence or absence of their covering sheath- intrasynovial and extrasynovial. An intrasynovial tendon has a double layered

synovial membrane containing synovial fluid such as the flexor tendons of the hand. Tendon sheath fluid assay has shown hyaluronic acid and protein concentrations similar to those in normal joint fluid, indicating that flexor tendon sheath fluid has a character similar to synovial fluid of joint (Hagberg et al., 1992). This fluid has been shown to be involved in specific functions such as tendon gliding and nutrition of tendon tissue (Lundborg et al., 1980).

An extrasynovial tendon such as the Achilles tendon has no such membrane but is covered by a layer of loose connective tissue called paratenon (Graf et al., 1990). The two types of tendons have been shown to heal by different mechanism following division and also when used as free graft (Gelberman et al., 1992b) and this is discussed in more detail in later sections.

1.2.4 Tendon Vasculature

Blood supply to the tendon has been widely studied using various different techniques. Intrasynovial tendons receive nutrition from both synovial fluid bathing them as well as from segmental blood vessels (Lundborg et al., 1980). Extrasynovial tendons receive blood supply from ossoetendinous and myotendinous junctions as well as blood vessels coming through the mesotenon from the paratenon (Mayer, 1916).

A substantial number of work has been done on the blood supply of Achilles tendon using various different techniques (Reviewed by Fenwick et al., 2002) Injection studies in fresh cadavers demonstrated numerous evenly distributed vessels in the paratenon from which vessels ran towards the tendon via the mesotenon (Carr and Norris, 1989).

Cadaveric angiographic testing and light microscopic histological study showed that the blood supply of the Achilles tendon comes from three different areas: the musculotendinous and osseotendinous junctions and the paratenon (Ahmed et al.,

1998) The vessels of the epitenon are chiefly derived proximally from the muscular branches and distally from vessels in the region of the heel. The vessels in the paratenon are thought to be derived from the main arteries of the leg and that the two systems communicate via the mesotenon (Kannus 1997).

Gross anatomy of the mouse leg vasculature follows nomenclature similar to human blood vessels. The leg is supplied by two deep vascular bundles- anterior tibial and posterior tibial vessels and the two superficial vascular bundles- sural and saphenous vessels (Figure 1.4).The peroneal vessels which contribute to the blood supply of the human Achilles tendon in the leg has not been described in the mouse.

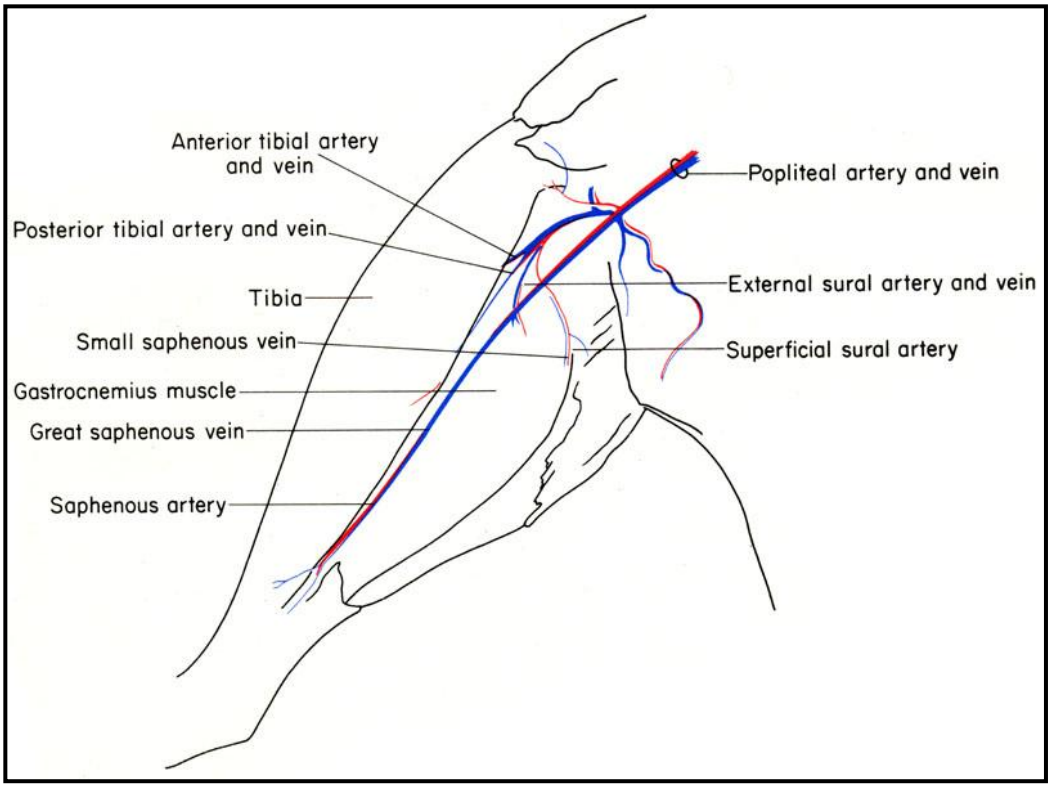

Figure 1.4 -Blood vessels of the mouse leg showing the posterior tibial vessels lying deep to the gastrocnemius muscle while the saphenous and sural vessels lie superficial to the muscle (The Anatomy of the Laboratory Mouse, Margaret J. Cook, 1965)

1.3 Anatomy of the Achilles tendon

The Achilles tendon is considered to be the thickest and strongest tendon in the human body. The tendon is consistently formed by the tendons of soleus and gastrocnemius muscle (Cummins et al., 1946) (Figure 1.5). The fibres converge as they descend but at the same time rotate toward the lateral side. The tendon then flattens out before insertion.

The tendon inserts on the posterior surface of the calcaneum bone. The distal tendon is protected from the calcaneum during dorsiflexion by the retrocalcaneal bursa (Rufai et al., 1995). One of the very few anatomical studies of mice shows that the bony anatomy is slightly different from mammalian bony skeleton and the tibia and fibula are fused together at the distal end (The Anatomy of the Laboratory Mouse, Margaret J. Cook, 1965). The arrangement of the calcaneum and talus appear similar to human skeleton (Figure 1.5-1.6).

Using immunohistochemical labelling for type II collagen and routine histology with toluidine blue has shown that there are interlocking pieces of calcified fibrocartilage and bone at the enthesis region of human Achilles tendon (Milz et al., 2002). Fibrocartilage is found in tendon in areas subjected to compression (Benjamin and Ralphs, 1998) and this can be visualised with histological cell morphology, Alcian blue stain (Tilman & Schünke 1991) or the presence of type II collagen by immunohistochemistry (Peterson et al 1999).

The tendon is covered by a thick layer of paratenon, lying deep to which is a shiny vascular membrane, the epitenon (Nisbet, 1960). In between these two layers is a thin film of fluid, which gave the tendon a close resemblance to synovial tendons.

In a comparative anatomy study Holmes demonstrated that 90% of cells in adult dog, cat, and monkey Achilles tendon were tenocytes (Holmes, 1971). The study also showed that the percentage of tenocytes increased with weight and age of the rat.

In a 50 gm rat 90% of the cells were tenoblasts whereas in a 65 gm rat (older) 71% of the cells were tenocytes.

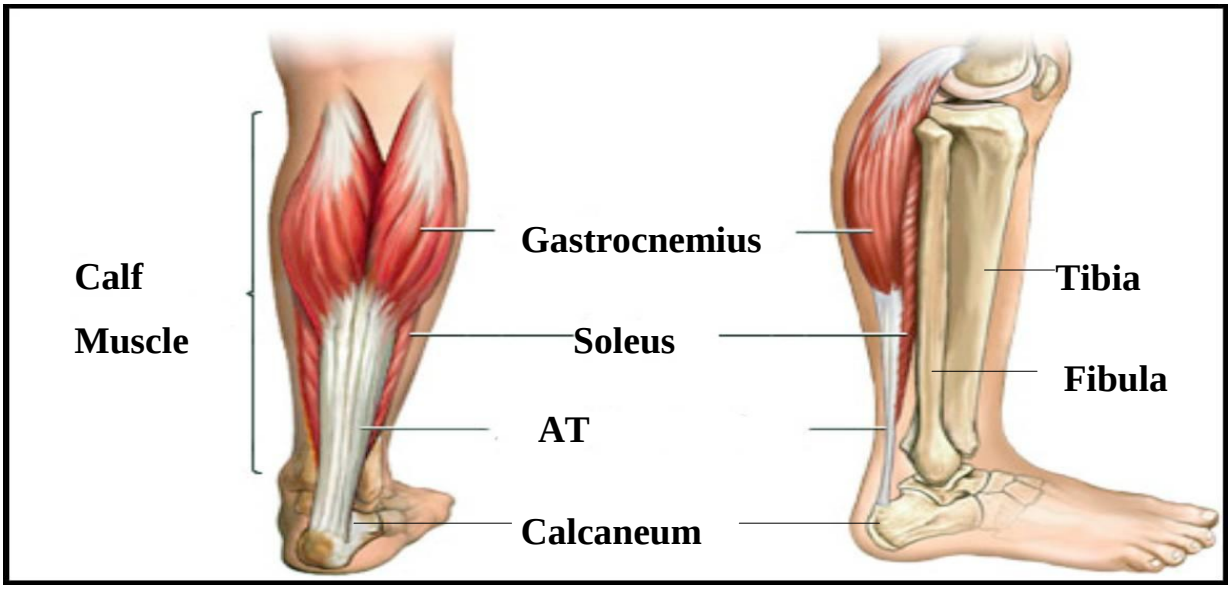

Figure 1.5- Formation of human Achilles tendon by the soleus and the gastrocnemius muscle in the human and inserting into the back of the calcaneum bone; AT- Achilles Tendon

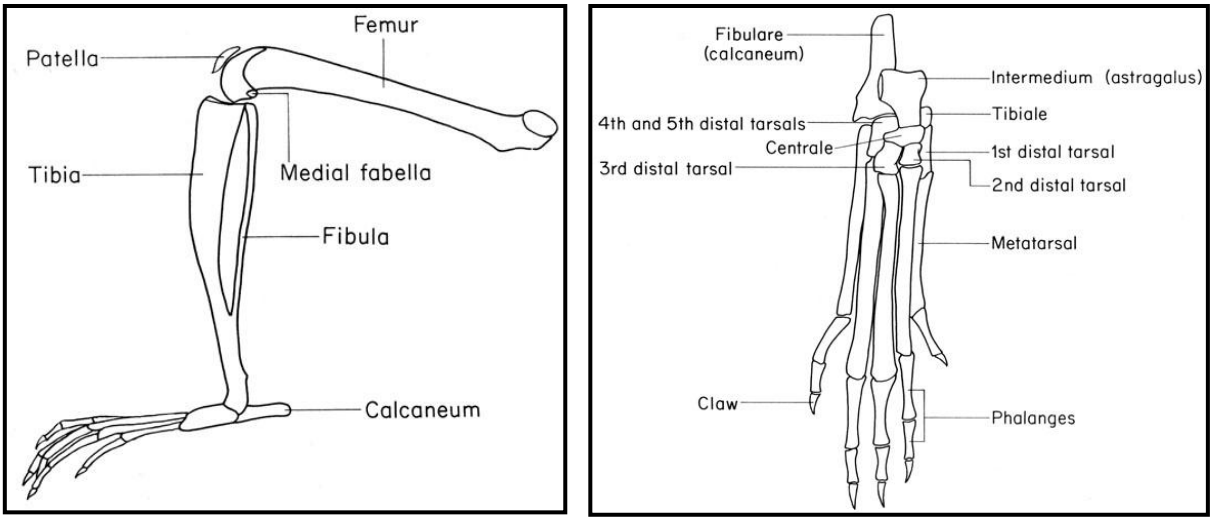

Figure 1.6--Bony skeleton of mice hind limb and hind foot showing fused tibia and fibula in the leg and projecting calcaneum in the foot, where the Achilles tendon inserts (The Anatomy of the Laboratory Mouse, Margaret J. Cook, 1965)

1.4 Biology of Tendon Healing

In the early twentieth century tendon grafting was considered the recommended treatment for all digital tendon injuries (Bunnell's Surgery of the Hand. 5th Edition. Philadelphia and Montreal, J. B. Lippincott Company). Over the years tendon grafting has become a less popular method for primary tendon repair and today direct repair is considered the best treatment for acute injuries (Strickland, 1983) of flexor and extensor tendons. Tendon grafting has remained of interest due to its applicability in delayed trauma management or severe injuries (Freilich and Chhabra, 2007; Moore et al., 2010) Tendon grafting is also used for reconstruction of ligaments (Victor et al., 1997) and to replace defective segments of tendon (Maffulli and Leadbetter, 2005).

1.4.1 Current concepts in Tendon healing

Tendon healing follows the general paradigm of healing tissues (Broughton et al., 2006) and has three chronologically overlapping stages- inflammatory phase, proliferative phase (fibroplasia) and remodeling phase (Sharma and Maffulli, 2006; Wong et al., 2009). Classic concepts of tendon healing are of extrinsic healing and intrinsic healing. Extrinsic healing denotes healing by cells extrinsic to the tendon, such as cells from the sheath, synovium and neighbouring tissues. Fibroblasts are thought to arrive to the injury site by vascular adhesions (Gelberman et al., 1984; Potenza, 1962). Intrinsic healing is described as healing by cells intrinsic to the tendon, more specifically by the tenocytes of the cut ends (Manske and Lesker, 1984; Matthews and Richards, 1975). Recent evidence suggest that the process is far more complex and cells from inside the tendon and cells from outside the tendon contribute to tendon healing (Wong et al., 2009).

1.4.2 Cellular activity during tendon healing

During the early period of healing Wu et al. have shown greater cellularity in both epitenon and endotenon areas (Wu et al., 2010). Using immunohistochemical techniques on chicken flexor tendon repair model, Wu showed that the total number of cells peaked at day 3, while the number of proliferating cells peaked at days 7 and 21. Apoptotic TUNEL positive cells peaked at day 3 and decreased after day 21 but remained greater than baseline levels. Based on Bcl-2 immunostaining the study also reported an inhibition of apoptosis between 2-4 weeks. In a patellar longitudinal incision model Lui reported that both TUNEL positive apoptotic cells and PCNA positive proliferative fibroblast like cells peaked at day 28 (Lui et al., 2007; Wu et al., 2010). The differences reported in the studies may be due to the differences in the types of the wound and types of repair used in each study.

On the basis of immunohistological studies in an intrasynovial mouse flexor tendon injury /adhesion model Wong et al (Wong et al., 2009) reported an early inflammatory reaction in the subcutaneous tissue surrounding the tendon followed by a peak of collagen synthetic activity inside the tendon substance at 21 days. The study showed that both the tendon and the surrounding tissue have a dynamic role in intrasynovial tendon healing.

Table 1.1 - Cellular activity in tendon healing as reported by Wong et al. (2009) in a Murine Flexor Tendon partial injury model

	Tendon	Subcutaneous tissue
CD45(Pan leukocyte marker)	Minimal at early time period, peaked at day 14 and 21 and reduced thereafter	Peaked at 24 hours and remained elevated till day14
Ly6G(neutrophil)	Minimal expression at all times with small peak at day3	Peaked at 24 hours and rapidly reduced thereafter
F480(Macrophage)	Marked increase at day 21	Remained high up to day 7
BrdU(Cell proliferation)	High levels between day 7 to day 28 but activity significantly lower than surrounding tissue	Remained high from Day3 to day21
Hsp47(Collagen synthesis)	Peaked at day 21 and was significantly higher than subcutaneous tissue	Peaked at day 10
Alpha-SMA (Pericyte and myofibroblast)	No expression in tendon	Remained high throughout experiment up to day 112 with peak at day 7
TUNEL(apoptosis)	Gradual increase reaching a peak at day 84, but at a reduced level than subcutaneous tissue at all times	Gradual increase reaching peak at day 84

An emerging concept of tendon healing is the biphasic healing modality where the blood and bone marrow derived cells are responsible for the early stages of tendon healing and the tendon derived cells contribute to the later stages of healing (Kajikawa et al., 2007). Both Kajikawa and Wong report a delayed but active involvement of the tendon cells in the healing process, supporting a bimodal healing pattern.

In their elegant and innovative study Kajikawa (Kajikawa et al., 2007) investigated the spatiotemporal distribution of reparative mesenchymal cells in patellar tendon using two types of GFP chimeric rat (Figure 1.7). One of the chimeric rats expressed GFP cells only in the patellar tendon and the other one expressed GFP in the bone marrow derived cells. In the study a perpendicular wound was made in both types of chimeric rat and fibroblast like GFP positive cells were measured in the wounds at various time points.

The GFP positive tendon-derived cells were observed in the wounded area from day 3 and their proliferative activity remained high till day 7. The authors therefore concluded that the circulation-derived cells primarily contribute to the healing process with the role of the tendon-derived cells increasing with time. A further study by the same group (Kajikawa et al., 2008) reported that marrow derived cells did not show any collagen synthetic activity (Hsp47) suggesting that these cells do not participate in forming neo-tendon. Therefore, despite wide interest in bone marrow derived cells in tendon healing their role remains yet undetermined. The studies suggest that cells from the tendon may play the major role in neo-tendon formation.

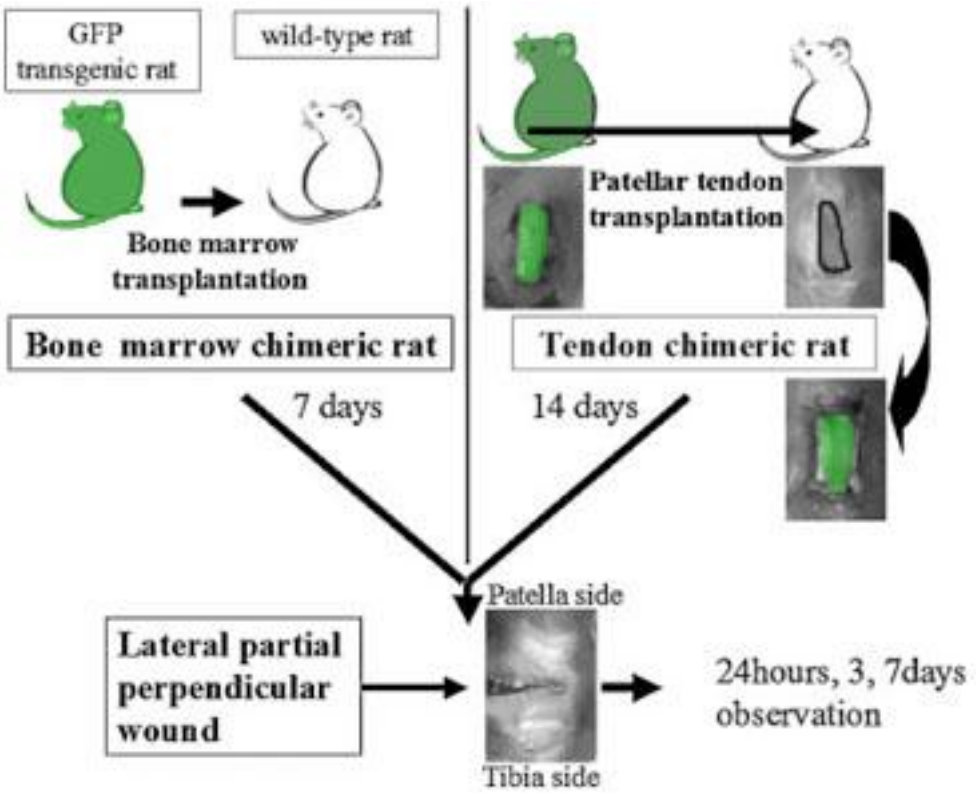

Figure 1.7 - Development of Bone marrow chimeric rat and tendon chimeric rat. Bone marrow chimeric rats were developed by irradiating the bone marrow of wild type rat followed by bone marrow transplantation from GFP transgenic rat (Left side). These rats therefore expressed GFP in the bone marrow derived cells. Tendon chimeric rats were developed by transplanting the patellar tendon from GFP rat to the wild type rat (Right side) of the figure. The tendon chimeric rats only expressed GFP in their patellar tendon. Both groups of animals received a longitudinal wound to the tendon and the studied at 24hours, 3, and 7 days. Modified from Kajikawa et al. (Kajikawa et al., 2007)

1.5 Biology of graft healing

The healing of grafts follows a more complex pathway than normal wound healing as the grafts need to reestablish their source of nutrition**.** The biology of graft healing has been widely studied for skin graft which is a common reconstructive surgical procedure. Studies of skin graft healing has shown that the graft is initially adhered to the recipient site through formation of a fibrin layer and undergoes diffusion of nutrients by capillary action from the recipient bed by a process known as plasmatic imbibition (Maeda et al., 1999). The next phase involves the process of inosculation, in which there is early anastomosis between donor and recipient vessels (O'Ceallaigh et al., 2006). Revascularization of the graft is accomplished through these capillaries as well as by neovascularisation which occurs by influx of host cells into the graft in a perivascular fashion (O'Ceallaigh et al., 2007).

Remodelling and repopulation of skin grafts is a relatively complex biological process. Using antibodies against GFP Matsuo et al (Matsuo et al., 2007) demonstrated that 6 months after full thickness skin graft transplantation from GFP to wild type mice, GFP positive grafted cells survived in the epidermis, hair follicle and sebaceous glands and only in part of the dermis, blood vessels, and nerves.

Stem cells of the epidermis localized in the bulge region of the hair follicles have been shown to contribute to the formation of the epidermal structures (Oshima et al 2001) and authors suggest that graft cell survival is dependent upon the presence of stem cells in grafted tissues.

The complex architecture of the skin makes it difficult to separate the role of various cells in graft healing. The role of graft derived stem cells in graft survival presents a new concept in graft healing and requires further investigation.

1.5.1 Biology of Tendon graft healing

The fate of tendon graft has been widely studied in the bone tunnel where it is frequently used for Anterior Cruciate Ligament Reconstruction. Arnoczky described the following stages of tendon autograft healing in the bone tunnel- -avascular necrosis, revascularisation, cellular proliferation and remodelling (Arnoczky et al., 1982). Amiel & co-workers (Amiel et al., 1986a; Amiel et al., 1986b; Kleiner et al., 1989) showed that autogenous patellar tendon grafts underwent rapid necrosis and repopulation occurred from cells of extra-graft origin.

The mechanism of tendon graft healing outside bone tunnels follows a slightly different pathway. Mason and Shearon used canine Extensor Carpi Radialis tendon as an autologous end to end graft and performed daily analysis of cellular events from day 3 to day 100 (Mason and Shearon, 1932). The authors grouped their results in two overlapping phases. The first phase compromised of events of the first two weeks and the second phase commenced from the second week. In the first phase tendon stump and graft is held together by proliferating tissue from the sheath and peritendinous area and by the end of this phase the sheath tissue appear to have organized into well aligned dense connective tissue. At this time the sheath has many leukocytic cells. In the second phase, the tendon and graft stump starts to show mitotic figures (as early as day 4) and cells gradually infiltrates the scar tissue situated between the graft and the tendon. The authors reported that on the basis of gross and histological criteria the graft remained alive throughout the healing process and its appearance was very similar to the rest of the tendon. One of the main limitations of the study was the huge number of variables in terms of immobilization, suture, use of sheath and the number of animals harvested each day.

Table 1.2 -Temporal events in tendon graft healing (Mason and Shearon 1932)

Days	Events
4-7 days	Tendon graft alive No sign of cell proliferation (Based on mitotic figures) Necrosis around silk suture
8-10 days	Graft held together by disorganised tissue of the stump and dense relatively more organised tissue of the stump WBC in sheath still present. Numerous oval shaped nuclei in the sheath Graft show some proliferative activity Areas of necrosis in the centre of the graft
12-14 days	Increased proliferative activity form the stump Union of graft and stump appear primarily by sheath proliferative activity
3 weeks	Graft and stump begins to regain uniformity of structure Reorganisation of cells and collagen fibre bundles
4-5 weeks	Tissue appearance begins to match normal adult tendon structure with parallel rows of cells in between parallel rows of collagen fibres Tendon strength improved
100 days	Histologically tendon graft inseparable from the rest of the tendon Stump still slightly wider than the rest of the tendon

Later studies (Potenza., 1964; Skoog and Persson., 1954) supported the argument that tendon graft remains alive by histological criteria. Potenza used intrasynovial flexor tendon grafts to reconstruct the flexor tendons but in order to minimise trauma he sutured the graft without displacing it. The graft therefore maintained its blood supply inside the flexor sheath area and was in most part undisturbed in its anatomical bed, a situation which is unlikely in the clinical setting. Potenza used inert stainless steel sutures which was in contrast to earlier grafting studies all of which used the highly reactive silk suture(Flynn et al., 1960; Mason and Shearon, 1932) . Potenza reported that the tendon cells did not participate in the healing process and the reparative cells at the stumps arrived from either the synovial sheath (distal stump) or the paratenon (Proximal stump).

Canine studies by Flynn et al (Flynn et al., 1960) also reported early healing by sheath tissue followed by healing from stump cells but reported that necrosis occurred in whole of the graft and that the transplant was completely replaced by tenoblasts from the stump. Use of silk suture, extrasynovial tendon graft and trauma to surrounding tissue may be some of the factors involved in Flynn's contradictory evidence.

The healing of tendon graft has also been shown to be affected by the type of donor tendon used as a graft. Canine studies (Seiler et al., 1997) showed that while both intrasynovial and extrasynovial tendons remain viable by histological criteria, the intrasynovial tendon grafts did not form adhesion. They hypothesized that where an intrasynovial tendon graft has been used, healing occurs from the stumps and cells migrate into the graft from the apposed ends whereas extrasynovial tendon grafts heal by cells invading from all directions through vascular adhesions. Whether the cells migrate into the graft or out of the graft is yet to be determined. Table 1.3 summarises the evidence provided by Gelberman's group in support of their hypothesis (Abrahamsson et al., 1995; Amiel et al., 1995; Ark et al., 1994; Gelberman et al., 1992b; Seiler et al., 1993a; Seiler et al., 1997).

Table 1.3 - Differences in healing of Extrasynovial and Intrasynovial tendon graft

Characteristics	Method	Intrasynovial	Extrasynovial
Tissue architecture	Light microscopy	Viable, normal appearing surface and internal fibroblast at all time points	Dense circumferential adhesion formation At 3 weeks degenerative changes in the endotenon and at 6 weeks hypercellular graft
Collagen alignment	Transmission Electron Microscopy	Well aligned collagen fibres through 6 weeks	Areas of thin, disorganised collagen fibres with high amplitude crimps
C2ellular survival and proliferation	Intravital fluorescent stain Ethidium Bromide and Calcein and confocal microscopy	Uniform viable surface layer	Predominantly nonviable fibroblast at 3 weeks Increase number of viable cells with repopulation
Neovascularisation	Microangiography	Blood vessels visualised at proximal and distal repair sites	Blood vessels all around the graft-vascular adhesions
Cellular productivity	mRNA for Type I procollagen - Insitu Hybridisation	No areas of increase mRNA	Areas of increased mRNA seen at 2 and 4 weeks in the fibroblasts of peritendinous adhesion
DNA synthesis	Exvivo 3H thymidine uptake and DNA content(Biochemical method)	Modest increase	Significantly higher than intrasynovial tendon
Mechanical strength	Mechanical testing device	Significantly increased angular rotation	Much lower angular rotation

Though intrasynovial tendons appear to be better candidates for tendon grafting, their low availability as grafts limit their use in the clinical setting and the commonly used tendon grafts remain of extrasynovial type (plantaris, palmaris, hamstring, patellar tendon etc).

1.5.2 Cellular repopulation in tendon graft

Recent studies on murine flexor tendon showed that acellular freeze dried allografts were repopulated by 42 days (Hasslund et al., 2008) (Figure 1.8).

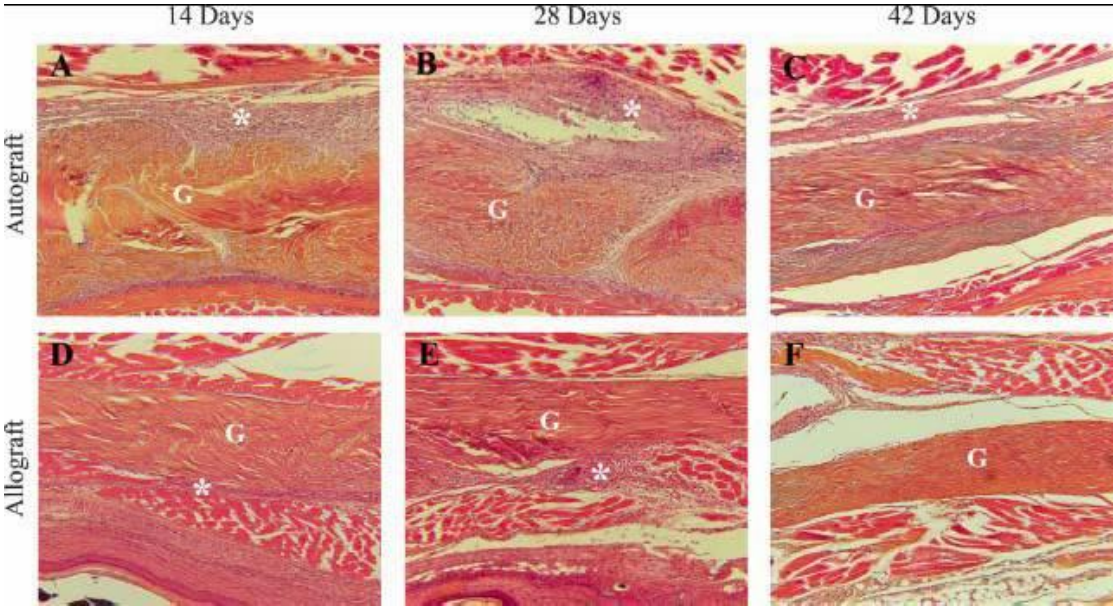

Figure 1.8 - Representative histologic sections of the middle segment of the FDL tendon autografts (A–C) and allografts (D–F) at 14, 28, and 42 days post-surgery. Sections were stained with Orange G/Alcian Blue (Scale bar-500μm). Hypercellular fibrotic scar (*) surrounding 14-day and 28-day autografts (A, B) that appears to be minimal around the acellular allografts (C, D). By 42 days, the scar tissue appears to have significantly remodeled in both autografts (E) and allografts (F). Graft tissue is marked G (Hasslund et al., 2008)

Confocal microscopic studies using GFP rat have shown that tendon grafts used for both rotator cuff tears (Iwata et al., 2008) and Anterior Cruciate Ligament (Kobayashi et al., 2005) reconstruction are replaced by host cells by 28 days. Iwata (Iwata et al., 2008) reported infiltration of GFP positive host cells into the grafted rotator cuff tendon as early as Day 1 day after transplantation and found that host cell invasion

occurred from neighbouring synovium, tendon and bone. The study could not comment whether the graft acted only as a scaffold or whether viable graft cells are required during the remodelling process. Insitu hybridization study of sex mismatched animals showed that reseeded cells of acellular tendon grafts persist up to 12 weeks and in a small number of animals up to 30 weeks (Thorfinn et al., 2009). The mechanism of repopulation and the source of cellular repopulation have not yet been established.

1.5.3 Role of other cells in tendon graft

1.5.3.1 Bone marrow derived cells

Apart from tendon and sheath cells other cells may influence graft healing. Much of the interest has been centred on the role of marrow derived cells in tendon/graft healing. Using GFPBMT mice Zantop showed that bone marrow derived cells accumulate in the wound in the early part of graft (both autologous and bioscaffold) healing and are predominantly associated with areas of inflammation and angiogenesis (Zantop et al., 2006). A reparative role of these cells is yet to be established.

1.5.3.2 Inflammatory cells

During tendon healing in a rat partial tenotomy model, tendons were seen to be filled with a neutrophilic infiltrate within 6 hours of injury followed by an influx of monocyte and macrophages within 24 hours (Iwuagwu and McGrouther, 1998). Further experiments in the same model showed that Cd45 positive leukocytes comprised of 18 % of the cells at 6 hours of tendon injury but reduced to 4% by 72 hours (Zavahir et al., 2001). In a rat Achilles tendon injury model neutrophil and ED1 positive systemic macrophages were found to be increased after 24 hours. Neutrophils reduced by 70% while the concentration of ED1 positive macrophages remained constant at day 3 post-injury (Marsolais et al., 2001). Neutrophils and ED1

positive macrophages returned to control values after 7 and 14 days, respectively. ED2 positive macrophages showed a tendency to increase at day 28 suggesting a very different role of these macrophages in the healing cascade. Similar results were reported for tendon graft healing in the bone tunnel. Immunohistochemical studies of rat autografts used for Anterior Cruciate Ligament reconstruction (Kawamura et al., 2005) found that mature tissue macrophages (ED2 positive) show increased proliferative activity (PCNA) at day 14 suggesting that a change in phenotype from proinflammmatory to pro-regenerative as healing progresses. In a c57Bl/6 mice Achilles tendon injury model liposomal clodronate induced macrophage depletion has also shown a reduction in the density of proliferative cells (BrdU positive) in tendons by 36% (Godbout et al., 2010). On the other hand a recent study (Hays et al., 2008) has shown that a reduction in liposomal clodronate induced macrophage depletion during rat ACL reconstruction led to better morphologic and biomechanical healing at the bone-tendon interface of such repairs. In culture conditions human monocytes and macrophages have been reported to express virtually all known collagen and collagen-related mRNAs (Schnoor et al., 2008). The macrophages secreted a large amount of type VI collagen which is known to be involved in modulation of cell-cell and cell-matrix interactions. The authors suggest that the production of type VI collagen is a marker for a nondestructive, matrix-conserving macrophage phenotype which may be involved in physiological and pathological conditions *in vivo*. It is possible that different macrophage play completely or even opposing functions and may therefore be an important player in tendon healing and graft integration than was previously thought and this possibility requires further investigation.

1.5.4 Cytokines and growth factors in graft healing

Histology, biomechanical and molecular testing of freeze dried allograft and autografts in murine model showed that adhesion reduced after 28 days and this peak in remodelling directly corresponded to high GDF-5 (Growth and Differentiation Factor- 5) level (Hasslund et al., 2008). The authors also report that live autografts

significantly upregulated VEGFa in 28-day autografts but the TGFβ1 expression levels were not increased. A further study by the group (Basile et al., 2008) tested the effect of GDF-5 gene delivery to the healing site and found limited efficacy due to the short duration of its action. It is likely that the cytokine and growth factor profile during tendon graft healing closely resembles that of tendon healing and the many growth factor, cytokines and other exogenous substances currently under investigation to improve tendon healing (Reviewed by Doure et al.,2008) may also be useful in improving tendon graft and construct integration.

1.5.5 Apoptosis in graft healing

Apoptosis has been shown to be a part of the healing process of wounded tendons. Lui (Lui et al., 2007) reported that TUNEL positive cells peaked at 28 days following tendon wounding while Wong (Wong et al., 2009) reported a peak at 84 days in a mice tendon adhesion model. A recent study reports a much earlier peak in apoptosis in the healing tendons at day 3, followed about 10 days later by the peak proliferation period (Wu et al., 2010). Using Bcl-2 immunohistochemistry, Wu also found that apoptosis was inhibited between 2 and 4 weeks. Apoptosis may be triggered by loss of mechanical integrity and the need for realignment by the neotendon cells. Apoptosis has been shown to be induced both by mechanical loading of intact tendon (Scott et al., 2005) or by the lack of it (Egerbacher et al., 2008). In terms of healing of transplanted tissue, apoptosis has been shown to contributes to both graft rejection and the establishment of graft tolerance (Zavazava and Kabelitz, 2000). The role of apoptosis in tendon graft healing has not been investigated.

1.5.6 Vascularisation of tendon grafts

Though tendons have been designated as relatively avascular tissue, neovascularisation has been shown to be an integral part of both tendon and tendon graft healing. Earlier work by Peacock showed a profuse vascular network during healing and maturation of graft (Peacock, 1959). Peacock injected a radioactive dye into the hind leg and measured the radioactivity over the various parts of the tendon 20 minutes after injection. His study showed that blood vessels entering long tendons from the muscular origin and periosteal insertion are able to nourish only the proximal and distal third of the tendon. Circulation to the central third of long tendons is by intermediate vessels entering through disorganised paratenon or a definite volar mesentery. In free grafts this portion of the circulation is restored through postoperative adhesions, which appeared vital for the survival of the graft.

Chaplin (1973) used microangiographic studies with barium sulphate injections (Chaplin, 1973). Chaplin's studies demonstrated a difference in both the basic vascular pattern of intrasynovial and extrasynovial tendons and also in the pattern of revascularisation of these tendons. Following simple division intrasynovial parts of flexor tendons had no significant revascularisation. When used as free grafts all extrasynovial tendons showed good revascularisation and adhesion formation while intrasynovial tendon grafts retained their avascularity and adhesion occurred only at either ends of the graft. Chaplin concluded that extrasynovial grafts were inferior to intrasynovial grafts when used to repair damaged flexor tendons, as the vascularity seems to support adhesion formation.

Sckell et al. assessed the role of peritendinous tissue in the revascularisation of patellar tendon graft in a murine model using intravital microscopy (Sckell et al., 1999). The peritendinous connective tissue envelope of the graft was completely removed, partially removed or not stripped at all. Intravital microscopy showed that grafts with intact peritendinous tissue showed accelerated vascularisation and histology confirmed higher viability compared to the other two groups. The authors

suggested that the intact connective tissue are either able to produce angiogenic factors or to stimulate host cells to generate and release these factors.

Perfusion studies with India ink showed neovascularisation of extrasynovial tendon grafts through vascular adhesions by two weeks (Gelberman et al., 1992a). In contrast, the flexor tendon grafts of intrasynovial origin healed without ingrowths of vascular adhesions and neovascularisation took place from the proximal and distal sites of the sutures. Cross sections extrasynovial tendon showed obliquely oriented intratendinous vessel while intrasynovial tendons showed vessels extending through the surface layer of the tendon graft.

Fenwick et al. reviewed the previous studies performed on tendon graft neovascularisation and concluded that neovascularisation is essential for the long-term survival of tendon graft (Fenwick et al., 2002).

1.6 GFP species and animal selection for tendon grafting study

A number of different species has been used to study various aspects of tendon graft healing. Many of these studies investigated the fate of tendon graft in the bone tunnel for Anterior Cruciate Ligament reconstruction. With increase use of tendon grafts for overuse injuries several studies recently have investigated tendon to tendon grafting

Table 1.4 - Animal models used for tendon grafting studies

Animal	Tendon graft for tendon repair studies	Tendon graft for ligament reconstruction studies
Mice	(Hasslund et al., 2008; Zantop et al., 2006)	
Rat	(Iwata et al., 2008; Kajikawa et al., 2008; Kajikawa et al., 2007; Tachiiri et al., 2010)	(Bedi et al., 2009; Hays et al., 2008; Kobayashi et al., 2005)
Rabbit	(Murphy et al., 2008)	(Karaoglu et al., 2008; Lim et al., 2004; Ouyang et al., 2004)
Avian	(Ashley et al., 1964; Cao et al., 2002)	
Porcine		(Lee et al., 2005; Liu et al., 1995; Milano et al., 2006; Wu et al., 2009)
Dog	(Potenza, 1964; Seiler et al., 1993b)	(Shino and Horibe, 1991; Yasuda et al., 2004)
Bovine		(Teli et al., 2005)
Primate	(Singer et al., 1989)	

Canine models are popular for studying both tendon healing and tendon grafting biology due to their large size and anatomical similarity to human tendons (Potenza, 1964; Seiler et al., 1993b). Larger animal models remain popular particularly when mechanical studies are planned (Shin et al., 2008; Singer et al., 1989). Requirement of genetically manipulable models have led to the increase in the use of rodent models (Chhabra et al., 2003). Mice and rat (Kajikawa et al., 2007; Kobayashi et al., 2005) are commonly used animals for tendon grafting studies and increase in their use is also aided by their low housing cost, large number of available antibodies, comparable properties to human tendons (Wong et al., 2006a).

Transgenic species like GFP allow easy tracking of cells (Hadjantonakis and Nagy, 2001; Kajikawa et al., 2007) in and out of grafts and has therefore become a popular technique to study grafting biology. (Hayashi et al., 2007; Matsuo et al., 2007; Muramatsu et al., 2007; Zantop et al., 2006). Some of the advantages of the GFP chimeric models are that they allow non invasive visualization and can be monitored real-time *in vitro* and *in vivo* and be quantified by flow cytometry, confocal microscopy and fluorometric assays (Hadjantonakis and Nagy., 2001). Moreover the availability of GFP BMT mice allows tracking of bone marrow derived cells in wounds, grafts etc therefore yielding useful information for tissue engineering (Zantop et al., 2006 ; Kajikawa et al., 2007). GFP species has therefore become an effective tool to study the fate of grafted tissue and has shown tissue specific differences in grafting biology.

The information available from various grafting studies using GFP animal models is summarized in table 1.5.

Table 1.5- Use of GFP species for the study of grafting biology

Author	Species	Specimen	Tools used	Main findings
Iwata et al., 2008	GFP rat	Achilles tendon graft to rotator cuff	Confocal microscopy	Graft cells disappear by 28 days and are replaced by host cells
Muramatsu et al., 2007	GFP rat	Whole limb allograft and immunosuppression	Fluorescent microscopy	Tissue specific variation in repopulation rate with skin cells repopulated first
Kimura et al., 2005	GFP rat	Sciatic nerve graft	Fluorescent microscopy	Retrograde transmigration of donor cells-contributing to axonal regeneration in the recipient nerve
Matsou et al., 2007	GFP mice	Skin graft	Immuno-histochemistry	Rejection of full thickness dorsal skin graft. Improved viability with tail skin grafts
Keijser et al., 2006	GFP rat	Cornea- limbal isograft, sibling allograft and nonsibling allograft	Fluorescence microscopy and Immuno-histochemistry for macrophage and lymphocyte	Average transplant survival 14±3 days

1.7 Role of cells in engineered tendon

Controversy surrounds the value of grafting of cell- based constructs in tendon and it is still unclear as to whether the cells in a tendon graft remain viable after the grafting procedure. It has been argued that cells are not necessary for healing of transplanted tendon (Hasslund et al., 2008) or construct (Badylak et al., 1999) as host cells would eventually repopulate them and that it would simplify the immunogenic aspect of construct transplant. On the other hand cell based constructs have been reported to have improved mechanical function than cell free constructs (Butler et al., 2004). Liu reported formation of structurally disorganised neo-tendon in the scaffold only group and concluded that an even distribution of cells is required in donor tendon/construct to form a homogenous tissue (Liu et al., 2006). The precise nature of cellular traffic into grafts or out of grafts is still largely unknown.

Tendon engineering has advanced significantly in the past 25 years. But one of the main limitations of engineered tendons is that their mechanical strength still remains much lower than that of a normal tendon (Butler et al., 2008; Liu et al., 2006). One potential means of improving collagen deposition and improving collagen alignment which in turn could influence recruitment of tendon strength would be to investigate tendon progenitor cells in a construct. Previous studies have shown that embryonic and neonatal tendon fibroblasts deposit collagen in parallel alignment through cytoplasmic protrusions termed "fibripositors" (Canty et al., 2004; Canty et al., 2006). These cells can be isolated from embryonic tendon and cultured *in vitro*. Furthermore, it has been demonstrated that these cells form a "neo-tendon" when under tension in the absence of a blood supply (Kapacee et al., 2008).

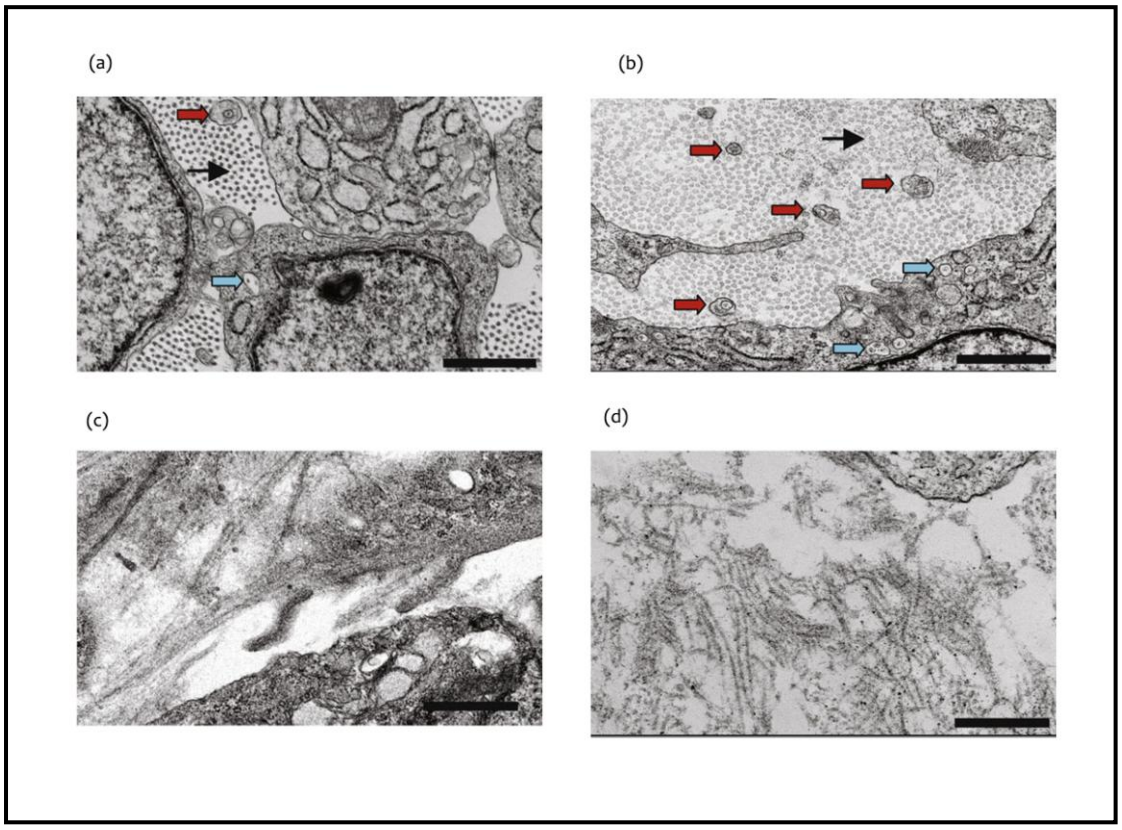

Figure 1.9 - Electron microscopy of fibripositor positive tendon construct. (a) Transverse section of a metatarsal tendon from a 13-day chick embryo showing fibripositors (red arrow) and a fibricarrier (blue arrow), (b) Embryonic tendon cells (ETC) in a construct 1-week post contraction, (c) Electron microscopy of ETCs on Aclar, (d) Disorganised arrays of thin filaments 1-week after severing a construct. Scale Bars - 500 nm (Kapacee et al., 2008)

1.7.1 Cell-free tendon constructs

Many scaffold based materials are under investigation as tendon replacement material. One successful biomaterial that has already been marketed is the extracellular matrix of porcine small intestinal submucosa (SIS-ECM). SIS-ECM has been used to repair Achilles tendon (Badylak et al., 1995; Derwin et al., 2004), rotator cuff (Dejardin et al., 2001; Iannotti et al., 2006)and flexor tendon (Derwin et al., 2004) and has been shown to regenerate neo-tendon with limited mechanical recovery.

1.7.2 Cell based tendon constructs

Numerous cell types have been investigated as potential cell based therapies in tendon grafting. Kryger investigated 4 cell lines (epitenon tenocytes, sheath fibroblast, bone marrow derived mesenchymal stem cell and adipoderived stem cell) and showed that all grafts had been populated by cells (Kryger et al., 2007). However it was unclear from these studies where the cells came from, whether the graft cells undergo apoptosis or remained viable due to the limitations of histological staining. These findings suggest that more work is required to identify whether cells migrate into the tendon, or are replaced, and whether apoptosis or cell migration is involved.

1.8 Summary

A review of the literature suggests that though some histological data exist regarding the fate of tendon grafts no study has been done so far to identify the role of the graft cells. Cell based therapy offers an exciting potential for the future of tendon healing and therefore a better understanding of the grafting biology may open new therapeutic possibilities. On the other hand it may also help us to understand and improve on current tendon grafting practices. A single report was found where tendon to tendon grafting was studied using transgenic animals (Iwata et al., 2008) to investigate persistence of fluorescence of grafted GFP tendon. Another study used wild type mice as a tendon grafting model (Hasslund et al., 2008) focussing on adhesion and growth factor profile during graft healing. Neither study investigated the role of the grafted cells in healing and the mechanism of cellular repopulation. Though earlier histology based experiments suggested that the graft remain alive and healing occur from the stump cells, newer evidence suggests that repopulation by host cells may play a major role in graft integration. A more detailed study looking into the activity of graft cells at various stages of healing will be undertaken to clarify these controversial points of interest.

1.9 Aims

1) To establish a model for the study of tendon grafting
2) To study the fate of graft cells after tendon grafting
3) To study the chronological events of tendon graft take
4) To identify the applicability of the model for testing of tendon constructs

Chapter two

Materials and methods

2.1 Experimental animals

The availability of large numbers of transgenic and knockout species makes the mouse a useful research model. For this study two varieties of transgenic mice species were chosen- the C57BL/6J and the enhanced Green Fluorescent Protein (eGFP) expressing mice C57BL/6-Tg (CAG-EGFP)1 Osb/J. The C57BL/6J mice are the most widely used inbred strain and the first to have its genome sequenced (http://jaxmice.jax.org/strain/000664.html). The GFP mice was generated in C57BL/6 mice with an "enhanced" GFP (eGFP) cDNA under the control of a chicken beta-actin promoter and cytomegalovirus enhancer which makes all of the tissues, with the exception of erythrocytes and hair, appear green under excitation light (Ikawa et al., 1995). C57Bl/6J mice and eGFP (commonly referred to as GFP in publications) mice were chosen to carry out transgenic grafting as the two strains are identical except for the transgene, have only a small number of reported rejections and have easily available antibodies for the detection of the GFP.

Both the C57 BL/6J and GFP mice were supplied by Harlan (Blackthorn, Oxfordshire) and housed at the Biological Unit, in the University of Manchester. Male mice aged 8-12 weeks were used for the study. Mice were matched on size and weight for grafting. Mice were housed together prior to surgery and individually after the surgical procedure. They were provided with mashed feed for the first week in order to prevent weight bearing on operated hind limbs. Standard recommended husbandry was provided by the technical staff at the biological unit.

Table 2.1- Number of animals used

	Type of study	Number of mice
Mouse Achilles tendon anatomy study	C57Bl/6J	16
	GFP	8
Transgenic grafting study	C57Bl/6J	12+3 (for graft harvest)
	GFP	12+4
Construct grafting studies	C57Bl/6J	12
	GFP	8

2.2 Method of anatomical characterisation of mouse Achilles tendon

2.2.1 Macroscopic anatomy

8 c57BL/6Jmice legs (4 left and 4 right) were viewed and dissected under a Leica MZ6 stereomicroscope (Leica Microsystems Ltd, Switzerland) using surgical micro instruments Dissected samples were kept moist by regular spraying with pH neutral phosphate buffered saline (PBS) (Sigma-Aldrich Company Ltd, Poole, UK).

2.2.2 Microscopic anatomy

8 legs (4 left and 4 right) of C57BL/6J and 8 legs (4 left and 4 right) of GFP mice were collected immediately after termination and fixed in fresh Zinc fixative solution (Appendix) for 48 hours at 4°C prior to transfer to 50% Industrial Methylated Spirit (IMS) (Genta Medical, York, UK) solution for preservation. 16 legs were then decalcified in 20% pH 7.4 EDTA solution (Tennants Brewery, Manchester, UK) (Appendix) for 15 days with solution changes every 5 days. Radiographs were performed on the 15th day to ensure complete decalcification. This was achieved by placing samples over unexposed 9 x 12 centimetre Industrex C radiograph film (Kodak, Rochester, New York) in black plastic wallets into a lead enclosed dental radiograph machine (Faxitron, Illinois, USA). The power settings were set to 45 kVp and the sample was exposed to 5 seconds worth of radiation. The radiograph machine was deactivated and the radiographic film was developed in a dark room with 3 minutes in Phenisol developer solution (Ilford Imaging ltd, Mobberley, England.) followed by 3 minutes in running cold water. The film was then placed in Hypam fixer solution (Ilford Imaging ltd, Mobberley, England.) for 3 minutes then further rinsed for 3 minutes in cold running water prior to leaving to air dry. Following decalcification the decalcified legs were put back into 50% IMS solution until further processing. Remaining 8 C57BL/6J (4 left and 4 right) mice legs and 8 GFP (4 left+ 4 right) legs were filleted to remove the bone from the specimen and immersed in 50% IMS.

Both the decalcified legs and filleted legs were processed in a Tissue-Tek Vacuum Infiltration Processor (Bayer Diagnostics, Newbury, Berkshire, UK) on a skin cycle program (Appendix). Following wax processing, legs were placed in wax wells that were filled with molten wax. Legs were positioned in either longitudinal alignment or in an axial alignment and left for the wax to set over 24 hours. The blocks were cut at 7 µm sections from paraffin embedded samples using a HM 335E electronic microtome (Microm, Walldof, Germany) using Accu Edge low profile disposal blades (Feather Safety Razor Co Ltd, Japan). Sections were floated on a warm water bath (37-40˚ C) and mounted on coated 1% poly-l-lysine slides (Cell Path). The sections were dried briefly on a hot plate prior to being labelled and placed into an oven overnight at 37˚C.

2.2.2.1 Basic staining-Haematoxylin and eosin

Haematoxylin & Eosin staining (Appendix) was used to highlight cell nuclei purple (Harris alum haematoxylin) and counter stain remaining tissue pink (Eosin Y)(Appendix). Following dewaxing, sections were placed into filtered haematoxylin for 4 minutes followed by a period of "bluing" which involves rinsing in running tap water for 5 minutes. Slides were subsequently transferred to Eosin Y for 30 seconds followed by rinsing in running water for 10 seconds and dehydrated through the alcohols prior to mounting in Pertex and glass cover slips.

2.2.2.2 Alcian Blue Staining

This stain highlights acid mucosubstances (Glycosaminoglycans) and acidic mucins that were used to highlight fibrocartilaginous areas within tendon. Sections were dewaxed and hydrated then placed in Alcian Blue Solution pH 2.5 (which stains weakly sulphated mucins-Appendix) for 5 minutes. Samples were then washed in tap water followed by counterstaining in 0.1% Nuclear Fast Red (Appendix) for 5 minutes. Further washing in tap water was performed and slides were then dehydrated and mounted with Pertex and glass cover slips.

2.2.2.3 Miller's Elastin

This stain highlights elastin fibres. Sections were dewaxed and hydrated through graded alcohols and then treated in 0.5% acidified Potassium Permanganate (Appendix) for two minutes then rinsed in tap water prior to washing in 95% IMS. Sections were then placed into Miller's Elastin Staining solution for two hours and then washed in 95% IMS solution. Counterstaining was performed in Van Gieson's stain (Appendix) for 2 seconds prior to washing and dehydrating through the alcohols and mounting in Pertex and glass cover slips.

2.2.2.4 Masson's Trichrome Staining

Masson's Trichrome stain (Appendix) for collagen and other components of the extracellular matrix. Slides were dewaxed and rehydrated followed by submersion in Harris' Haematoxyllin for 4 minutes and bluing for 5 minutes. Samples were then transferred to 1 % (v/v) picric acid for 30 seconds, rinsed in running water until only a yellow tint remained for 1 minutes, transferred to 0.1 % (w/v) Biebrich scarlet for 2 minutes and then quickly rinsed in water for 10 seconds. Slides were then placed into 50% phosphomolybdic acid/50% phosphotungstic acid (50:50 PMA/PTA) for 10 minutes then transferred directly to Fast Green for 5 minutes and rinsed in tap water for 10 seconds. The slides were dehydrated and mounted with Pertex and glass cover slips.

2.2.2.5 Hoechst and Phalloidin stain

Slides were dewaxed, rehydrated and rinsed in 0.1% Triton X-100 in PBS three times, five minutes each. Sections were incubated for one hour with of TRITC-labelled phalloidin (1:500 dilution, Sigma, Dorset, UK). Slides were then rinsed again and incubated with Hoechst 33258 bisbenzimidazole nuclear counterstain (1:500 dilution) for 30 min. After one further rinse, sections were mounted in Gelvatol anti-fade aqueous mountant.

2.2.2.6 Immunohistochemistry with Alpha Smooth Muscle Actin (Alpha SMA)

Alpha Smooth Muscle Actin (αSMA) is expressed by pericytes which are cells present in the endothelium of blood vessels. Experimental and control slides were selected and rehydrated through xylene and graded alcohols (5 minutes in xylene twice, then 10 seconds in each graded alcohol 100% -> 100% ->90% ->70% -> 50% -> PBS) and then washed in PBS-Tween twice for 5 minutes each time. Sections were immersed in 3% H202 solution for 10 minutes and washed again in PBS- Tween (.01%) twice for 5 minutes each time. Sections were dried and segregated with ImmEdge Hydrophobic Barrier Pen (Vector Lab) and then washed in PBS tween for 5 minutes. Horse blocking serum (2.5%) was added to all sections (Immpress-Vector Lab) and incubated for 30 minutes. Sections were washed in PBS-tween twice for 5 minutes. Primary antibody (Rabbit polyclonal-Abcam) were added to alternate sections and incubated at 37˚C for 1 hour. PBS was added to rest of the sections. The slides were washed twice in PBS-Tween and ImmPRESS anti-rabbit Ig (Immpress-Vector lab)) was added to all sections and incubated at 37˚C for 30 minutes. The slides were washed in PBS twice for 5 minutes and then 3, 3'-diaminobenzidine (DAB -Vector Lab) solution was added to each section for 5 minutes minimum or until DAB precipitated, rinsed in PBS twice for five minutes, counter stained in Nuclear fast red for minimum of five minutes, dipped in water twice and dehydrated through graded alcohols and into clean xylene twice for 5 minutes and mounted in Pertex and dried.

2.3 Tendon Grafting

2.3.1 Operative procedure for tendon grafting

4 GFP and 4 C57BL/6 mice were used for each time point. Graft harvested from the GFP mouse was applied to a defect in the C57 BL/6 mouse Achilles tendon as an onlay or patch graft using one securing sutures on each end to minimise trauma and handling (Figure 2.1- 2.2). Similarly graft harvested from the C57 BL/6 mouse was placed into the GFP mouse.

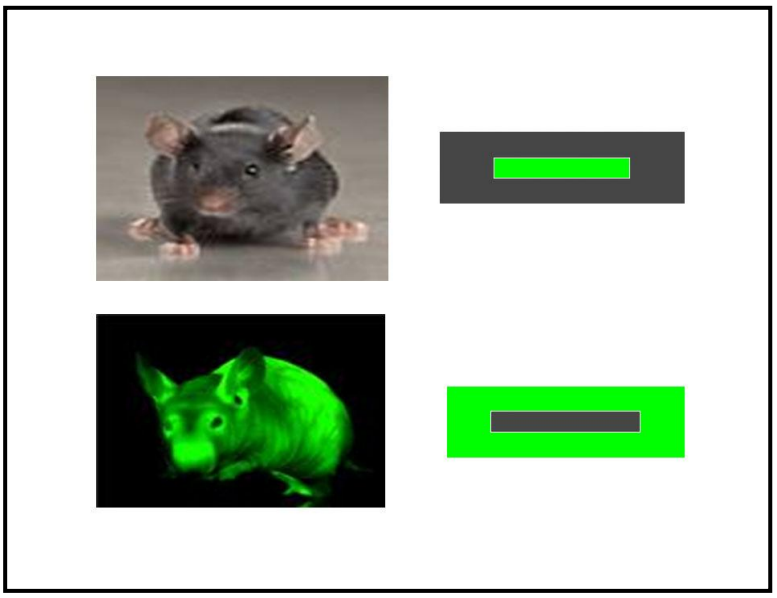

Figure 2.1- Diagrammatical representation of design of syngenic and autologous grafting showing the C57BL/6 mouse receiving a green GFP graft (above) and the green GFP mouse receiving a C57 BL/6 graft (below)

All equipment and instruments were checked thoroughly prior to surgery. Anaesthesia was induced by 4% Isoflurane (Abbott Laboratories, UK) and Oxygen (BOC) at 4 litre/minute and maintained by 2% Isoflurane and Oxygen at 2 litre/minute, with an Oxygen drive.

Achilles tendon was harvested from freshly euthanized donor mice under magnification (Leica Surgical microscope). The donor tendon was placed in CO_2 independent media (Gibco-Invitrogen) to maintain viability during transfer.

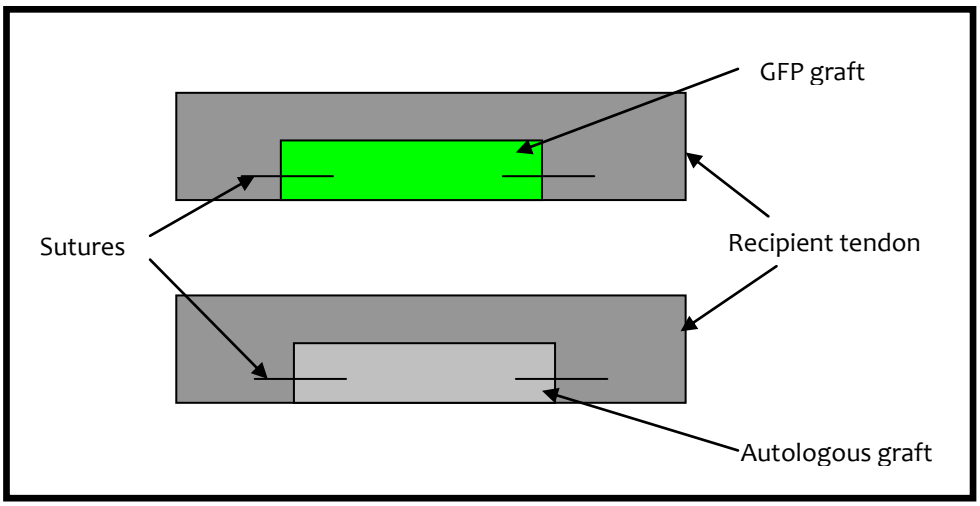

Figure 2.2- Diagrammatic representation of surgical technique of tendon grafting studies showing placement of the graft in a 50% defect of the tendon and the placement of the proximal and distal holding sutures

The recipient mouse was placed in prone position on a custom made operating table made of thermoplastic material. The legs were shaved and hair removed with a handheld vacuum cleaner. The area was cleaned with Hibiscrub (Chlorhexidine Gluconate 4% w/v-Molnlycke Health Care). The left leg was stretched out, immobilized with blue tack (Bostik, UK) underneath and over the foot(Figure 2.3- 2.4). A tourniquet was applied at the thigh using elastic ribbon. A 1 cm longitudinal incision was made at the midposterior line on the back of the right leg from the musculotendinous junction

to just distal to the ankle joint. The direction of plantaris was confirmed by its insertion into the plantar aponeurosis. The plantaris was separated from the body of the Achilles tendon by sharp dissection of their fascial connections. A distal transverse incision was made in the Achilles tendon comprising 50% of the width of the tendon. The incision was extended longitudinally up to 4 mm and then the segment was divided proximally. In the left leg, the donor tendon placed in media previously (GFP tendon graft to C57 mice and C57 tendon graft to GFP mice) was placed into the defect and secured with 10-0 polyamide (Braun Medical, UK) sutures proximally and distally. Fascia and plantaris were replaced back into position. The tendon was kept moist and well hydrated with regular normal saline irrigation. Skin was closed with 8-0 interrupted suture. Subcutaneous Buprenorphine (Reckitt Benckiser Healthcare, UK-Appendix) was administered to all animals for postoperative analgesia.

In the left leg, a cut segment from the same tendon was put back into the defect as autologous graft. Mice were weighed and recovered in individual cages with standard animal husbandry.

After the procedure mice were monitored carefully on a daily basis. Weight, ambulation and wounds were recorded. The mice generally had excellent postoperative recovery and was fully weight bearing within 24 hours. No clinical signs of rejection were noted at any stage.

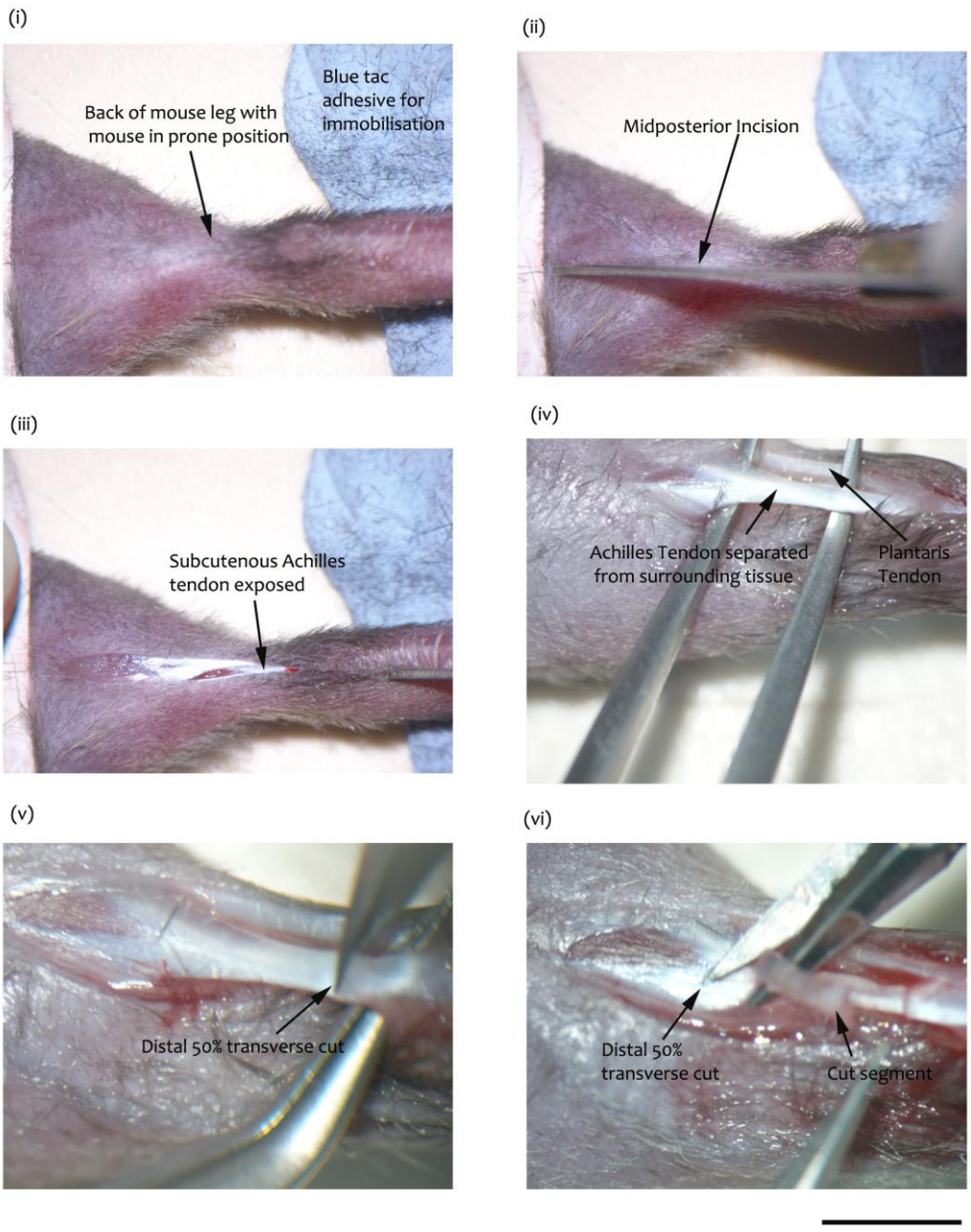

Figure 2.3 -Photographic representation of surgical procedure for tendon grafting showing i) Positioning of mouse leg , ii) Longitudinal incision for exposure, iii) Exposed Achilles tendon (iv) Achilles Tendon separated from surrounding tissue (v) Distal 50% transverse cut and vi) Excising a 50% segment of tendon. Scale Bar-3 mm

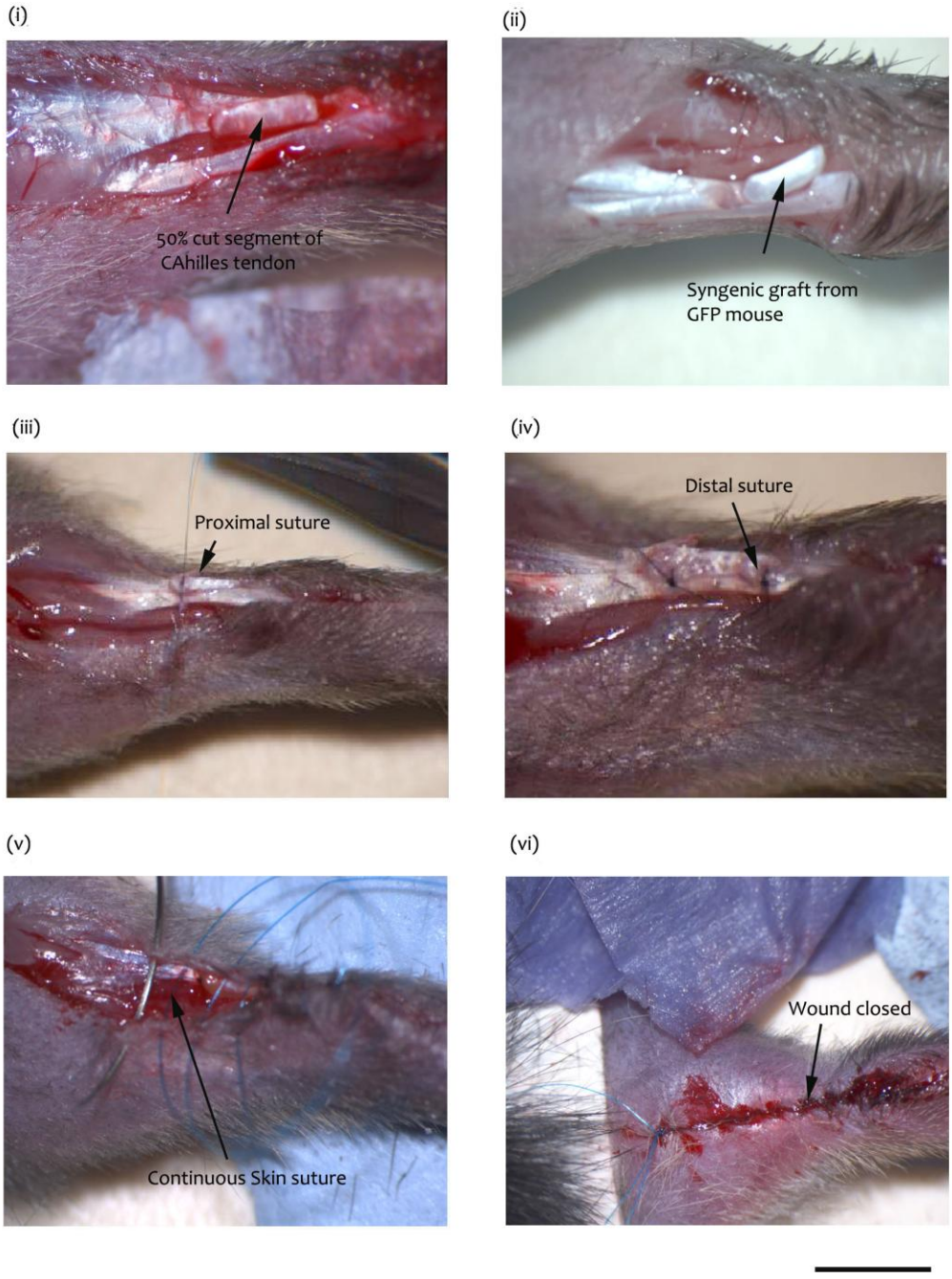

Figure 2.4 -Photographic representation of surgical procedure for tendon grafting showing -i) 50% cut segment of the Achilles tendon, ii) Syngenic or autologus graft placed in the defect, iii) proximal suture, iv) distal suture to secure graft, v) continuous suture for skin closure, vi) skin closed; Scale Bar-1 mm

2.3.2 Tissue Harvest

4 GFP and 4C57BL/6 (n=8) mice that had underwent tendon grafting procedures were harvested at each of the following time point- Day 3, Day 21 and Day 90 (total n=24). The time points were chosen in keeping with the three classic stages of healing- inflammation, proliferation and remodelling.

Mice were euthanized by an overdose of CO_2 inhalation followed by cervical dislocation. The legs were removed at the knee joint. Longitudinal incisions were made on the medial and lateral side of the leg for better penetration of fixatives. The specimens were submerged in a Zinc based fixatives for a minimum of 48 hours and then changed into 50% IMS until further processing.

Hair was removed by application of hair removal cream for 20-30 minutes and then washed in PBS and re-submerged in 50% IMS. The posterior compartment of the leg was sharply filleted. The excised specimen was carefully assessed for residual bone fragments.

2.3.3 Tissue processing

All fixed samples were processed in a Tissue-Tek Vacuum Infiltration Processor (Bayer Diagnostics, Newbury, Berkshire, UK) on a skin cycle program (Appendix). Following wax processing legs were placed in wax wells that were filled with molten wax. All legs were carefully positioned to allow for longitudinal sections. The wax blocks were left to set over 24 hours.

7µm sections were cut from paraffin embedded samples using a HM 335E electronic microtome (Microm, Walldof, Germany) using Accu Edge low profile disposal blades (Feather Safety, Japan). Sections were floated on a warm water bath (37-40° C) and mounted on 1% poly-l-lysine (Cell path, UK). The sections were dried briefly on a hot plate prior to being labelled and placed into an oven overnight at 37°C.

2.3.4 Histology for tendon graft characterisation

2.3.4.1 Dewaxing

Before staining, the paraffin embedded sections were immersed in two consecutive xylene (Genta Medical, York, UK) baths for 5 minutes to dissolve wax. Then slides were transferred to consecutive solutions of 100% IMS, 100% IMS, 90% IMS, 70% IMS then 50% IMS for 10 seconds each to rehydrate samples.

2.3.4.2 Dehydrating and slide preservation

Following staining slides were transferred to consecutive solutions of 50% IMS, 70% IMS, 90% IMS, 100% IMS, and 100% IMS for 10 seconds each. The slides were then placed into two consecutive xylene baths for 5 minutes each prior to coating with Pertex mounting media (Cellpath plc, Powys, UK) and 50mm x 22mm glass coverslips (Scientific laboratory supplies Ltd, Nottingham, UK) and allowed to dry at room temperature before light field microscopy.

2.3.4.3 Haematoxylin and eosin staining (H & E)

Haematoxylin and Eosin staining was performed on every 4^{th} slide for orientation.

2.3.5 Immunohistochemistry

Table 2.2 shows list of antibodies that were used to identify the types of inflammatory cells, presence of GFP cells, collagen synthetic activity, proliferative activity, apoptosis and vascularisation.

Table 2.2 - List of antibodies used and their targets

Antibodies	**Function**
CD45	Pan Leukocytic marker
Ly6G	Predominantly Neutrophil and subset of Eosinophil
F4/80	Mature tissue macrophages and activated macrophages
CD3	T-lymphocytes
Alpha SMA	Pericytes in blood vessels
BrdU	5-Bromo-2-deoxyuridine-Thymidine analogue incorporated into newly synthesizing DNA of replicating cells. Antibody to BrDU can then be used to detect this
Hsp47	Heat Shock Protein 47- A molecular chaperone that interacts with and stabilizes procollagen
TUNEL	Terminal-deoxynucleotidyl Transferase Biotin dUTP End labelling for DNA fragment-marker for apoptotic cells
GFP	GFP positive cells

Table 2.3 - Antibodies and their pre-treatment, primary, secondary, amplifier and chromogens used

Antibody	Pre-treatment	Block	Primary	Secondary	ABC	DAB	Control
CD 45 (BD Pharmingen)	None	1% rabbit serum	1:100 Rat anti-mouse	1:200 rabbit anti- rat	Yes	Yes	Spleen
Ly6G (BD Pharmingen)	None	1% rabbit serum	1:200 Rat anti-mouse	1:200 rabbit anti-rat	Yes	Yes	Skin wound
F4/80 (Serotec)	None	1% rabbit serum	1:200 Rat anti-mouse	1:200 rabbit anti- rat	Yes	Yes	Spleen
CD3 (BD Biosciences)	None	1% rabbit serum	1:200 Rat anti-mouse	1:200 rabbit anti- rat	Yes	Yes	Spleen
Alpha SMA (Abcam) Ab5694-100	None	2.5% Goat serum	1: 200 Rabbit polyconal	Immpress kit(Vector Lab)	No	Yes	Spleen
Hsp 47 (Stressgen)	None	MOM block	1:200 Mouse Monoclonal	MOM kit 2 IgG	Yes	Yes	Skin wound
BrdU (Abcam)	10 min in 4 M HCl, 10 min in borate buffer	1% rabbit serum	1:200 Rat anti-mouse	1:200 rabbit anti-rat	Yes	Yes	Spleen
TUNEL (Roche)	30 min in Tris HCl+ Proteniase K	None	2:3 -enzyme: solution	1:2:1 sheep serum: PBS: POD kit	No	Yes	Large intestine
GFP (Abcam)	None	1% Rabbit serum	1:200 Rat anti-mouse	1:200 rabbit anti-rat	Yes	Yes	GFP spleen

2.3.5.1 Protocol for GFP antibody staining

Slides were dewaxed in Xylene twice for 5 minutes each and then rehydrated through descending alcohol-100%, 100%, 90%, 70% and 50%, 5 seconds in each and then washed in water for 30 seconds . They were then washed in PBS-Tween (Appendix) three times for 5 minutes each and gently stirred on a shaker during all washes. Endogenous peroxidase activity was blocked by using 3% H_2O_2 (made from 30% H_2O_2-Sigma) for10 minutes and the washed again in PBS-Tween twice for 5 minutes. Slides were dried individually in between sections and sections were separated using a wax pen (Immedge- Vector Lab) to allow the solution to stay on the section and separate them from controls. The wax was allowed to dry and then washed twice again in PBS-Tween to remove any excess wax. 1% rabbit serum was used to block nonspecific antigens and 35µl of blocking serum was added to each section. Alternate sections in the slide were used as negative control and GFP spleen was used as positive control. The slides were incubated with blocking serum for one hour at room temperature and then washed again in PBS-Tween x 2 for 5 minutes. Primary antibody (Sheep anti-mouse) was added to experimental sections in 1:100 dilutions and blocking serum was added to control sections. Slides were incubated at 4 degrees overnight and washed in PBS-Tween x 2 for 5 minutes. Slides were gradually rewarmed to room temperature and secondary antibody (Rabbit anti-sheep) at 1:200 dilutions were applied to all sections and incubated at 37 degrees for one hour. Slides were then washed in PBS twice for 5 minutes, ABC was (Avidin Biotin Complex) added to all sections and incubated for 30 minutes in room temperature and then washed in PBS for 5 minutes twice. DAB (Vector Lab) was added for 5-8 minutes or until change of colour and then washed in PBS twice for 5 minutes each. The slides were counterstained with nuclear fast red for 10 minutes, then dipped in water, dehydrated through ascending alcohol 5 seconds each in 50%, 70%, 90%, 100%, 100% alcohol and in Xylene twice for 5 minutes. All slides were mounted in Pertex with coverslip and left overnight to air-dry.

2.3.5.2 Immunostaining for Inflammatory markers

A similar protocol was followed for inflammatory marker immunostaining with the exception of application of primary antibodies (Figure 2.5) and a rabbit anti-rat secondary. Three of the four sections of the slide were incubated with a different primary antibody at 37° overnight while the 4th control section received no primary.

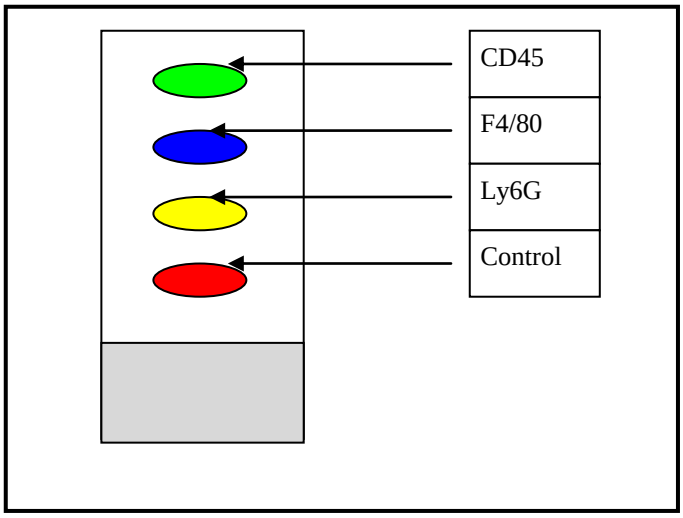

Figure 2.5 - Diagrammatic representation of a slide showing immunostaining for inflammatory markers using serial sections of the same slide

2.3.5.3 Immunostaining for Cellular activity markers- Proliferation, collagen synthesis, apoptosis, vascularisation (Pericyte)

Experimental and control slides were selected and rehydrated through xylene and graded alcohols (5 minutes in xylene twice, then 10 seconds in each graded alcohol 100% -> 100% ->90% ->70% -> 50% -> PBS) and then washed in PBS-Tween twice for 5 minutes each time. Sections were immersed in 3%H202 solution for 10 minutes and washed again in PBS- Tween twice for 5 minutes each time. All slides had a minimum of four sections on them. Sections were dried and segregated with a wax pen and then washed in PBS-Tween for 5 minutes.

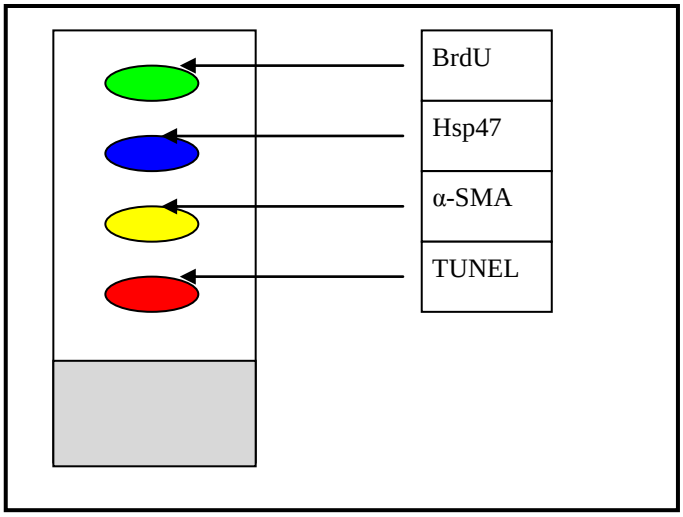

Figure 2.6 - Diagrammatic representation of a slide showing immunostaining for proliferation, synthesis, apoptosis and vascularisation using serial sections of the same slide

Slides were placed in the incubator and two drops of 4M HCL were added to the top section only and left for 10 minutes. PBS was added to the rest of the sections. Slides were quickly rinsed in PBS and then two drops of borate buffer were applied to the top section of each slide only and left for 5 minutes. Slides were washed again twice in PBS-Tween for 5 minutes. Blocking solution was added to BrdU (1% Rabbit serum), Hsp 47 (MOM Blocking agent) and Alpha-SMA (ImmPRESS) sections and PBS to TUNEL sections and left for30 minutes. After 30 minutes proteinase k (Roche, UK) in Tris HCL

solution was added to TUNEL sections. Sections were washed in PBS-Tween twice for 5 minutes. Primary antibodies were added to the sections (Figure 2.6) and incubated at 37˚C for 1 hour. The slides were washed twice in PBS-Tween and secondary antibody was added firstly to BrdU (Rabbit anti-rat) and Hsp47 (MOM secondary) for 30minutes and kept at room temperature. Sections were washed in PBS-Tween twice for 5 minutes and ABC was added to BrdU and Hsp 47 sections, ImmPRESS to SMA sections and POD development kit to TUNEL and incubated at 30°C for 30 minutes. The slides were washed in PBS twice for 5 minutes and then DAB solution was added to each section for 5 minutes minimum or until DAB precipitated, rinsed in PBS twice for five minutes, counter stained in Nuclear fast red for minimum of five minutes, dipped in water twice and dehydrated through graded alcohols and into clean xylene twice for 5 minutes and mounted in Pertex and dried.

2.3.6 Image capture

Gross anatomical structures were captured using a Nikon Coolpix 4500 digital camera (Nikon, Japan) mounted on Leica M650 operating microscope (Leica, Germany). Files were captured at 2272 x 1704 pixels of resolution and saved as uncompressed .tiff files. Histological images were captured on a Leica DMRB microscope for direct transmission brightfield microscopy with a mounted Spot RT digital camera. Images were captured using Spot advanced capture software version 3.1 (Diagnostic Instruments, Inc., MI, USA) on a Silicon graphics Pentium III 230 mhz PC and saved as uncompressed .tiff files prior to transfer to external hard drives. 5x and 10x objectives were used to magnify images.

2.3.7 Image analysis

All images were montaged and aligned in Adobe Photoshop CS5 (Adobe Systems Inc. USA). Standard sized areas were selected in the graft tendon, host tendon and in the subcutaneous tissue using adobe Photoshop (n=3 slide/mouse/ stain). A total of 12 (3 slides/mice x 4 mice/time point) slides per time point were analysed for each stain. For quantitative analysis, Individual cells showing markers of inflammation, proliferation, synthesis or apoptosis were counted using the cell counter in the Image J software (http://rsbweb.nih.gov/ij). Data was put into Microsoft excel data sheet and analysed using SPSS version 16 (SPSS Inc. Chicago, USA). Three dimensional reconstructions of serial sections were done using "Reconstruct" software ("Reconstruct" by John C. Fiala).

2.3.8 Statistics

Mean values were calculated using SPSS version 16 (SPSS Inc. Chicago, USA) and expressed with the standard error of means following "±" symbol. The Kolgomorov-Smirov test was used to show that the data were normally distributed. Independent T testing was used to analyse differences between autogenic and syngenic grafting biology. Differences in cellular biology between control and different time points were assessed by analysis of means using one-way ANOVA and post hoc Tukey test. In all cases p value was considered significant if below 0.05. Significance was recorded with * in the graph if p-value was less than 0.05 and ** if p was less than 0.001.

2.4 Application of The mouse Achilles Tendon model for Biomaterial Testing

Two different varieties of engineered tendon constructs were investigated using the mouse Achilles tendon model. One was a GFP positive cell based construct developed by a collaborative group using techniques described by Kapacee et al (Kapacee et al., 2008). The second construct was Polycaprolactone 3D electrospun bundles, an acellular biocompatible construct developed by Downes Lab at the material Science centre at the University of Manchester.

2.4.1 Cell Based Fibrin Construct

Cells were extracted from 3 weeks old GFP mouse tail tendon with trypsin (37,000 U) and bacterial collagenase. Each well of a six well plate was coated with a 2 mm-thick layer (1.5 ml) of SYLGARD In each well. Fixed-position posts were created by pinning minutiens insect pins. Cells were suspended in fibrinogen and thrombin and incubated at 37 °C in DMEM4 supplemented with penicillin (100 U/ml), streptomycin (100 µg/ml), L-glutamine (2 mM), L-ascorbic acid 2-phosphate (200 mM), and 10% fetal calf serum. The plates were scored every 2 days to release fibrin gel that had adhered to the SYLGARD. The Cells contracted the fibrin gel during 6 days and formed a tendon like structure (Figure 2.7).

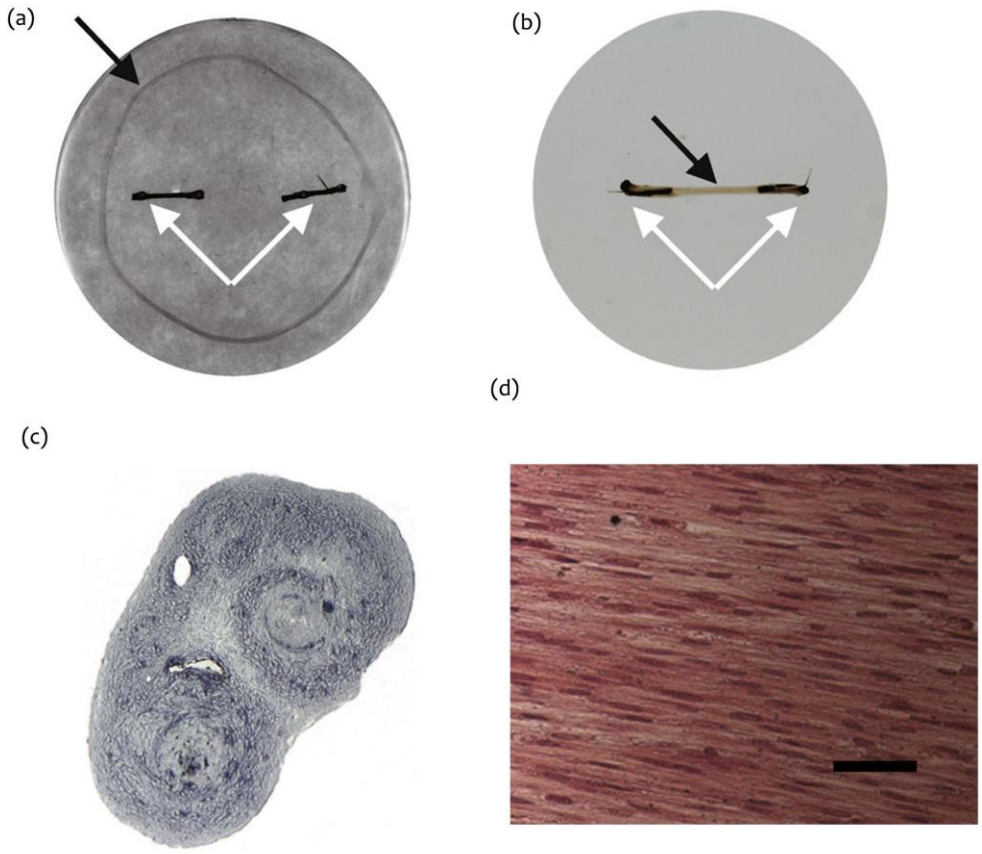

Figure 2.7 Formation of a construct from embryonic tendon cells. (a) plan view of a fibrin gel during contraction. The black arrow shows the outer edge of the gel. (b) plan view of a fully-contracted gel (black arrow), White arrows point to short lengths of suture material attached by minutien pins (c) transverse section of a construct 1-week post contraction stained with toluidine blue (d) longitudinal section of a construct 1-week post-contraction stained with haematoxylin-eosin showing the parallel alignment of cells. Scale Bar- 50 µm (Kapacee et al., 2008).

2.4.2 Acellular Construct Polycaprolactone 3D electrospun bundles

Acellular Polycaprolactone 3D electrospun (PCL) bundles were supplied by a collaborative group. The material has previously been tested as a peripheral nerve conduit (Sun et al., 2010).

The bundles had a low melting point of 50˚C and therefore attempts at testing them with wax sections failed. The specimens were tested with Scanning Electron Microscopy (SEM)

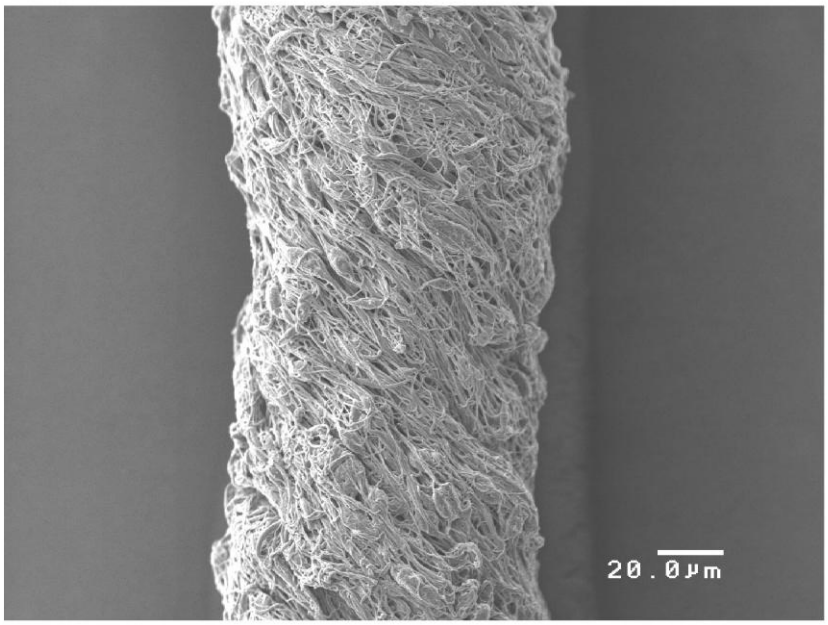

Figure 2.8 – Scanning Electron Micrograph demonstrating the structural morphologies of 3D fibrous bundles fabricated by the techniques described in the appendix – fine mandrel. (Magnification x 500). Photpgraph by Lucy Bosworth

2.4.3 Surgical Procedure for *in vivo* contsruct testing

The recipient mouse was placed in prone position in the operating board. The legs were shaved and hair removed with a handheld vacuum cleaner. The area was cleaned with Hibiscrub (Chlorhexidine Gluconate 4% w/v-Molnlycke Health Care). The left leg was stretched out, immobilized with blue tac (Bostik, UK) underneath and over the foot. Tourniquet was applied at the thigh using elastic ribbon. A 2 cm longitudinal incision was made at the midposterior line on the back of the right leg from the musculotendinious junction to just distal to the ankle joint. The direction of plantaris was confirmed by its insertion into the plantar aponeurosis. The plantaris was separated from the body of the Achilles tendon by sharp dissection of their fascial connections. A distal transverse incision was made in the tendon comprising 50% of the width of the tendon. The incision was extended longitudinally up to 4 mm and then the segment was divided proximally.

The cell based fibrin construct was cut at both ends, lifted from its culture media and was trimmed to the size of the defect. Either a fibrin construct or an a acellular PCL construct was placed into the defect and secured with 10-0 polyamide (Braun Medical, UK) sutures proximally and distally. Remaining part of the surgery was carried out as described for tendon grafting surgery.

In the PCL construct study mice (n=6, 2 mice/time point) were harvested at the following time points- Day 0, Day 3 and Day 21. At the time of harvest, mice were euthanized and the left leg dissected with the Achilles tendon removed from the bone. The tissue was stored in zinc fixative. The initial and final time-points were analysed by variable pressure SEM (VPSEM) (Zeiss), which allowed tissue samples to be viewed without dehydration and gold sputter-coating. An accelerating voltage of 5 keV was used to scan the tissue surface.

In the fibrin construct study a shorter time course was chosen to determine persistence of construct. Mice were harvested at Day 0, Day 3 and Day 7 (n=2/time point). The legs were processed using the same methodology described for syngenic grafting studies.

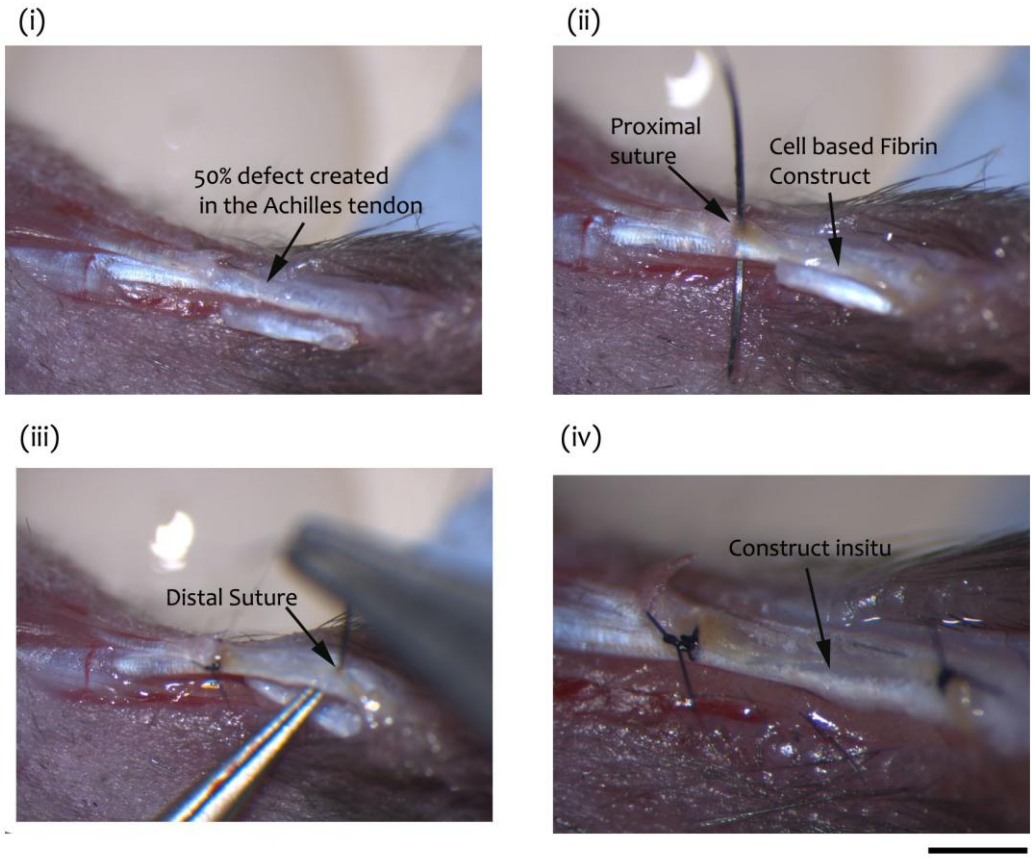

Figure 2.9 -Fibrin construct *in vivo* testing- (i) Construct lifted from culture into the wound, (ii) Construct being secured with a proximal suture and (iii) a distal suture (iv) Construct secured in tendon defect; Scale Bar- 1 mm.

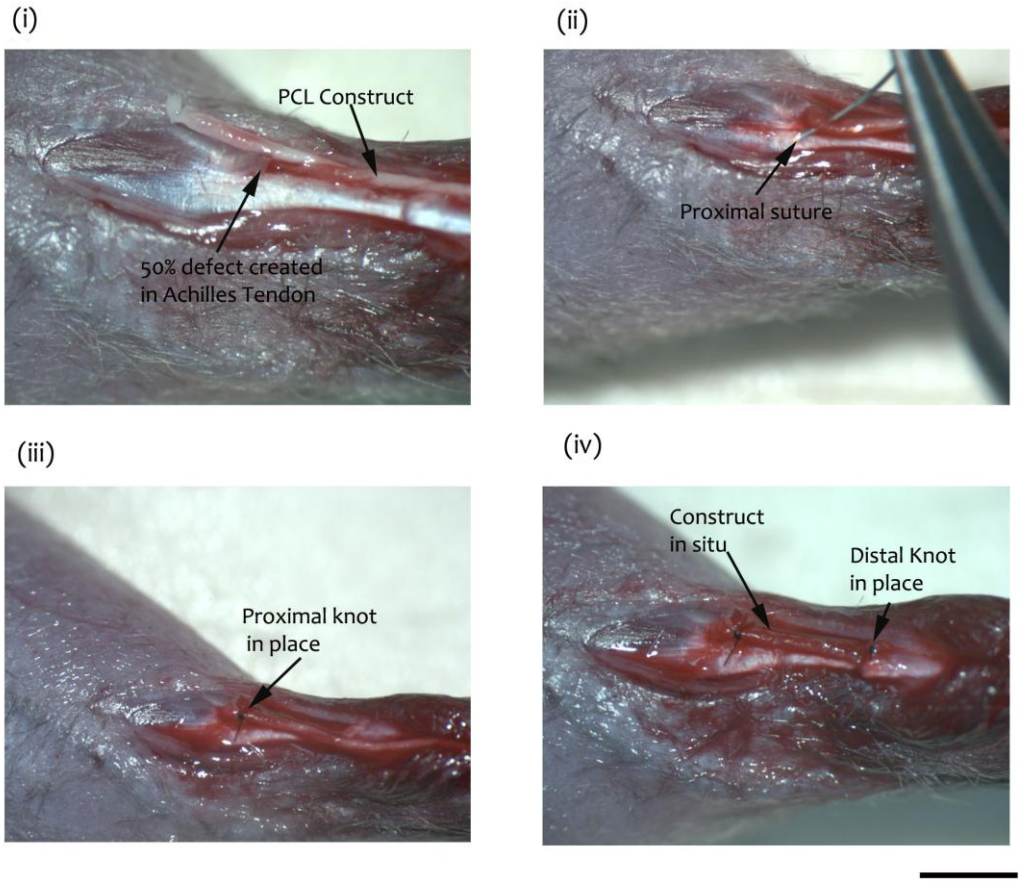

Figure 2.10 -Acellular PCL construct *in vivo* testing- (i) Defect being created in the wound, (ii) PCL Construct placed into the wound (iii) Construct being secured with a proximal suture and (iv) a distal suture, Scale Bar= 1 mm

Chapter Three

Results

3.1 Results- Anatomical characteristics of Mouse Achilles tendon

3.1.1. Macroscopic Anatomy

The Achilles tendon is formed by the union of the tendons of gastrocnemius and soleus (Figure 3.1). The average length of the tendon (from musculotendinous junction to calcaneal insertion) is 0.63 ±0.10 mm. The tendon is closely related on its posterior and medial aspect to the tendon of plantaris which travels from the medial side of the tendon to lie at its posterior aspect and passes over the posterior surface of the ankle to insert into the plantar fascia in the sole (Figure 3.2). The plantaris tendon was found to be present in all experimental animals and cadavers. The Achilles tendon spirals in its long axis and the medial fibers become posterior distally. The tendon consistently received contribution from both the soleus and the gastrocnemius muscles and tendons.

Anteriorly there is an obvious plane of demarcation between the superficial and deep group of muscles of the posterior compartment and the muscle belly of gastrocnemius can be easily separated from the deep flexor compartment by either sharp or blunt dissection. The flexor compartment lies in close proximity to the tibia proximally and distally to the united tibia and fibula. In the distal one-third of the leg the Achilles tendon is separated from the tibia and the flexor tendons by a constant presence of loose areolar tissue. Neurovascular bundles are seen to run in the loose areolar tissue close to the anterior aspect of the Achilles tendon. The tendon is inserted into the posterior aspect of the calcaneum. It is surrounded by a layer of paratenon which can be dissected away. The tendon is round in cross section at its waist but flattens out at insertion.

The tendon is subcutaneous and is easily accessible through a midline incision at the back of the leg. The plantaris tendon is separated from the body of the Achilles tendon by gentle dissection so as to prevent bleeding from the fragile vessels in the paratenon

particularly near the ankle region. The plantaris is retracted to one side and the tendon is ready for manipulation.

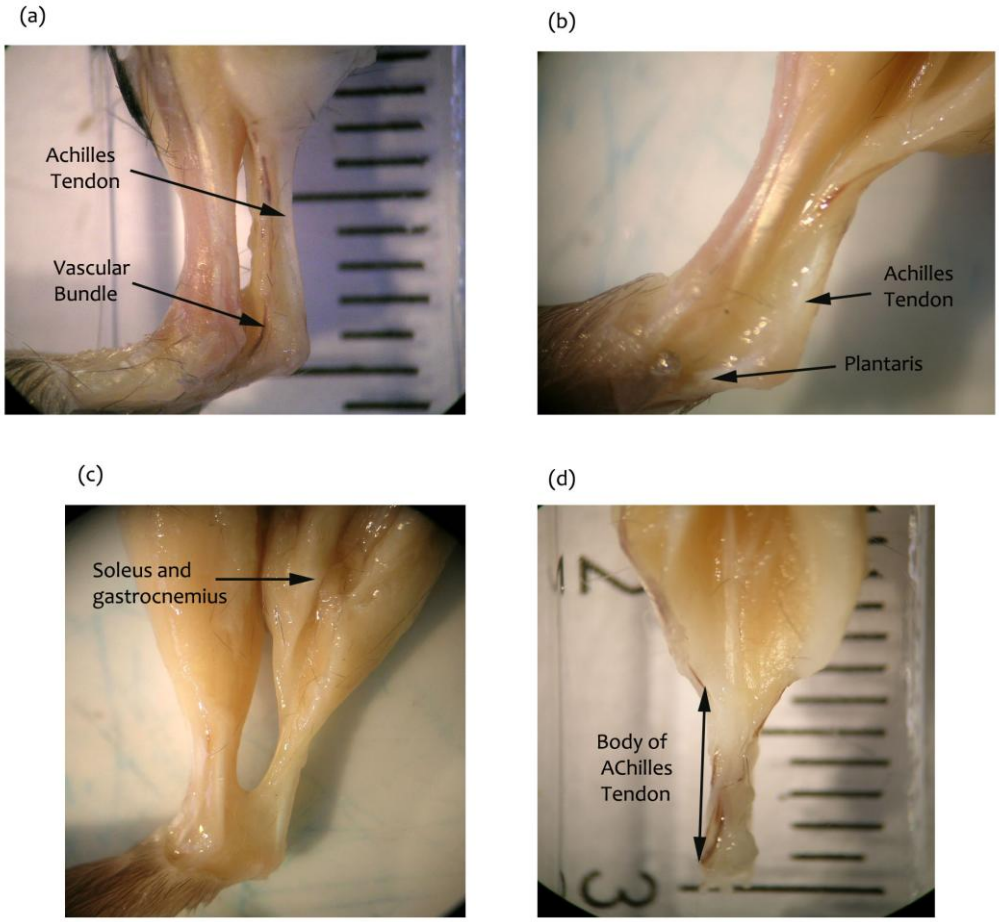

Figure 3.1 - Macroscopic anatomy of Achilles tendon by cadaveric dissection- a) and b) Fascial plane between superficial and deep compartment, c) and d) Formation of Achilles tendon with blood vessels lying anterior to the tendon

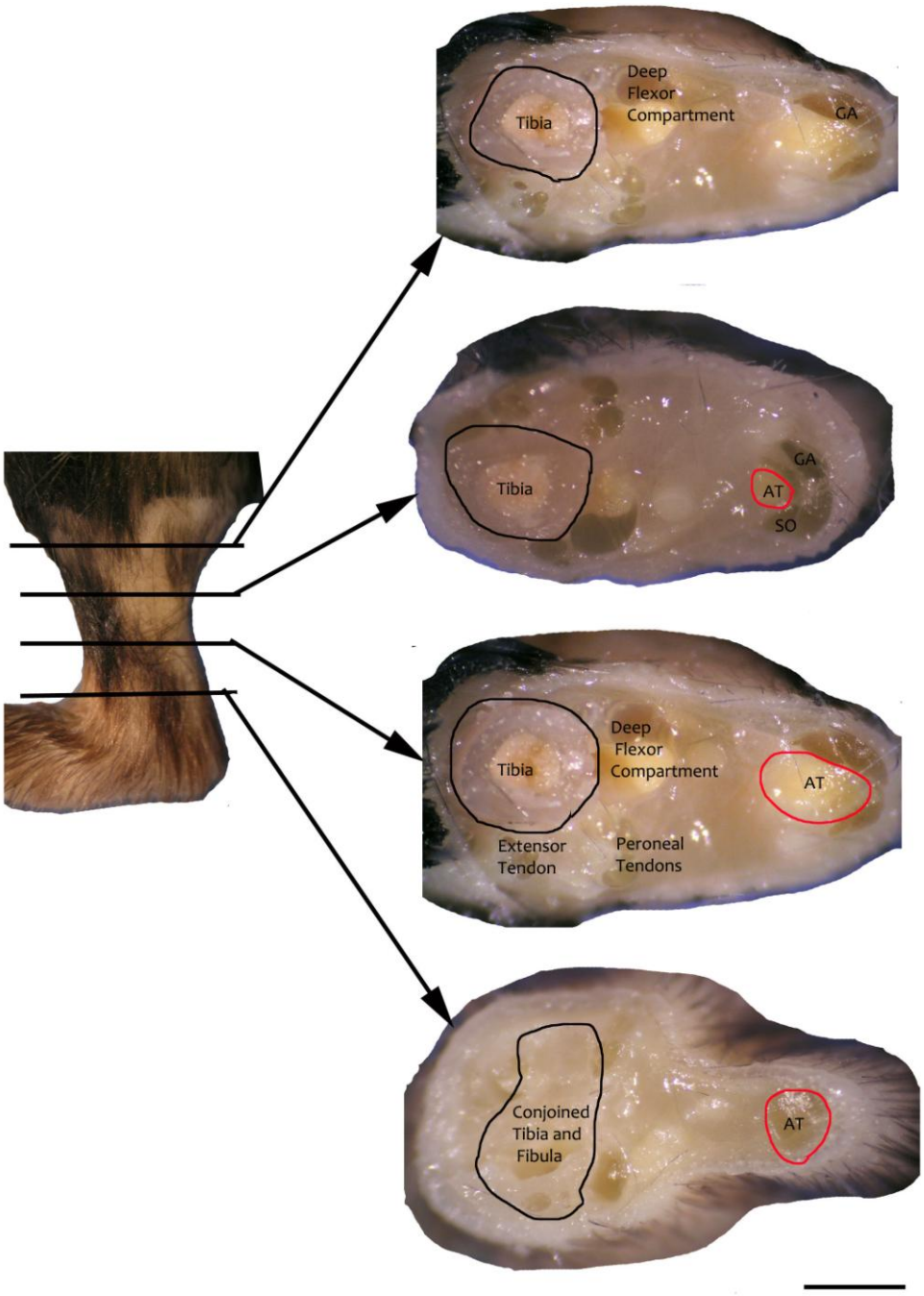

Figure 3.2 -Transverse serial section through Decalcified mouse leg from Proximal to Distal (Top to Bottom) – 2mm segments, image captured from above and below the cuts, AT-Achilles tendon, So-Soleus, GC- gastrocnemius. Scale Bar- 1 mm

The Achilles tendon is covered by a thin layer of fascial covering which is commonly termed the paratenon. Fascial extensions are seen passing from the skin to the paratenon. The paratenon is continuous anteriorly with a fascial sleeve, commonly termed the mesotenon where blood vessels could be visualised with the naked eye. Individual components of the tendon (soleus and gastrocnemius) can be stripped separately as they each have their own fascial sheath.

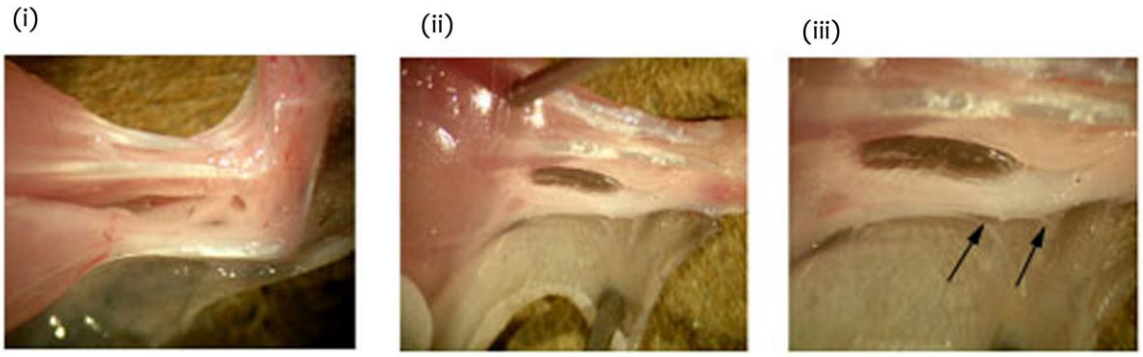

Figure 3.3 - Fascial extensions of the Achilles tendon sheath showing gradual separation of the skin from the tendon (i) and (ii) and thin fascial extensions(iii) (Black arrow) passing from the skin into the tendon sheath /paratenon

3.1.2 Microscopic anatomy

Transverse and longitudinal sections of the decalcified leg showed the relationship of Achilles tendon to other structures in the leg. The tendon is seen to be formed by the union of two separate tendons of soleus and gastrocnemius (Figure 3.4 and Figure 3.5). It flattens out to insert into the calcaneum. The thin plantaris tendon is seen passing into the foot and continuing into the plantar fascia. Three dimensional reconstruction of the mouse leg was done using H&E stained serial sections. The reconstruction shows the relationship of the Achilles tendon to its surrounding structures (Figure 3.4).

Hoechst and TRIT-C Phalloidin stain demonstrated the parallel distribution of cells along the long axis of the tendon (Figure 3.6). Alcian blue staining did not reveal any areas of fibrocartilage in the main body of the tendon but showed increased blue hue and rounded cells at the enthesis region adjacent to calcaneal insertion (Figure 3.7). There was also an increase in proteoglycan content at the region where soleus and gastrocnemius tendons join to form the Achilles Tendon(Figure 3.9). The collagenous and elastic component of Achilles tendon was demonstrated by Masson's Trichrome stain (Figure 3.10) and Miller's Elastin stain resepectively (Figure 3.11).

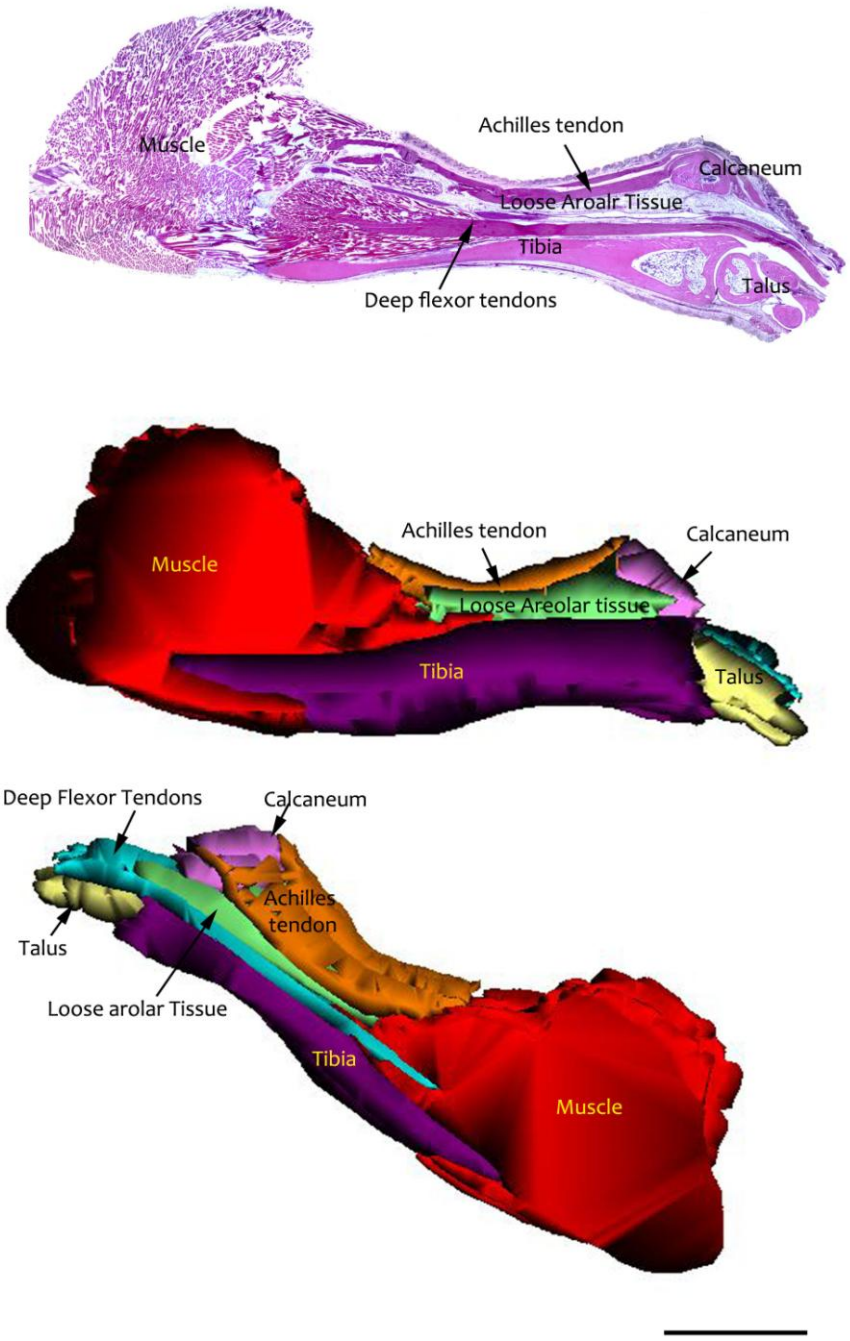

Figure 3.4 -Three dimensional reconstruction of the posterior compartment of mouse leg using H&E stained serial section showing relative relationship of structures. Scale Bar 1mm

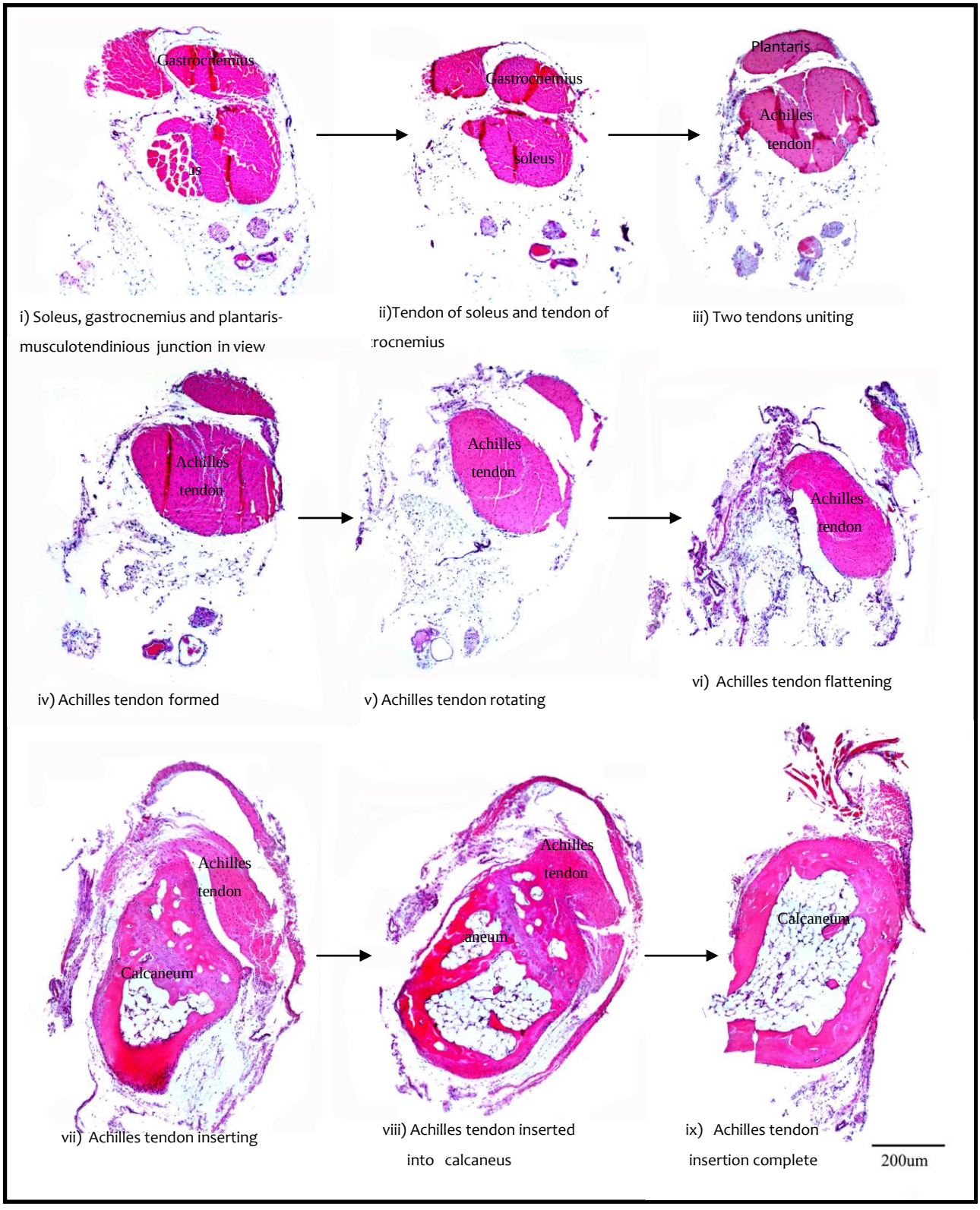

Figure 3.5 - Histological study of Achilles tendon in serial cross section from proximal to distal (stained with H&E) showing formation, rotation and insertion of the tendon

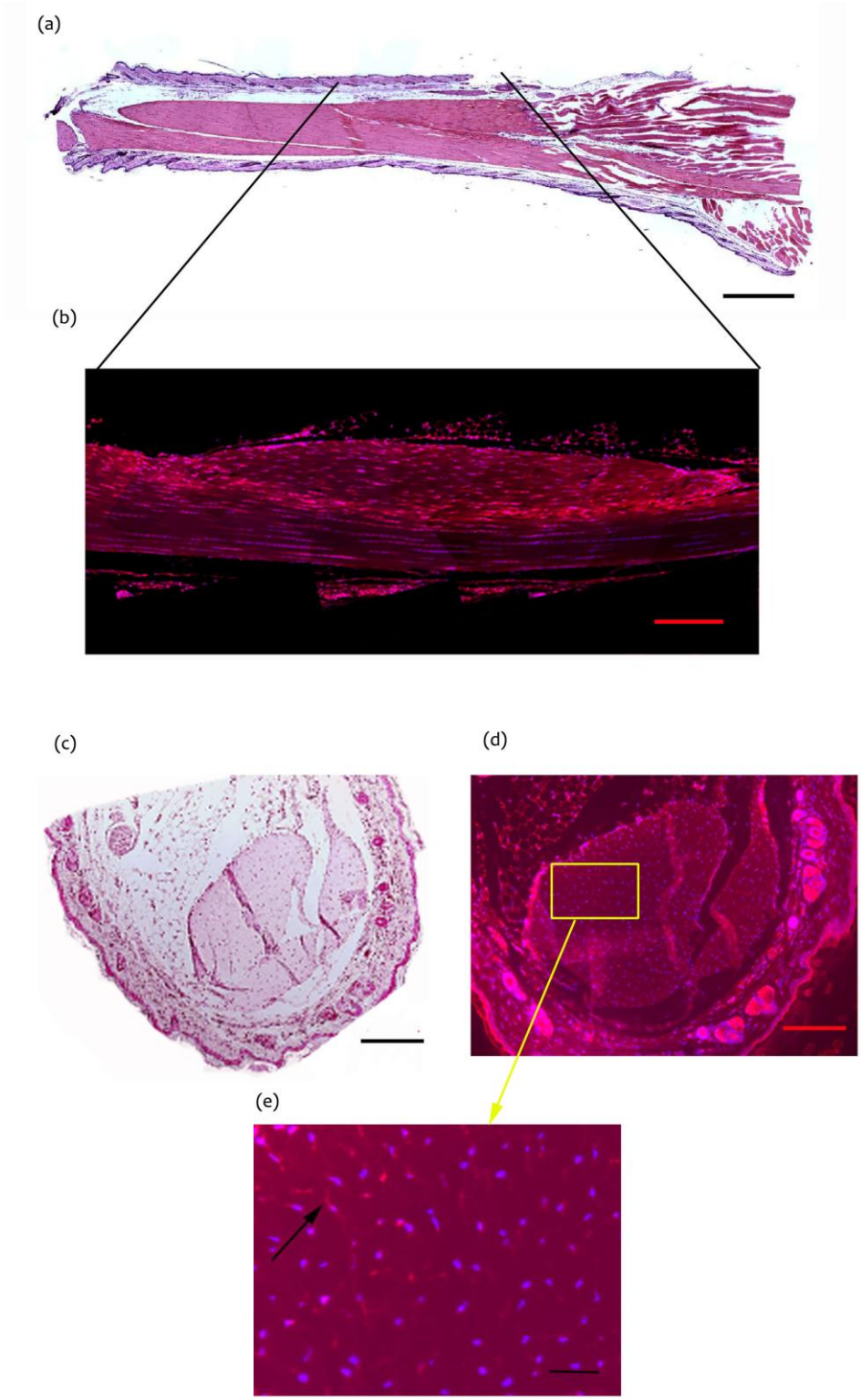

Figure 3.6 - (a) and (b) Longitudinal Section of filleted Achilles tendon , (a) H&E stain ; (b) Hoechst and TRITC Phalloidin stain showing Cellular arrangement in parallel rows and. Magnification x5; ScaleBar- 500 µm

(c-e) Cross section of the Achilles tendon showing intercellular cytoplasmic projections,(c) H&E and(d) and (e) Hoechst and TRITC Phalloidin stain on the right, (c) and (d) Magnification x5 ; Scale Bar-200 µm, (e) Magnification x10; scale bar- 50 µm

Alcian blue staining showed that the fascial envelope is high in proteoglycans and has a loose areolar distribution (Figure 3.8). An increase in proetoglycans at the region of union of soleus and gastrocnemius was seen and this could be demonstrated both in longitudinal and cross sections of the tendon. The tendon proper shows no obvious areas of fibrocartilaginous zones. Cellular morphology changed from oval to rhomboid as the tendon approached the bony insertion (Figure 3.7).

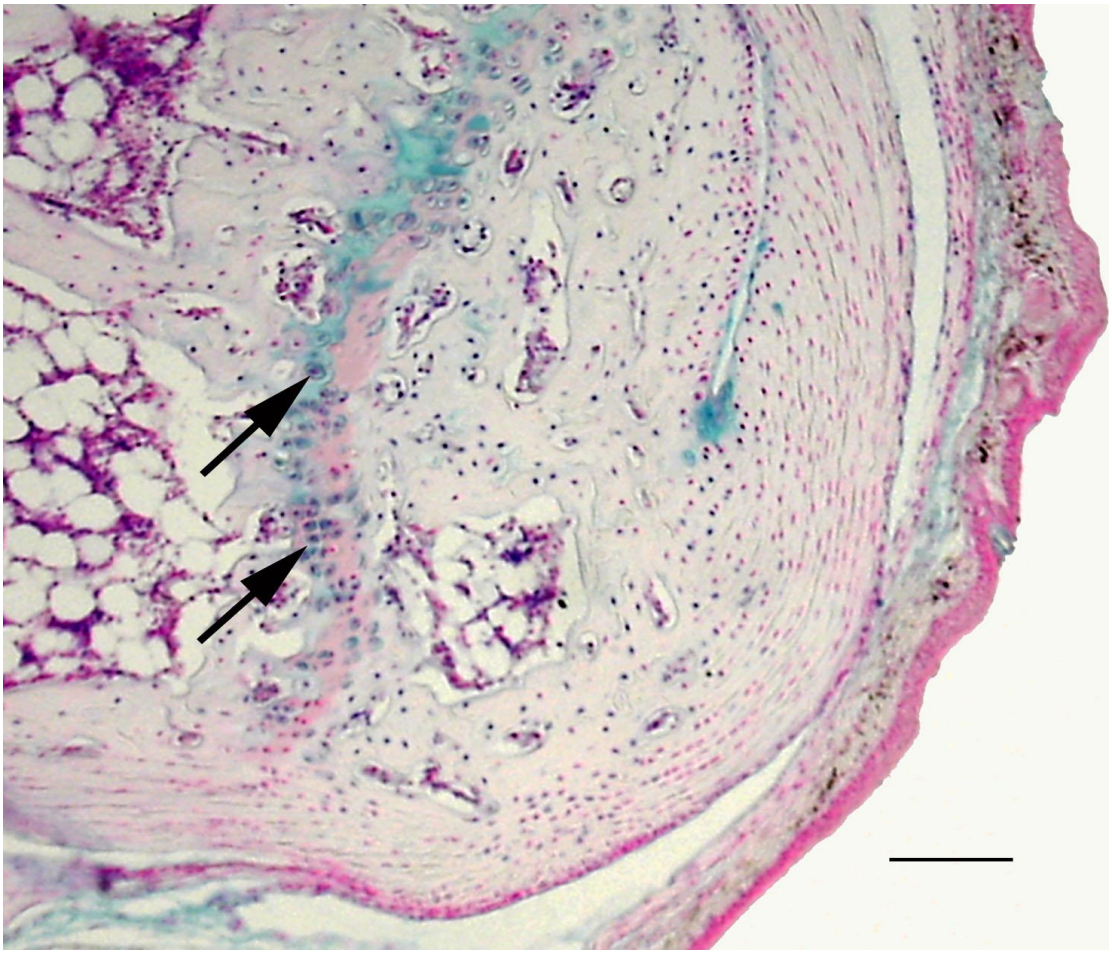

Figure 3.7- Longitudinal Section of the enthesis region showing change in cell morphology from elongated to rounded with cells of fibrocartilage staining blue x10 (Alcian blue stain), Fibrocartilage shown with Black Arrow, Magnification x 10 ; Scale Bar-500µm

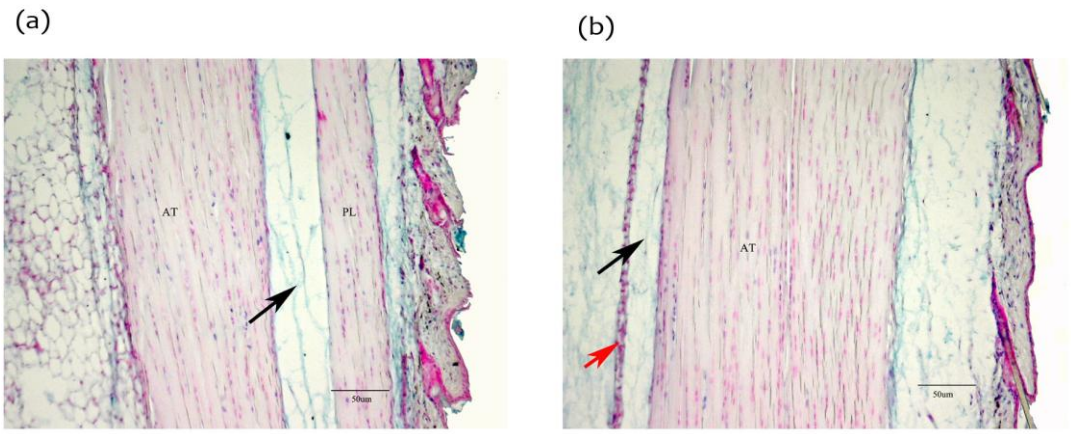

Figure 3.8 - The gliding fascia around Achilles tendon. Black arrow in (a) denotes fascial layer between Achilles tendon and plantaris. (b) Black arrow indicates space between Achilles tendon and paratenon and Red arrow indicates paratenon, Magnification -x5 - alcian blue stain

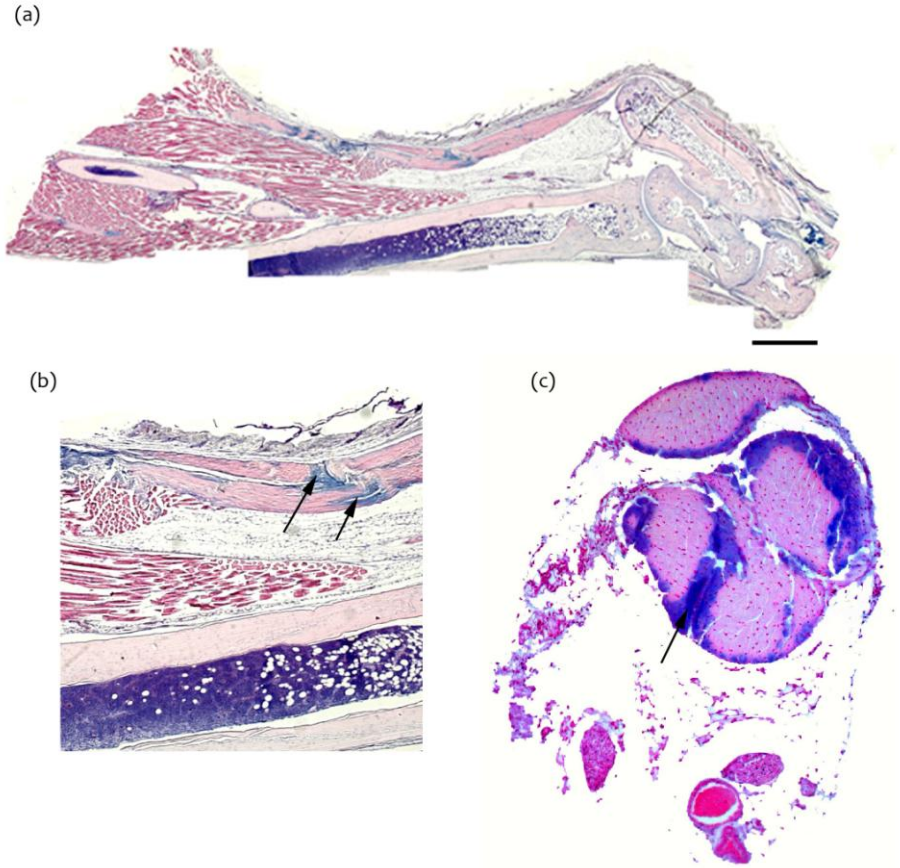

Figure 3.9 - Alcian blue staining showing increase bluish hue where the soleus and the gastrocnemius tendons join together to form the Achilles tendon (Black arrow). This is demonstrated both in longitudinal (a and b) and cross sections (c) of the Achilles tendon Magnification x 5; Scale Bar- 500 µm

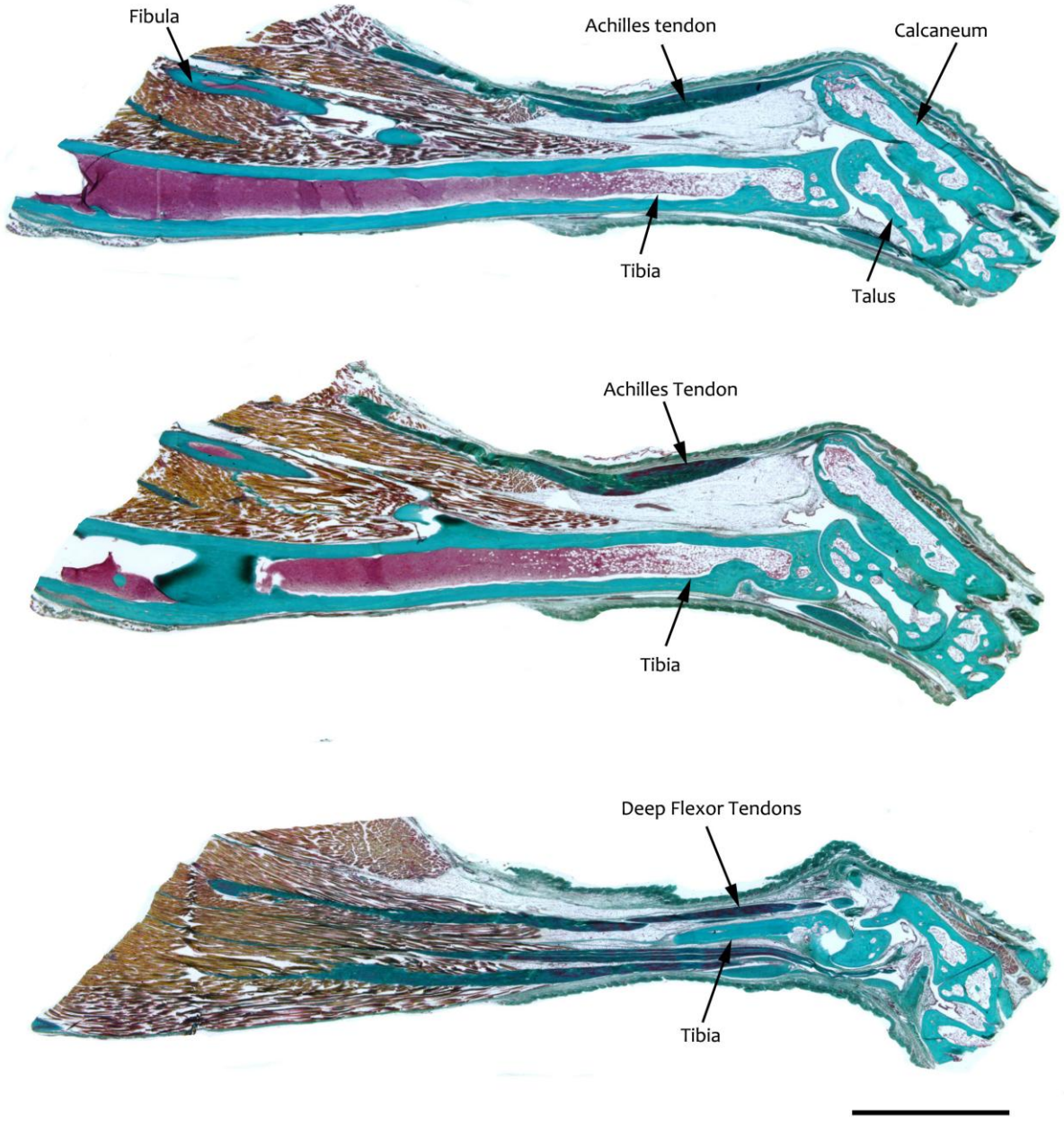

Figure 3.10- Serial longitudinal sections of mouse leg stained with Masson's Trichrome stain showing collagenous content of Achilles tendon. Magnification x 5, Scale Bar- 1 mm

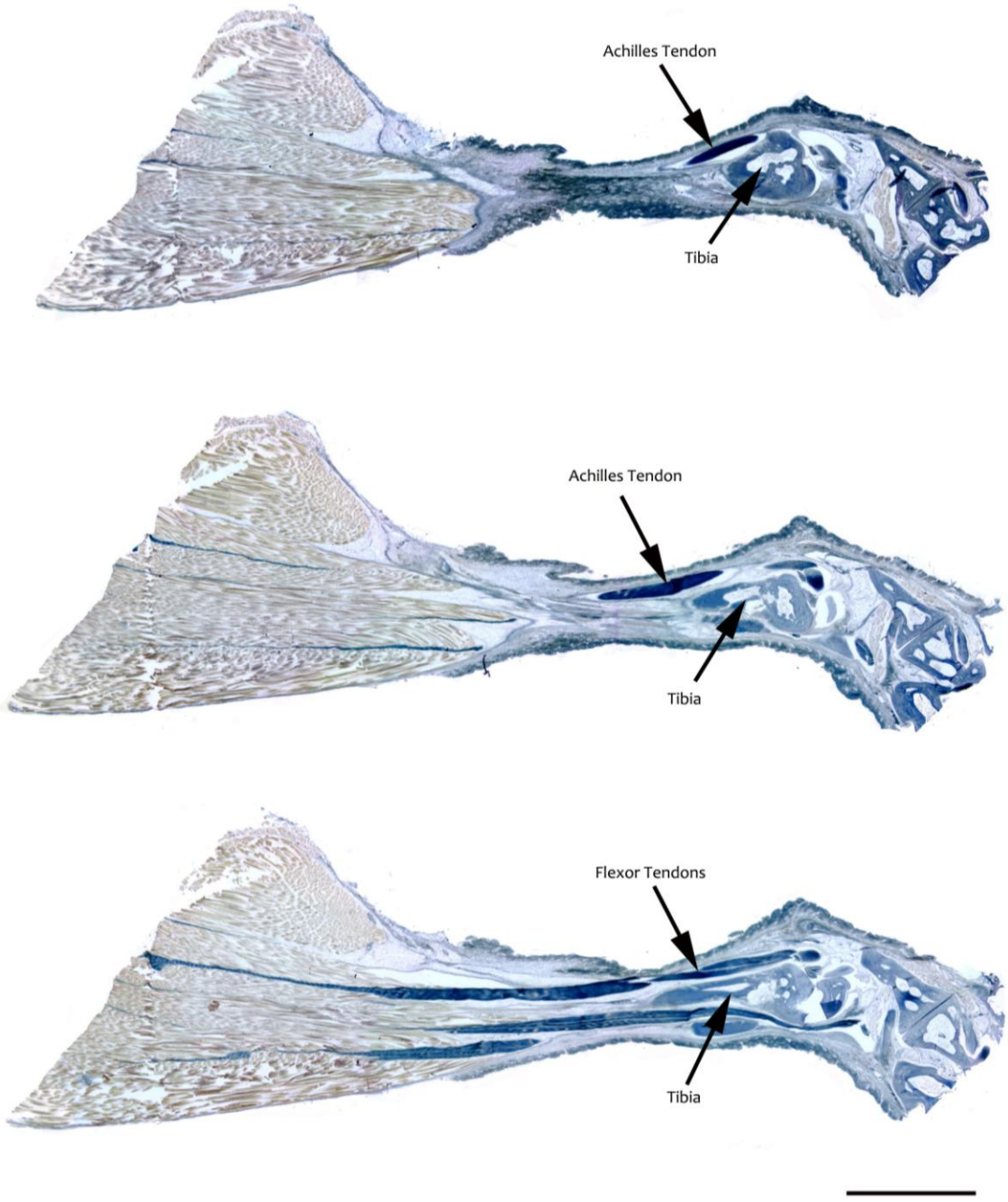

Figure 3.11- Serial sagittal section of the mouse leg (Decalcified sections) stained with Miller's elastin showing the highly elastic nature of the Achilles tendon. Magnification x 5; Scale Bar- 1mmm

3.1.3 Study of vascular architecture with Alpha-SMA immunostaining

Alpha SMA staining showed that the tendon substance was avascular (Figure 3.12 - 3.14). In transverse sections abundant blood vessels were seen in the loose areolar tissue anterior to the tendon. The mesotenon appears to bring the blood vessels to the tendon as demonstrated by serial cross section immunohistochemistry (Figure 3.14). At the musculotendinous junction blood vessels were seen in the connective tissue between soleus and gastrocnemius muscle/tendon. Two sets of vessels were seen on either side of the tendon but only one of these appears to be contributing to the vessels supplying the tendon through the mesotenon (Figure 3.14). Nonlumen related Alpha-SMA staining was found in the epitenon areas of the Achilles tendon (Figure 3.13b).

Figure 3.12 - Longitudinal section of the leg showing large calibre lumen related Alpha-SMA stain in the paratenon proximal to the tendon proper likely to represent the Posterior Tibial vessels Magnification x5 ; Scale Bar 200 µm

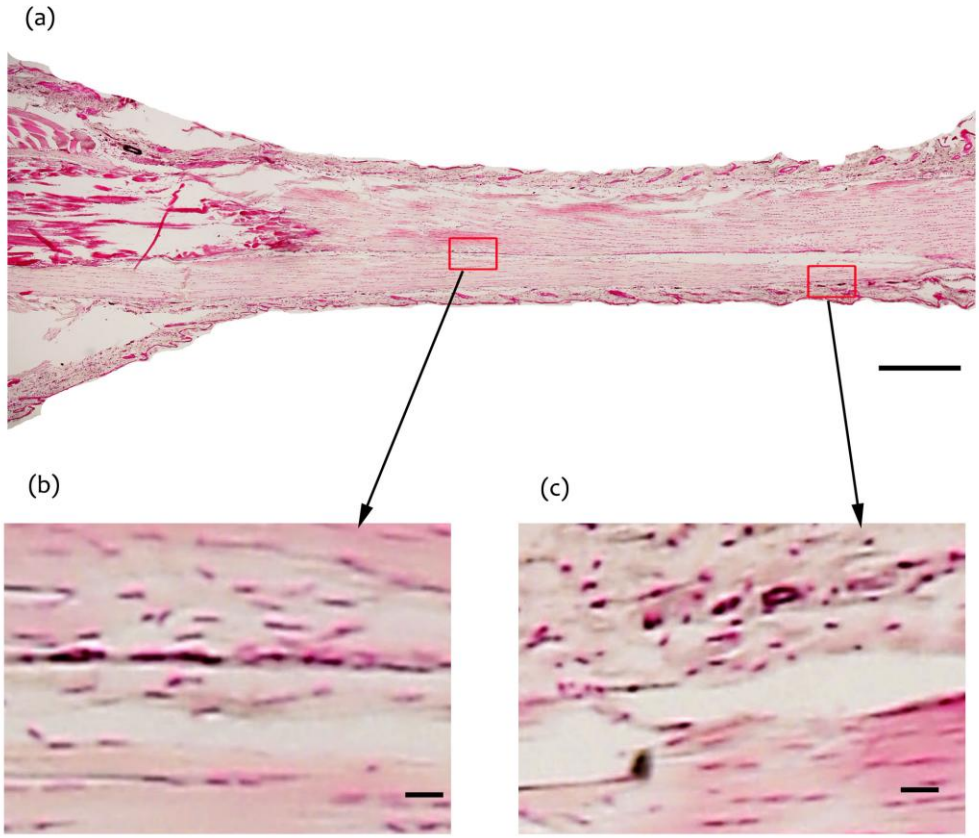

Figure 3.13- Longitudinal section of the Achilles tendon with Alpha SMA Stain showing (b) non-lumen related Alpha- SMA positive cells (Myofibroblasts) in the epitenon and (c) lumen related Alpha- SMA positive cells in the paratenon and skin and; (a) Scale Bar- 500 µm (b) and (c) Scale bar-50 µm

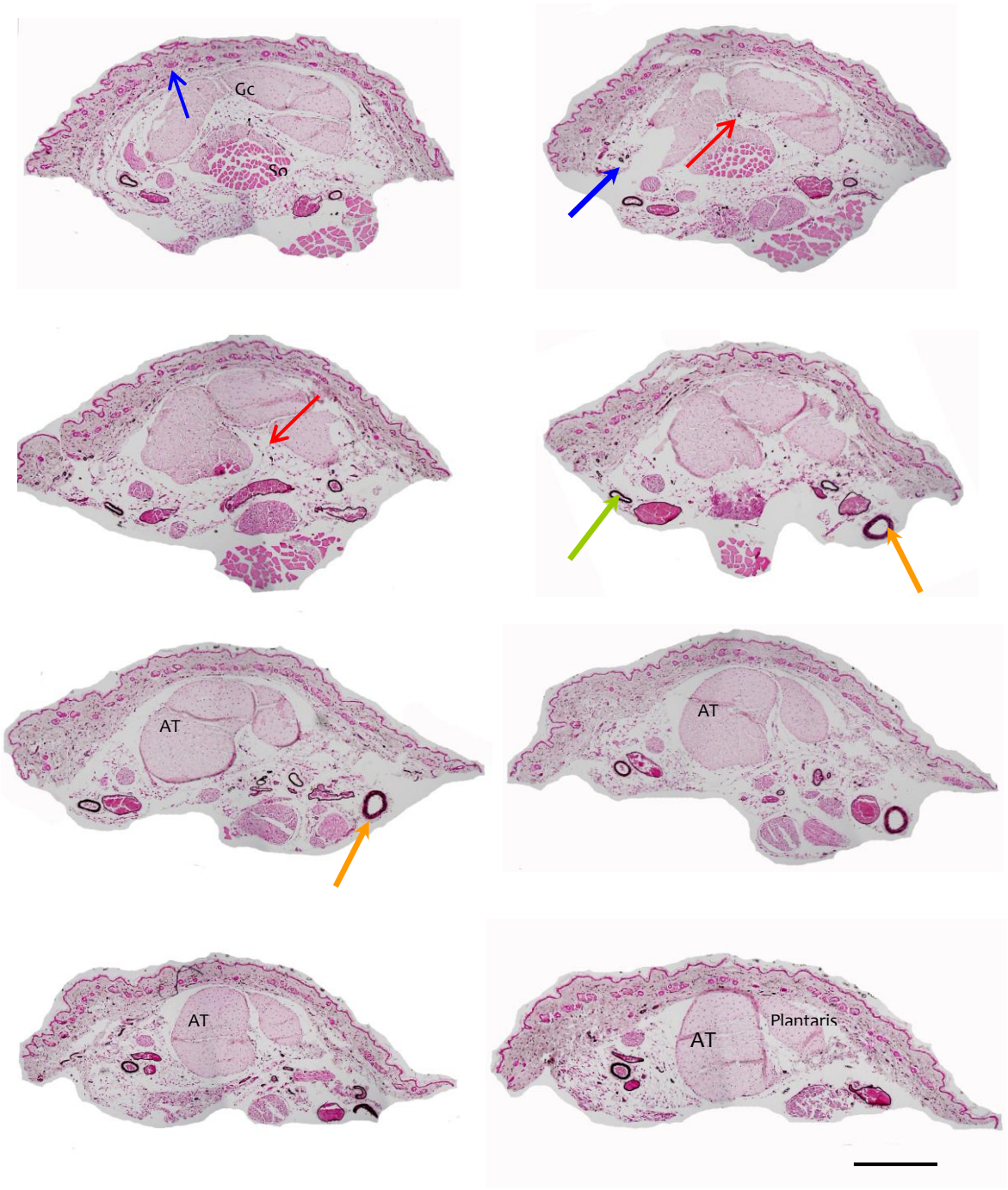

Figure 3.14- Serial transverse section, top left proximal to bottom right distal, of the Mouse Achilles tendon (Filleted off the bone) showing blood vessels present in the loose areolar tissue- anterior(Orange arrow) and lateral (Green arrow)to the Achilles tendon and in the dermis of the skin (Blue arrow). Small blood vessels are also seen in the epitenon and endotenon (red arrow). GC- Gastrocnemius, So-Soleus. Distance between sections shown are 70 um, captured at x5; Scale Bar-500 µm

3.2 Results of tendon grafting studies

3.2.1 Summary

At Day 3 the transgenic tendon graft was intact (GFP staining) and was separated from the main tendon by a fibrin clot. No obvious sign of necrosis was seen. No cellular invasion was apparent. The sheath was hypercellular with predominantly neutrophils (Ly6G staining) and macrophages (F4/80 staining). The recipient tendons also appeared intact showing no cellular invasion from the sheath.

At Day 21 the GFP positive graft continued to express GFP and both graft tendon cells and host tendon cells show marked collagen synthetic activity (Hsp47). By this time sheath hypercellularity had reduced. Staining with apoptotic marker (Tunel) showed a number of apoptotic cells both in the graft and in the host tendon.

At Day 90 the grafts appeared almost completely integrated to host tissue and GFP positive cells were no longer present in the GFP graft. There was a moderate amount of collagen synthetic activity in the tendon and sheath and a number of cells continued to show signs of apoptosis.

Autologous grafts showed similar cellular events with a slightly lower neutrophilic response. Control unwounded tendons showed almost no synthetic or apoptotic activity at any point.

3.2.2 Staining for inflammatory cells- CD45, Ly6G and F4/80

The pattern of the cellular changes following grafting was similar between autografts and syngenic grafts however the amount of cellular activity did differ between certain aspects of the healing process. The pattern of inflammation following grafting showed an intense inflammatory reaction in the subcutaneous tissue at Day 3, followed by an increase in inflammatory cells in the host tendon and grafted tendon at Day 21, which gradually diminished but never quite reached baseline levels in all tissues at Day 90 (Figure 3.15). The initial inflammatory response (Day 3) as measured by CD45 and Ly6G was greater in syngenic grafting subcutaneous tissue when compared with the subcutaneous tissue of autografts (CD45 2075 ±181 vs. 1211 ±81 cells/mm^2 and Ly6G 1587 ±65 vs. 1050 ±52 cells/mm^2) (Figure 3.15- Figure 3.22). However F480 expression was greater in autograft subcutaneous tissue when compared with syngenic subcutaneous tissue (autogenous 1355 ±50 vs. syngenic 1044 ±30 cells/mm^2) at Day 3 (Figure 3.23- Figure 3.26). These findings were shown to be statistically significant ($p < 0.001$).

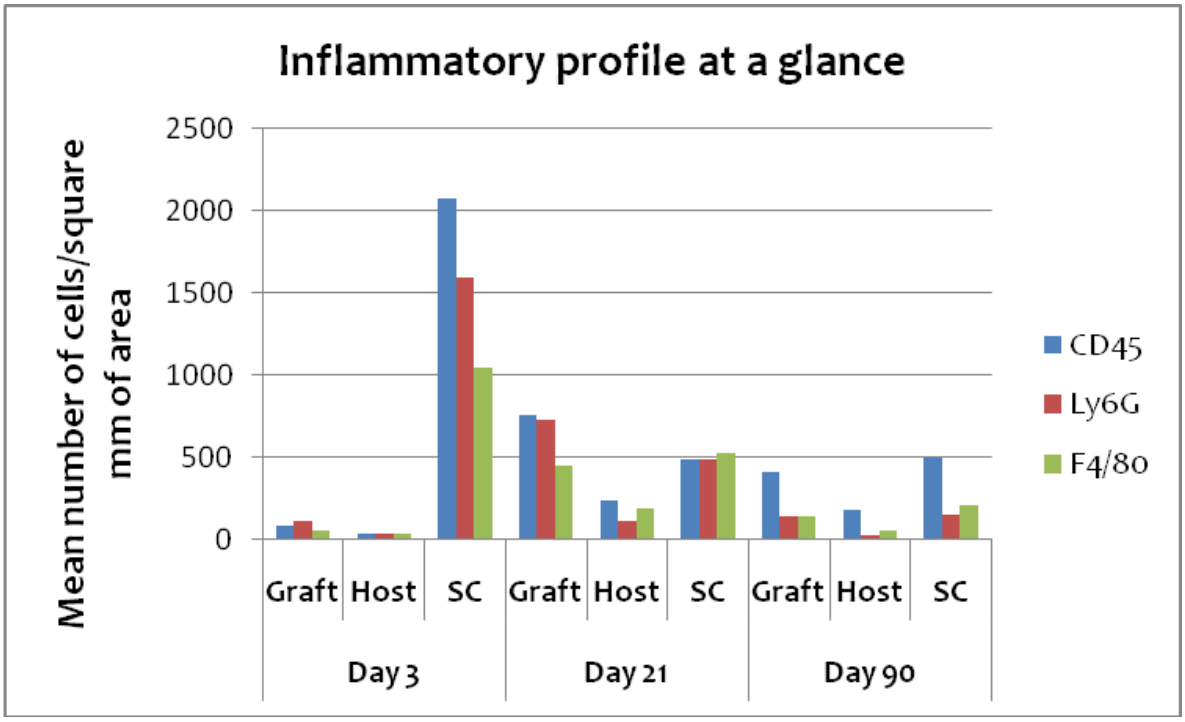

Figure 3.15 - Graphical representation of inflammatory cells in the graft, host tendon and in the subcutaneous tissue at Day 3, Day 21 and Day 90. Inflammation in the tendon lags behind subcutaneous tissue and only reaches similar activity at Day 21.

3.2.2.1 CD45 Staining

Tendon grafting invoked a marked inflammatory response in the subcutaneous tissue surrounding the grafted tendon with a large number of CD45 positive cells found homogeneously distributed in dermis, epidermis and paratenon (1211± 81 in autograft and 2075 ± 181 in syngenic graft). The number of CD45 positive cells in the subcutaneous tissue reduced significantly by Day 21 and only a very small number of these cells were present at Day 90. At Day 3, there were insignificant numbers of CD45 positive cells in both the donor and the host tendons. The small number of cells present in the tendon was found in the epitenon and around the sutures. By Day 21 the core of the tendon graft was invaded by a large number of CD45 positive cells (445 ± 53 in autograft and 757 ± 118 in syngenic graft). The host tendon remained unaffected and only a few cells were found inside it (199 ± 21 in autograft and 238 ± 58 in syngenic graft). At Day 90, the inflammatory influxes were reduced from all areas of the leg but a small number remained in the graft and the paratenon (Table 3.1).

Table 3.1- CD45 Stain- Number of cells/mm^2 and corresponding SEM (n=4 mice/time point, 3 slides/mice)

CD45	Control	Day 3	Day 21	Day 90	Control SEM	Day 3 SEM	Day 21 SEM	Day 90 SEM
Syngenic Tendon Graft	0	83.32	757.81	406.25	0	21.35	118.31	53.90
Syngenic Host Tendon	21.87	36.40	238.28	180.98	7.95	9.48	58.28	34.68
Syngenic Subcutaneous tissue	206.25	2075	489.53	496.09	42.33	181.87	40.78	79.06
Autograft Tendon Graft	0	45.45	445.31	281.25	0	13.71	53.06	47.21
Autograft Host Tendon	21.87	62.5	199.21	209.63	7.96	14.73	21.93	29.93
Autograft Subcutaneous tissue	206.25	1211.56	407.55	253.90	42.32	81.06	44.5	27.53

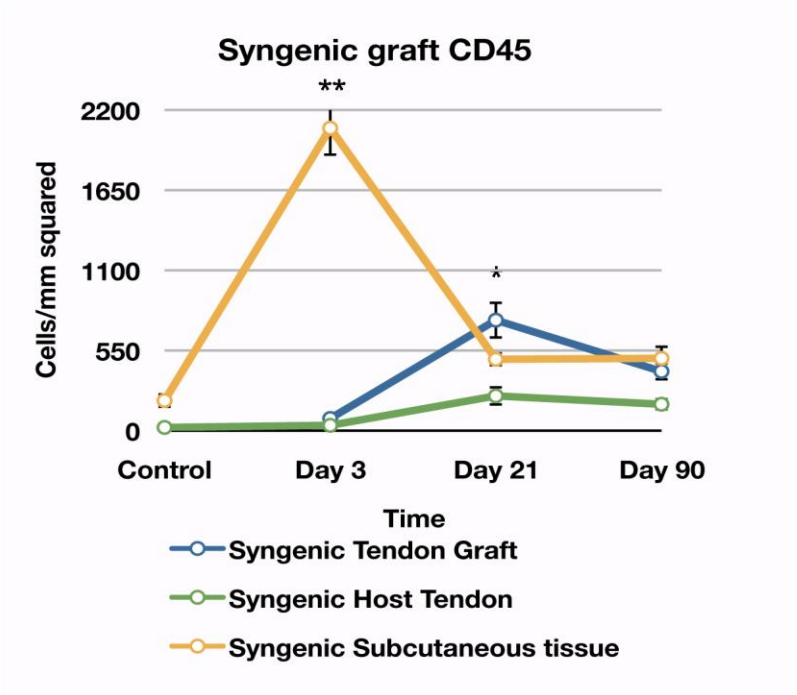

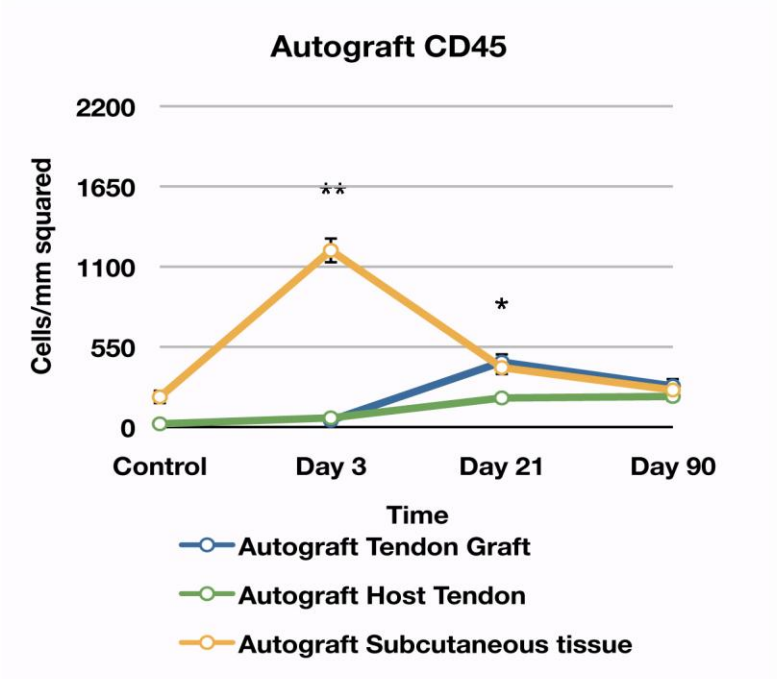

Figure 3.16 -Graphical Representation of the Chronological events after syngenic and autologous Tendon grafting- CD45 Stain for panleukocytes. The initial inflammatory response (Day 3) as measured by CD45 was greater in syngenic grafting subcutaneous tissue when compared with the subcutaneous tissue of autografts (CD45 2075 ±181 vs 1211 ±81 cells/mm2). Significance recorded with ***** in the graph if p-value was less than 0.05 and ****** if p was less than 0.001.

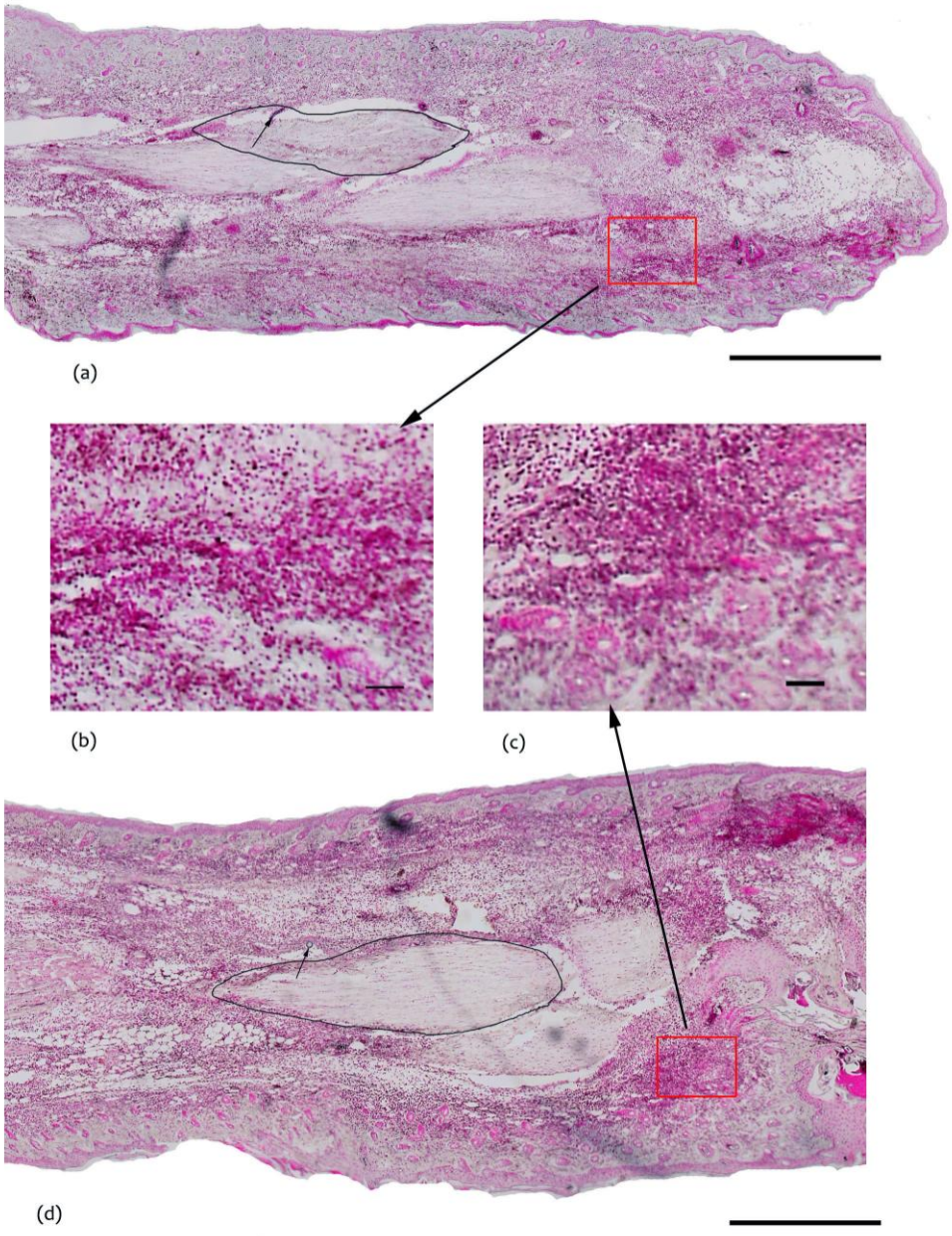

Figure 3.17 - Sagittal section of (a) Syngenic and (d) Autologous grafting at Day 3 showing staining for leukocytes with CD45 Magnification x5; Bar-500 µm. (b) and (c) Subcutaneous tissue in both grafts show massive influx of CD45 positive cells; Magnification x 10; Bar-100 µm

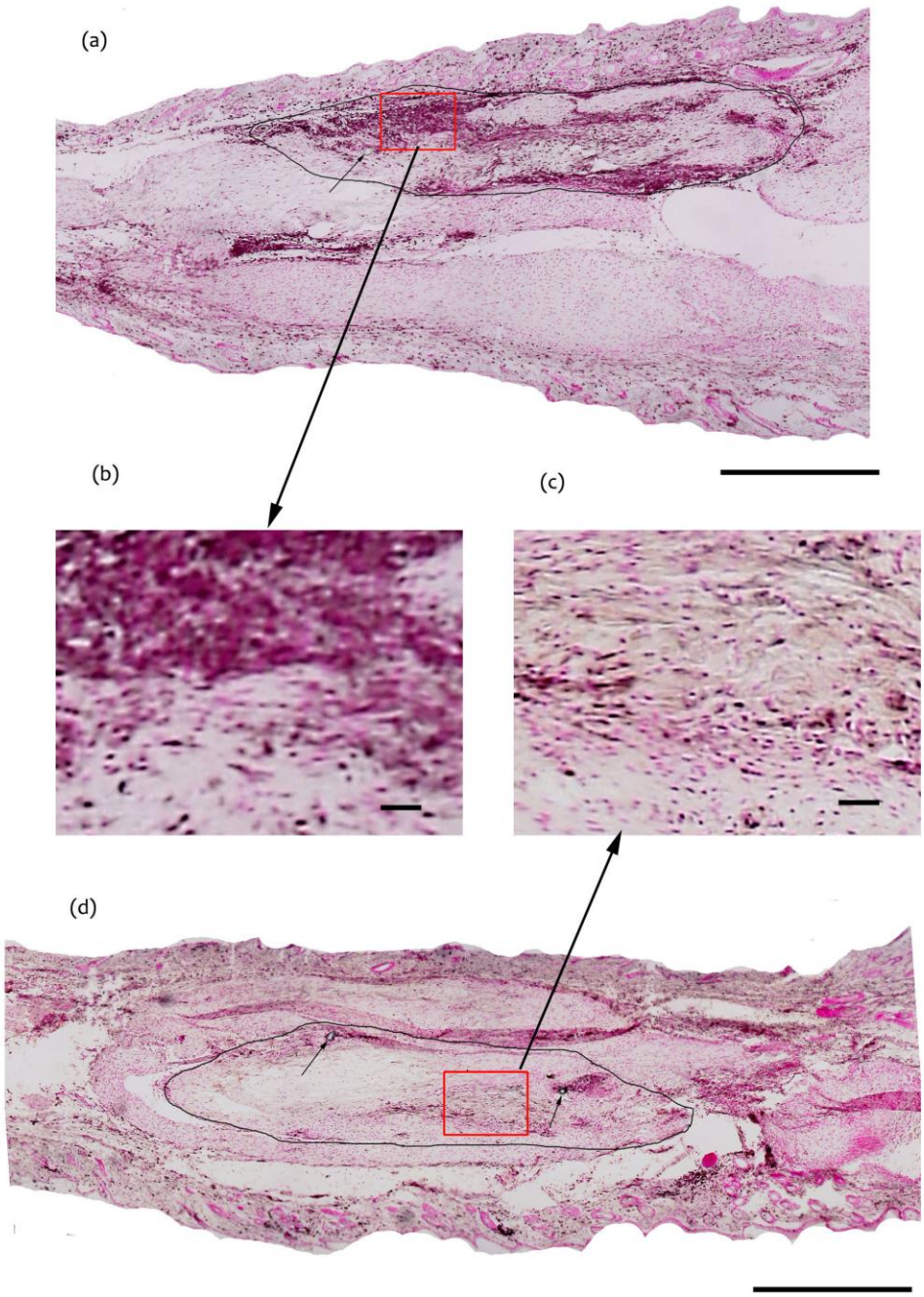

Figure 3.18- Sagittal section of (a) Syngenic and (d) Autologous grafting at Day 21 showing staining for leukocytes with CD45. Magnification x5; Bar-500 µm Subcutaneous tissue in both grafts show infiltration of Cd45 positive cells inside the tendon graft in (b) Syngenic and (c) Autologus grafts; Magnification x10; Bar-100 µm

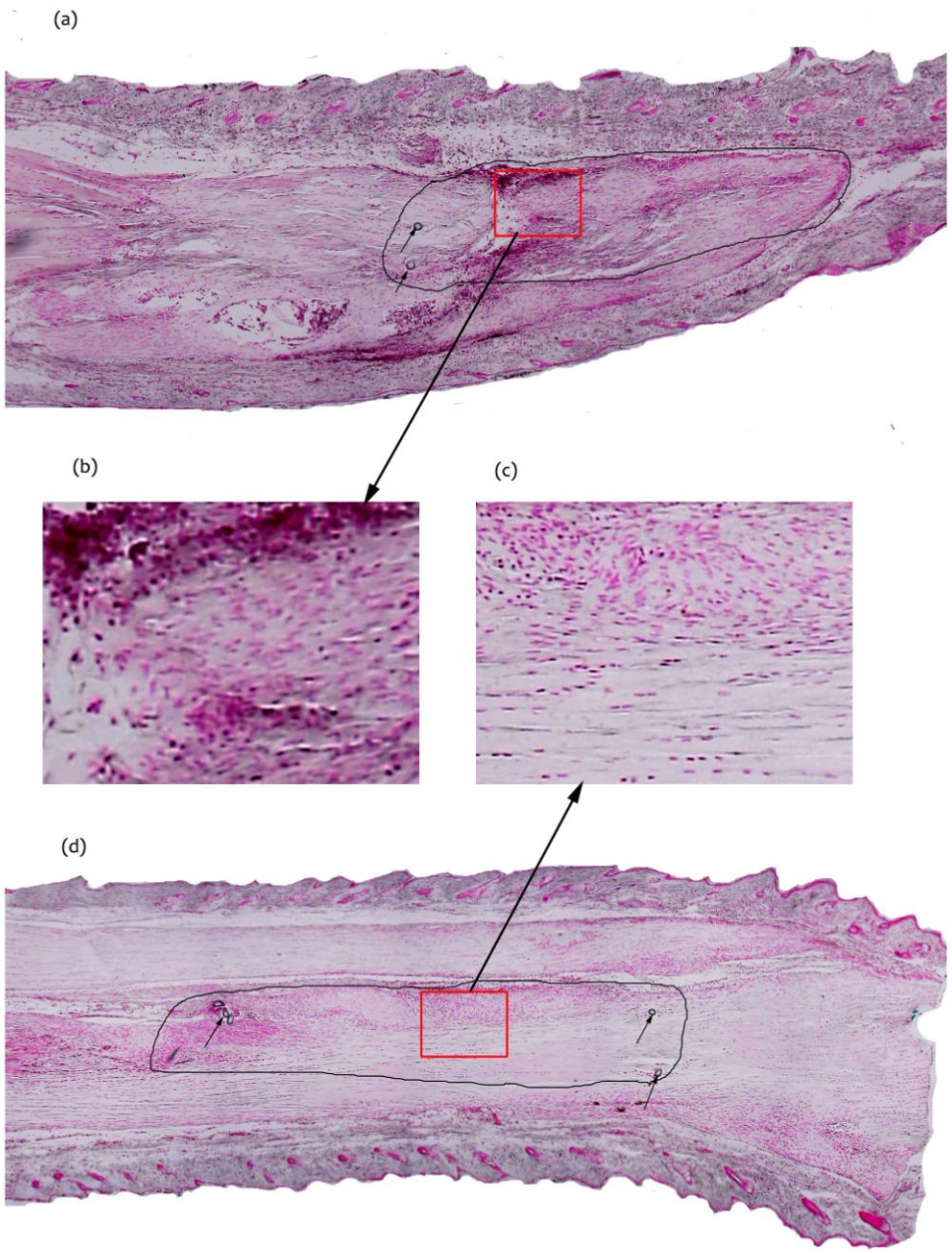

Figure 3.19 - Sagittal section of (a) Syngenic and (d) Autologous grafting at Day 90 showing staining for leukocytes with CD45. Magnification x5; Bar-500 µm Subcutaneous tissue in both grafts show very few Cd45 positive cells; Only a small number of Cd45 cells remained in the(b) syngenic and (c) autologous tendon; Magnification x10; Bar-100 µm

3.2.2.2 Ly6G Staining

At Day 3, many of the cells in the subcutaneous tissue were positive for Ly6G, indicating a significant neutrophilic infiltration (1050 ± 52 in autograft and 1587 ± 64 in syngenic graft) . The number of Ly6 positive cells in the subcutaneous tissue reduced significantly by Day 21 and remained at a similar level of activity at Day 90.

At Day 3, there were very few Ly6G positive cells in both the donor and the host tendon. The majority of the inflammatory cells were seen at the periphery of the tendons near the epitenon. By Day 21, the core of the tendon graft had a significantly large number of Ly6G positive cells (433 ± 37 in autograft and 725 ± 70). The host tendons were not invaded by the neutrophils at any time point and only a few cells were found inside it from Day 3 to Day 90 (Table 3.2).

Table 3.2- Ly6G Stain- Number of cells/mm^2 and corresponding SEM (n=4, 3 slides/mice)

Ly6G	Control	Day 3	Day 21	Day 90	Control SEM	Day 3 SEM	Day 21 SEM	Day 90 SEM
Syngenic Tendon Graft	0.00	110.68	725.16	136.72	0.00	29.56	70.47	23.72
Syngenic Host Tendon	15.63	35.16	109.38	28.59	4.94	18.55	26.41	10.68
Syngenic Subcutaneous tissue	131.25	1587.19	489.53	153.64	25.48	64.80	31.74	27.26
Autograft Tendon Graft	0.00	39.06	433.59	225.16	0.00	8.92	37.19	35.47
Autograft Host Tendon	15.63	27.34	285.16	208.28	4.94	8.63	39.69	21.78
Autograft Subcutaneous tissue	131.25	1050.78	486.97	404.84	25.47	52.14	27.11	35.16

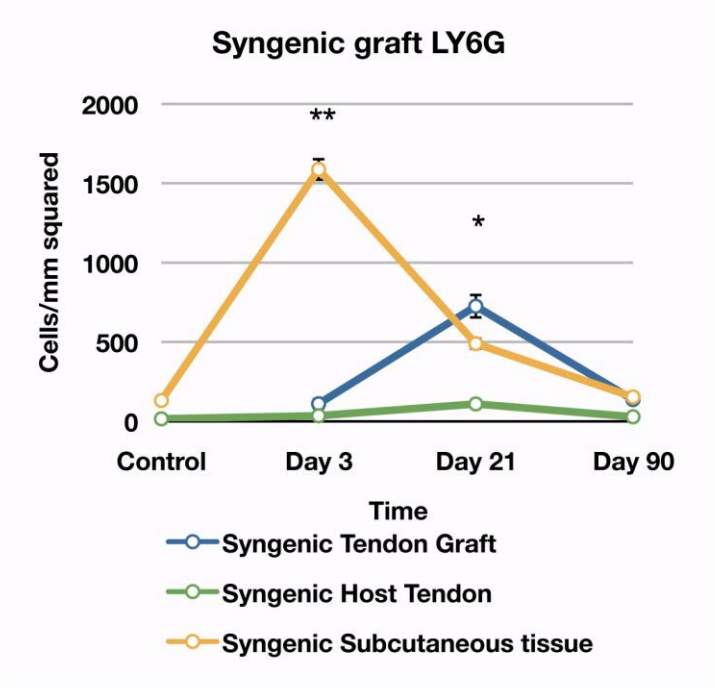

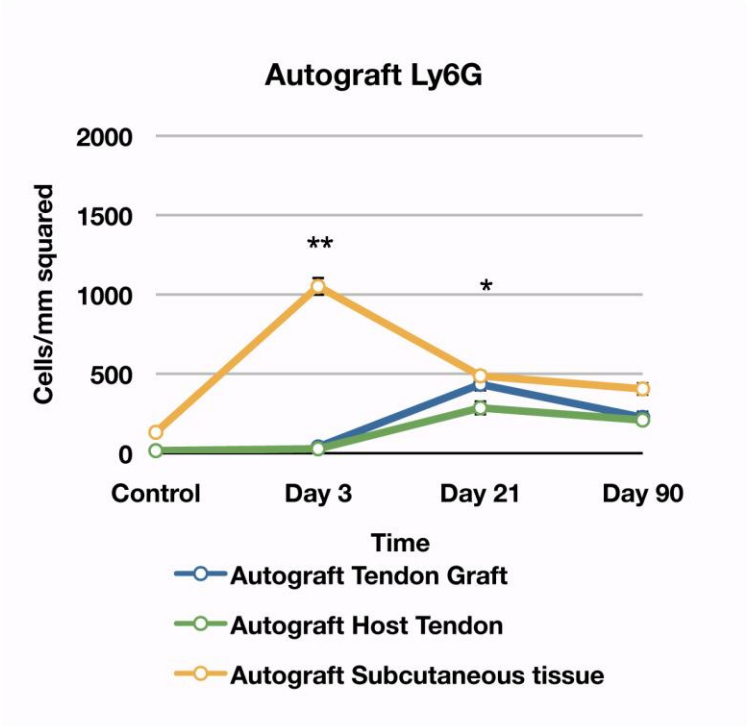

Figure 3.20- Graphical representations of chronological events after syngenic and autologus grafting with Ly6G stain. The initial inflammatory response (Day 3) as measured by Ly6G was greater in syngenic grafting subcutaneous tissue when compared with the subcutaneous tissue of autografts (1587 ±65 vs 1050 ±52 cells/mm2). Significance recorded with * in the graph if p-value was less than 0.05 and ** if p was less than 0.001.

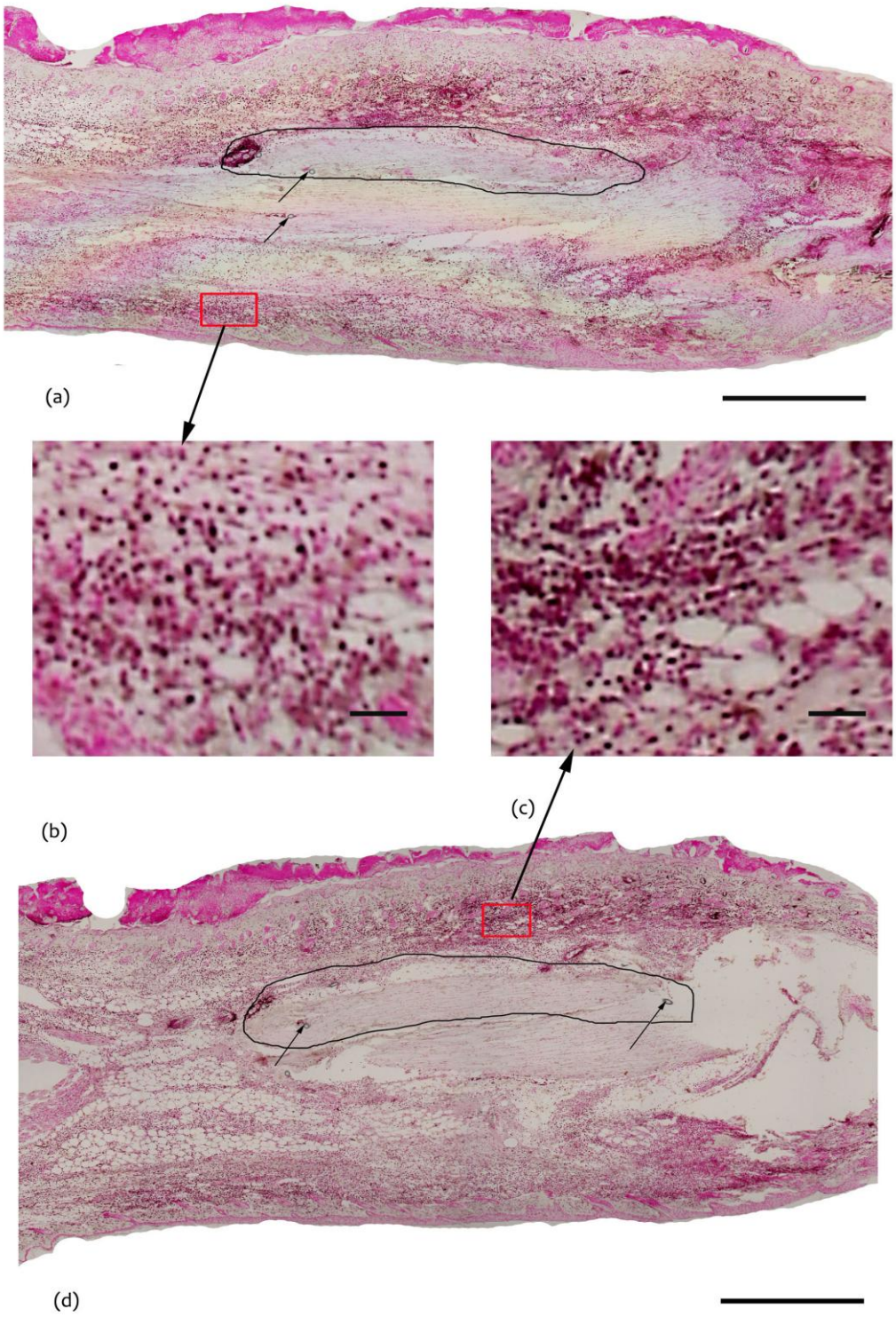

Figure 3.21 -Sagittal section of (a) Syngenic and (d) Autologous grafting at Day 3 showing staining for neutrophils with Ly6G. Magnification x5; Bar-500 µm Subcutaneous tissue show large number of Ly6G positive cells in both (b) syngenic and (c) autologous tendon; Magnification x10; Bar-100 µm

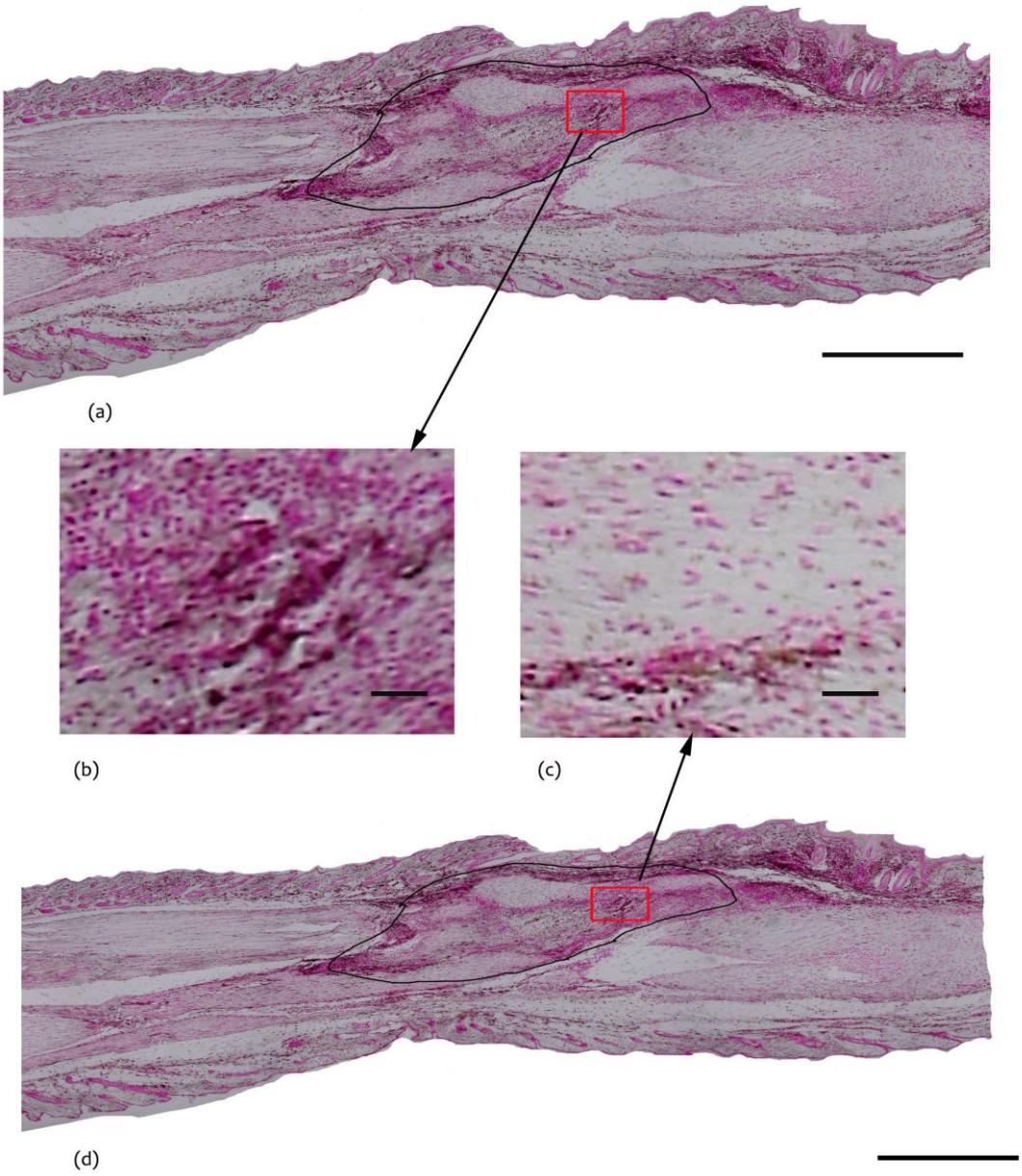

Figure 3.22 - Sagittal section of (a) Syngenic and (d) Autologous grafting at Day 21 showing staining for neutrophils with Ly6G. Magnification x5; Bar-500 µm. Grafts show infiltration with Ly6G positive cells both in the(b) syngenic and (c) autologous tendon; Magnification x10; Bar-100 µm

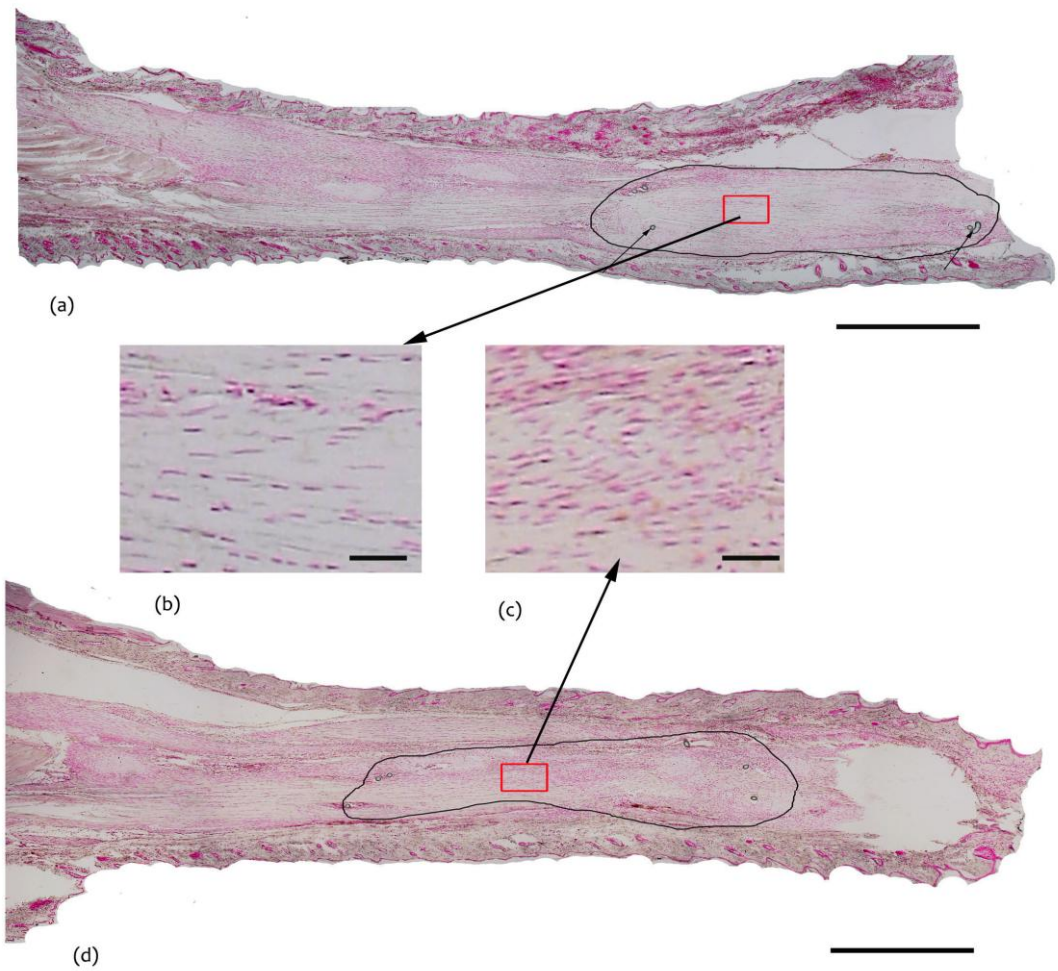

Figure 3.23 -Sagittal section of (a) Syngenic and (d) Autologous grafting at Day 90 showing staining for neutrophils with Ly6G. Magnification x5; Bar-500 µm Subcutaneous tissue in both grafts show very few Ly6G positive cells; Only a small number of Ly6G positive cells remained in the(b) syngenic and (c) autologous tendon; Magnification x10; Bar-100 µm

3.2.2.3 F4/80 Staining

At day 3, the subcutaneous tissue was hyper cellular and the presence of large numbers of F4/80 positive cells was indicative of accumulation of macrophages in this area (1355 ± 50 in autograft and 1044 ± 29 in syngenic graft). The number of F4/80 positive cells in the subcutaneous tissue reduced gradually by Day 21 and remained higher than normal at day 90.

At Day 3, there were very few F4/80 positive cells in both the donor and the host tendon. By Day 21 the core of the tendon graft was highly cellular with whirling patterns of cells, many of which were positive forF4/80 (385 ± 42 in autograft and 445 ± 40 in syngenic graft). The host tendon also showed a small rise in the numbers of macrophages at Day 21. At Day 90, macrophages had reduced from all areas of the leg but a small number remained in the graft and the paratenon (Table 3.3).

Table 3.3- F4/80 Stain- Number of cells/mm^2 and corresponding SEM (n=4 mice/time point, 3 slides/mice)

F480	Control	Day 3	Day 21	Day 90	Control SEM	Day 3 SEM	Day 21 SEM	Day 90 SEM
Syngenic Tendon Graft	0.00	57.30	445.31	143.13	0.00	15.30	40.22	23.69
Syngenic Host Tendon	28.13	31.25	190.10	52.08	14.31	12.16	44.38	14.81
Syngenic Subcutaneous tissue	193.75	1044.22	523.44	207.03	13.62	29.97	62.66	29.53
Autograft Tendon Graft	0.00	67.70	385.41	342.44	0.00	12.36	42.89	63.83
Autograft Host Tendon	28.13	55.94	231.72	196.61	14.32	14.19	26.25	27.09
Autograft Subcutaneous tissue	193.75	1355.47	395.78	265.63	13.62	50.00	45.47	30.64

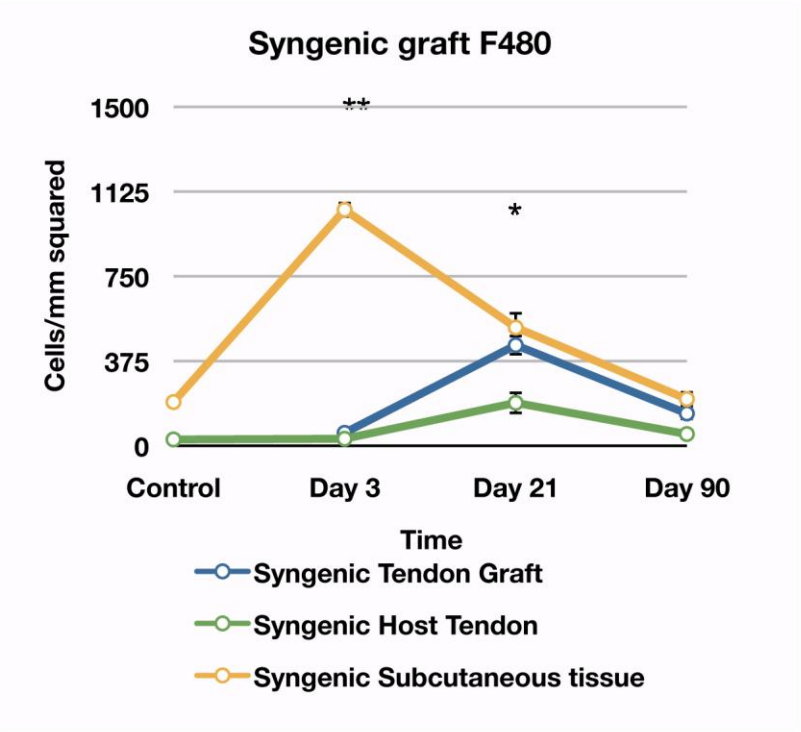

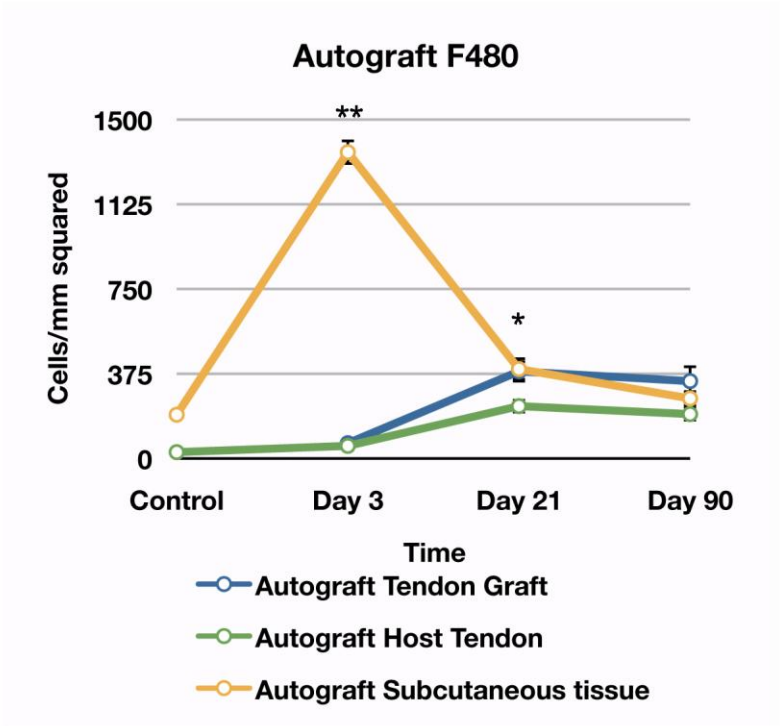

Figure 3.24 - Graphical representations of chronological events after syngenic and autologus grafting with F4/80 stain. Significance recorded with * in the graph if p-value was less than 0.05 and ** if p was less than 0.001.

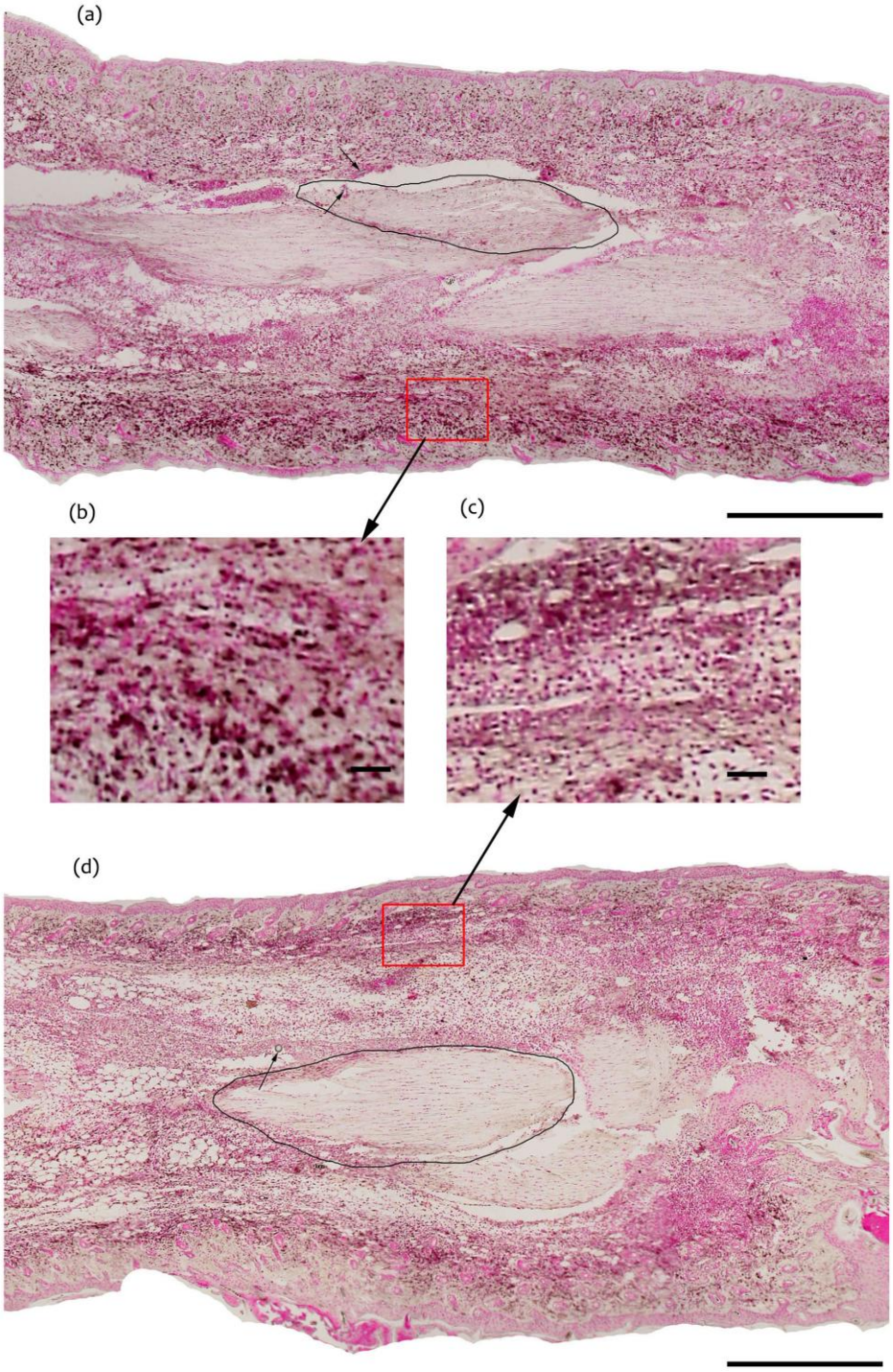

Figure 3.25- Sagittal section of (a) Syngenic and (d) Autologous grafting at Day 3 showing staining for Macrophages with antibody against F4/80. Magnification x5; Bar-500 µm Subcutaneous tissue in both grafts shows huge influx of macrophages in the subcutaneous tissue both in the (b) Syngenic and (c) Autologous grafts; Magnification x10; Bar-100 µm

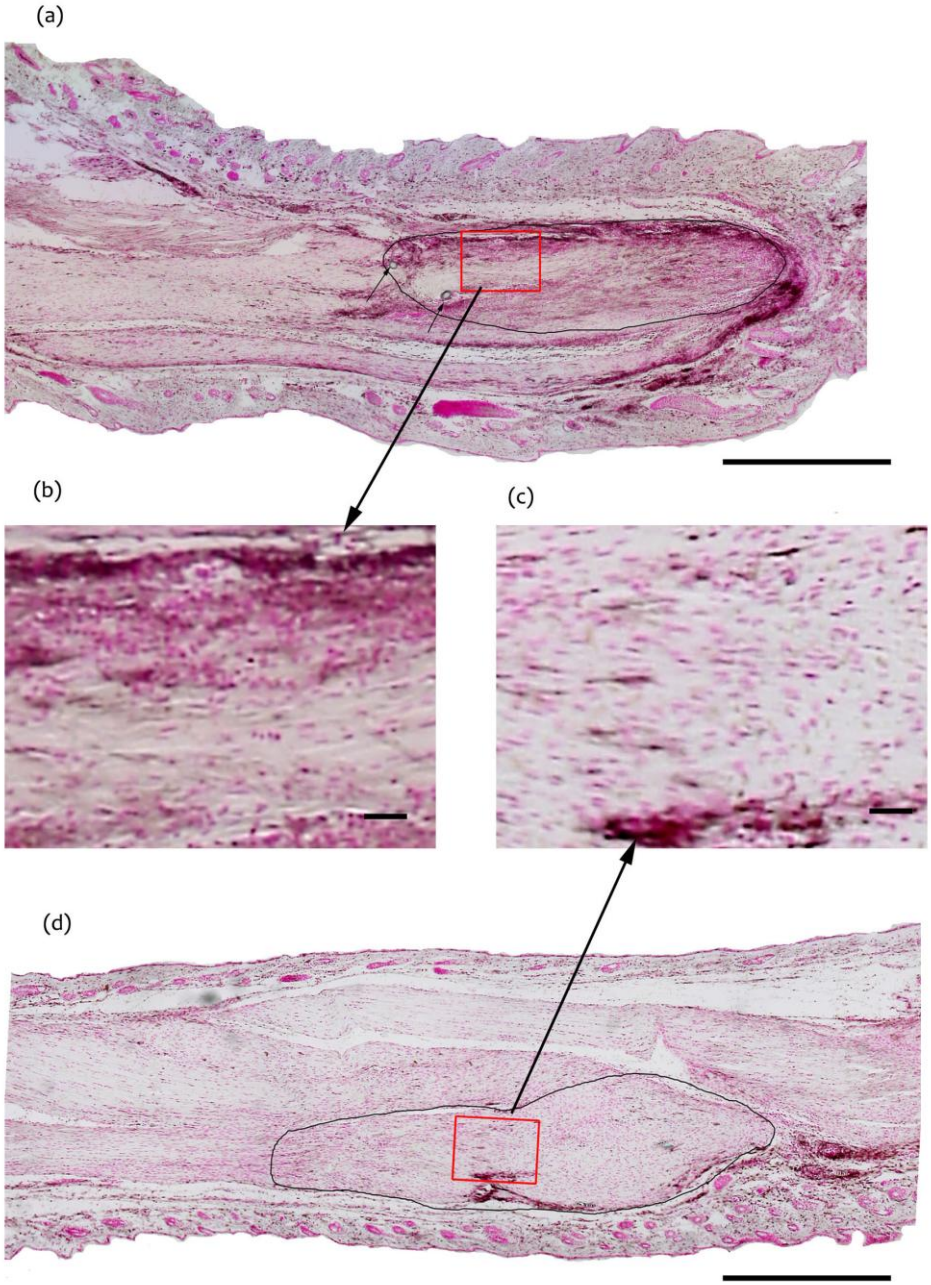

Figure 3.26 - Sagittal section of (a) Syngenic and (d) Autologous grafting at Day 21 showing staining for macrophages with antibody against F4/80. Magnification x5; Bar-500 µm. Both grafts shows infiltration of F4/80 positive cells inside the tendon graft in (b) Syngenic and (c) Autologous grafts; Magnification x10; Bar-100 µm

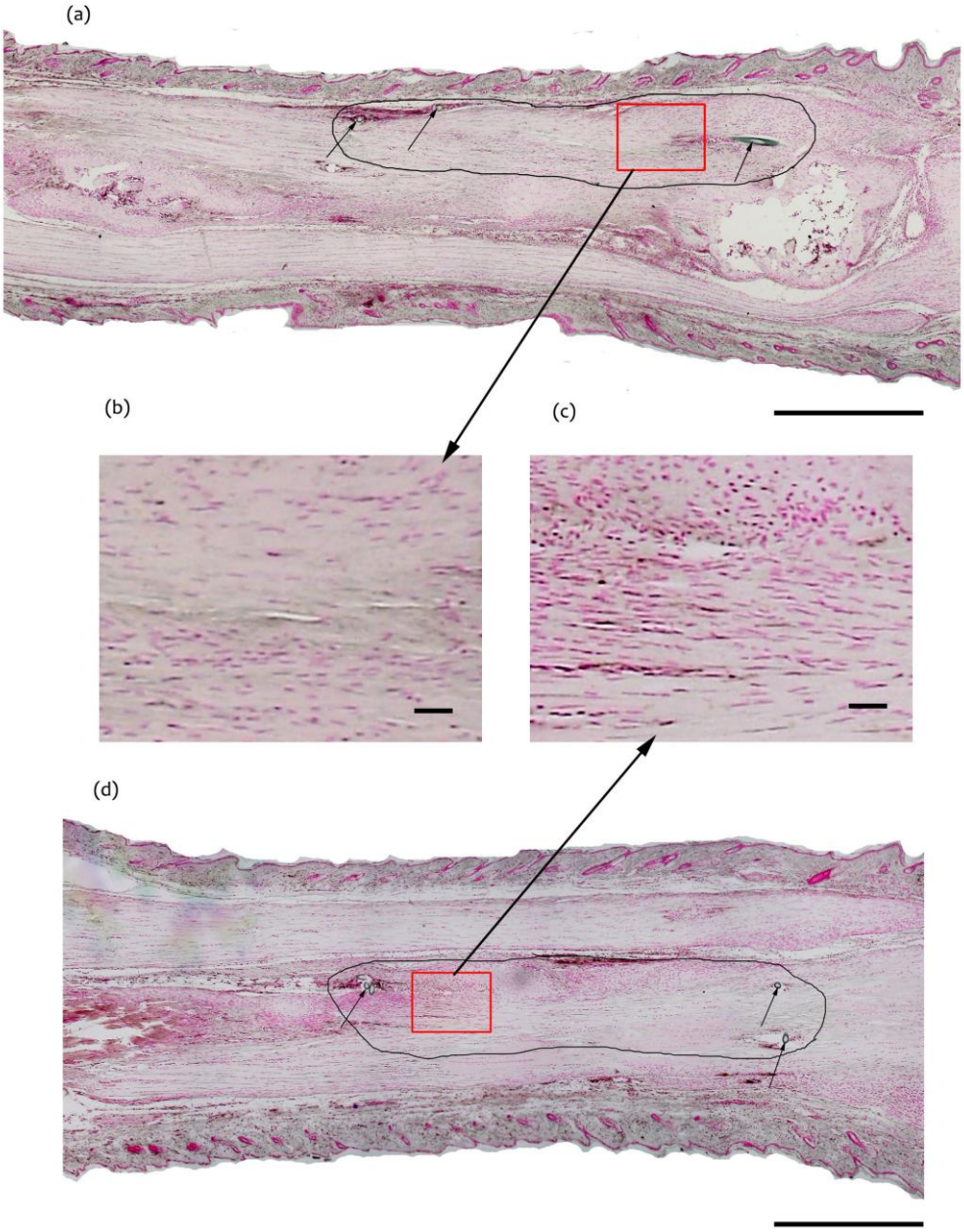

Figure 3.27- Sagittal section of (a) Syngenic and (d) Autologous grafting at Day 90 showing staining for macrophages with F4/80. Magnification x5; Bar-500 µm. Small number of macrophages remain in the tendon of both (b) Syngenic and (c) Autologous grafts; Magnification x10; Bar-100 µm

3.2.3 Cellular repopulation- GFP Immunisation

When GFP tendon was grafted onto a C57 host, the number of GFP increased per unit area due to the GFP labelled cells coalescing (Figure 3.28c and Figure 3.29 a-e). However GFP expression rapidly disappeared by Day 90. At day 3 the cellular architecture of the graft appeared normal and cell nuclei were oval in shape and distributed parallel to the long axis of the tendon. At Day 21, the oval GFP positive tendon cells were surrounded by a huge number of round cells many of which stained positive for CD45 and F4/80 confirming the inflammatory nature of the infiltrate. Though the tendon cells retained their shape, their longitudinal orientation was lost and a whirling pattern was seen. The graft tendon was enveloped in a rim of inflammatory cells which indicated the previous margin of the graft. The actual outline of the graft at day 21 was indistinct. The placement of the suture, the rim of inflammatory tissue, the pattern of distribution of cells and the presence or absence of GFP stains all contributed to the identification of the outline of the graft. At day 90, a few isolated GFP positive cells were present in the area of the graft.

When a graft harvested from C57 mice was placed in the GFP host (Figure 3.28a) or a GFP graft in the GFP mouse was done (Figure 3.28b), at day 3 the GFP stain showed GFP positive cells in the subcutaneous tissue and host tendon and only a small number of GFP positive cells in the non GFP graft. These GFP positive cells were rounded and most likely inflammatory in origin. At day 21, the C57 graft had many GFP positive non tendon cells in the core. At day 90, the outline of the graft could only be demarcated if sutures were viewed.

Table 3.4- GFP Stain- Number of cells/mm² and corresponding SEM (n=4 mice/time point, 3 slides/mice)

	Control	Day 3	Day 21	Day 90	Control SEM	Day 3 SEM	Day 21 SEM	Day 90 SEM
C57 graft on GFP mouse								
C57 Tendon Graft	0.00	23.44	593.75	372.39	0.00	10.47	67.02	99.69
GFP Host Tendon	387.50	466.09	356.77	263.02	29.38	64.84	42.95	77.53
GFP Host Subcutaneous tissue	584.38	653.59	575.47	520.78	37.17	252.66	101.41	110.16
GFP graft on C57 mouse								
GFP Tendon Graft	0.00	963.55	1283.75	111.98	0.00	158.19	203.58	37.92
C57 Host Tendon	0.00	13.02	18.23	0.00	29.39	13.02	18.23	0.00
C57 Host Subcutaneous tissue	0.00	7.81	65.09	7.81	0.00	7.81	42.66	7.81
GFP graft on GFP mouse								
GFP Autograft Tendon Graft	0.00	359.38	593.75	559.84	0.00	39.52	67.02	83.69
GFP Autograft Host Tendon	387.50	401.04	356.72	489.58	29.38	55.47	42.95	55.55
GFP Autograft Subcutaneous tissue	584.38	596.35	575.47	604.17	37.17	252.19	101.41	49.84

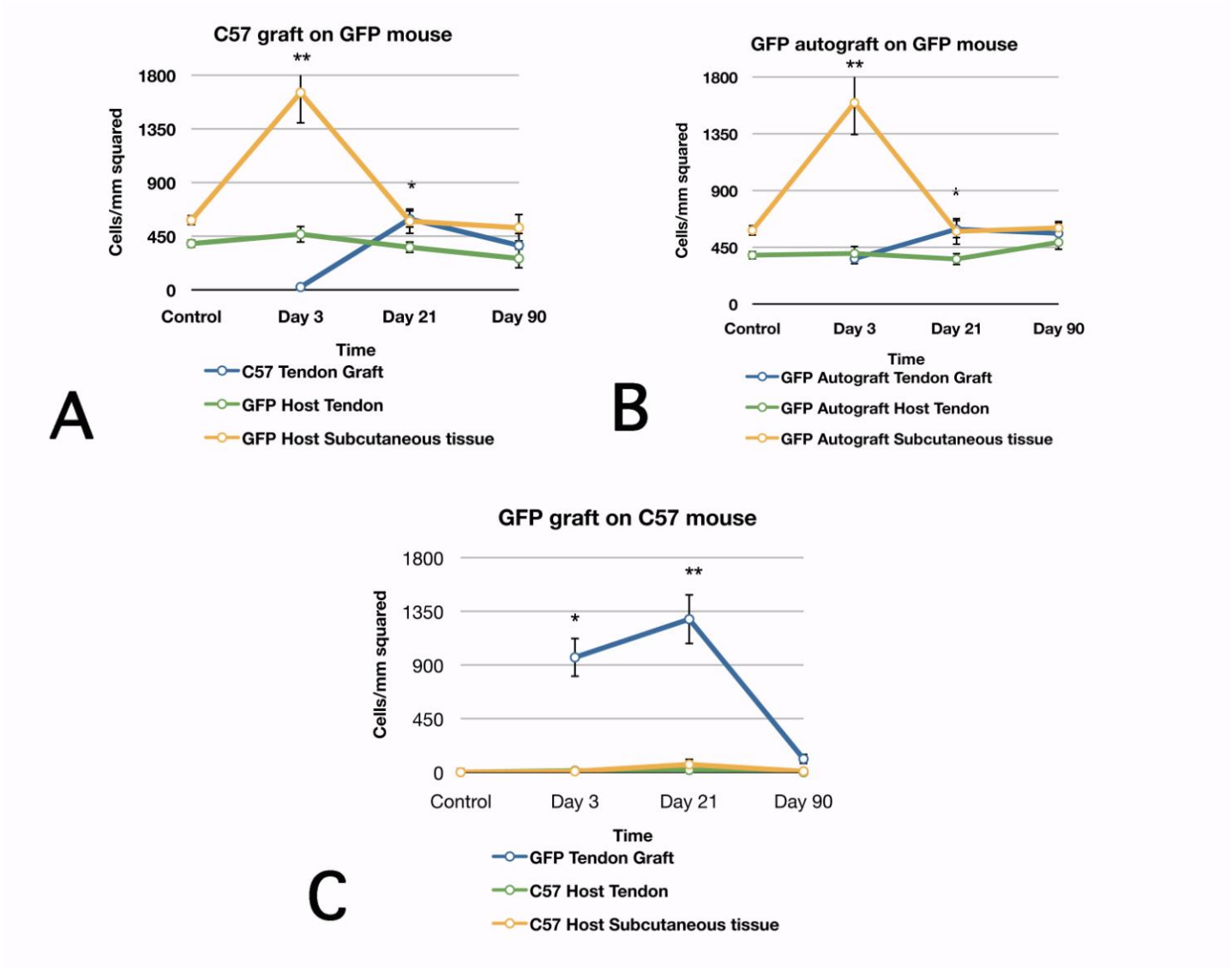

Figure 3.28- Graphical representation of chronological events after syngenic and autologous grafting with GFP stain. In both(A)- C57 graft on GFP mouse and (B)- GFP autograft in GFP mouse- GFP staining peaked in the subcutaneous tissue at Day 3 due the large inflammatory influx and in (C) GFP graft in C57 mouse- GFP staining in the graft peaked at Day 21 due to crowding of the graft cells and disappeared by Day 90. Significance recorded with * in the graph if p-value was less than 0.05 and ** if p was less than 0.001.

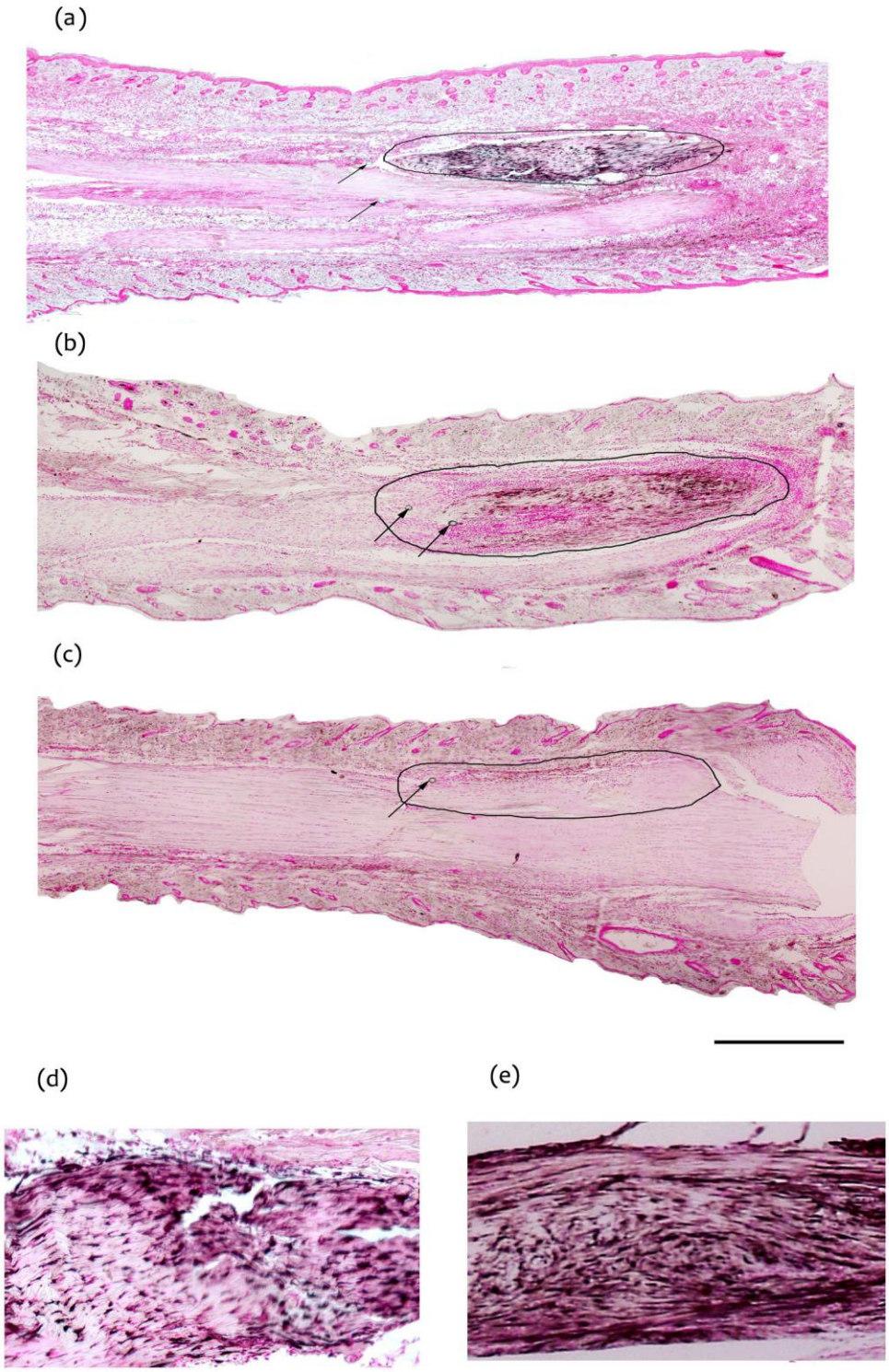

Figure 3.29 - Fate of grafted cells with GFP stain after grafting of GFP positive graft into C57 mice showing results at (a) Day 3, (b) Day 21, and (c) Day 90 . Graft is outlined in black. Arrows indicate securing sutures. Magnification x5, Bar- 500 µm. (d) Day 3 and (e) Day 21 GFP stained cells showing increaseed cell density of cells at Day 21

3.2.4 Cellular proliferation- BrdU immunostaining

The pattern of cellular proliferation showed a gradual increase in BrdU staining from control levels after grafting that mainly occurred in the subcutaneous tissues, whereas BrdU expression peaked in the host tendon and the tendon graft at Day 21 and gradually diminished at Day 90 (Figure 3.30- Figure 3.33). BrdU expression at Day 21 was significantly greater in the subcutaneous tissue in the syngenic model compared with the autograft (1275 ±117 vs. 843 ±139 cells/ mm^2) and greater in the syngenic tendon graft when compared to autograft at Day 90 (523±117 vs. 244±37 cells/mm^2) ($p < 0.05$) (Table 3.5).

Table 3.5- BrdU Stain- Number of cells/mm^2 and corresponding SEM (n=4 mice/time point, 3 slides/mice)

BrdU	Control	Day 3	Day 21	Day 90	Control SEM	Day 3 SEM	Day 21 SEM	Day 90 SEM
Syngenic Tendon Graft	0.00	57.29	632.81	523.44	0.00	19.21	88.59	117.03
Syngenic Host Tendon	84.38	28.64	393.23	286.45	15.30	13.02	22.61	52.34
Syngenic Subcutaneous tissue	425.00	734.38	1275.94	1166.56	34.02	100.47	117.97	105.94
Autograft Tendon Graft	0.00	92.44	584.63	244.69	0.00	22.81	111.17	37.48
Autograft Host Tendon	84.38	32.55	406.25	234.38	15.31	7.78	91.98	13.94
Autograft Subcutaneous tissue	425.00	760.42	843.75	1010.31	34.02	18.59	139.06	87.34

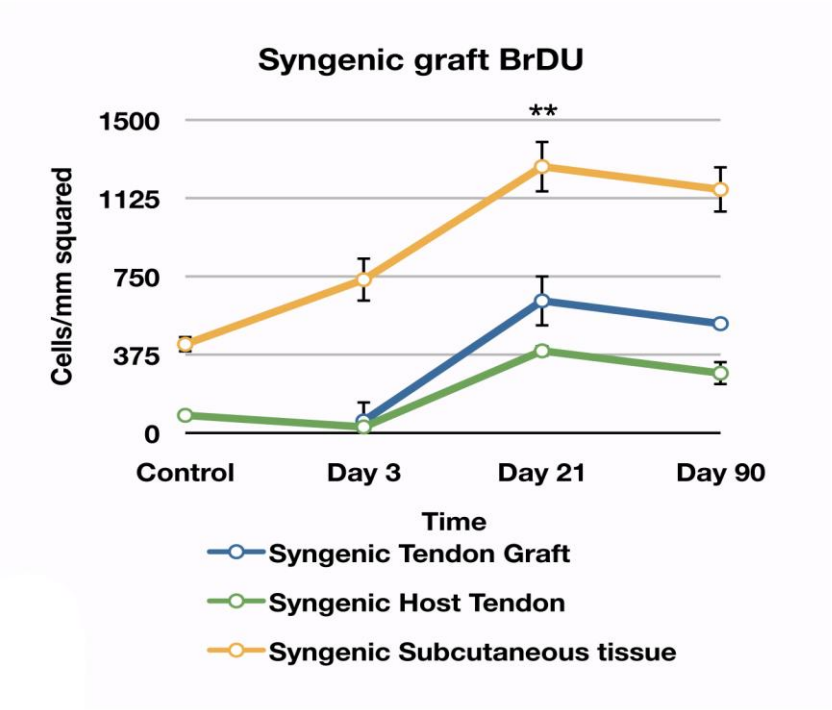

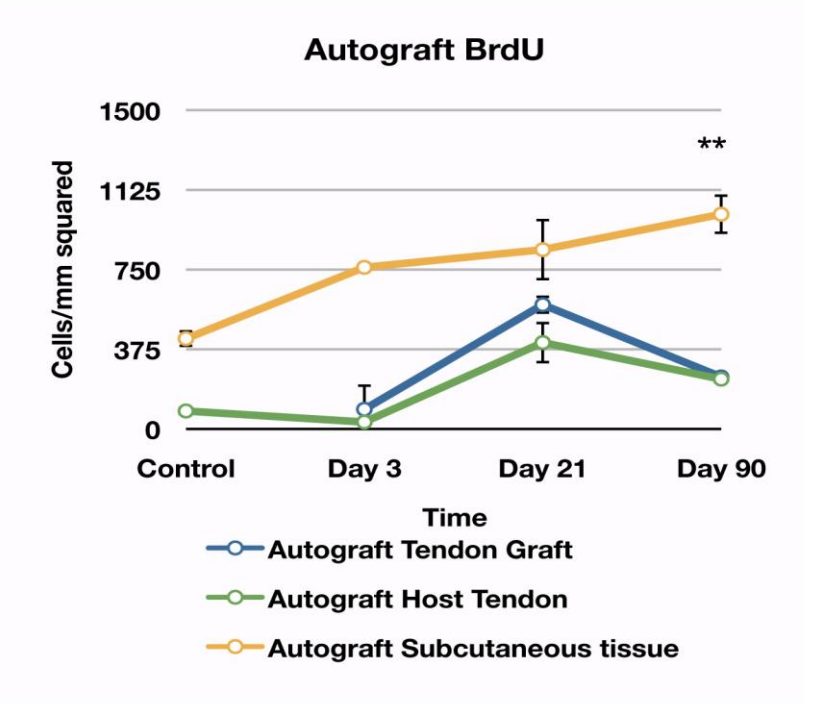

Figure 3.30 -Graphical representation of BrdU positive cells in syngenic and autografts at Day 3, Day 21 and Day 90. Activity in subcutaneous tissue remains much greater than tendon tissue at all time points. BrdU expression at Day 21 was significantly greater in the subcutaneous tissue in the syngenic model compared with the autograft (1275 ±117 vs 843 ±139 cells/ mm2) and greater in the syngenic tendon graft when compared to autograft at Day 90(523±117 vs 244±37 cells/mm2) ($p < 0.05$). Significance recorded with * in the graph if p-value was less than 0.05 and ** if p was less than 0.001.

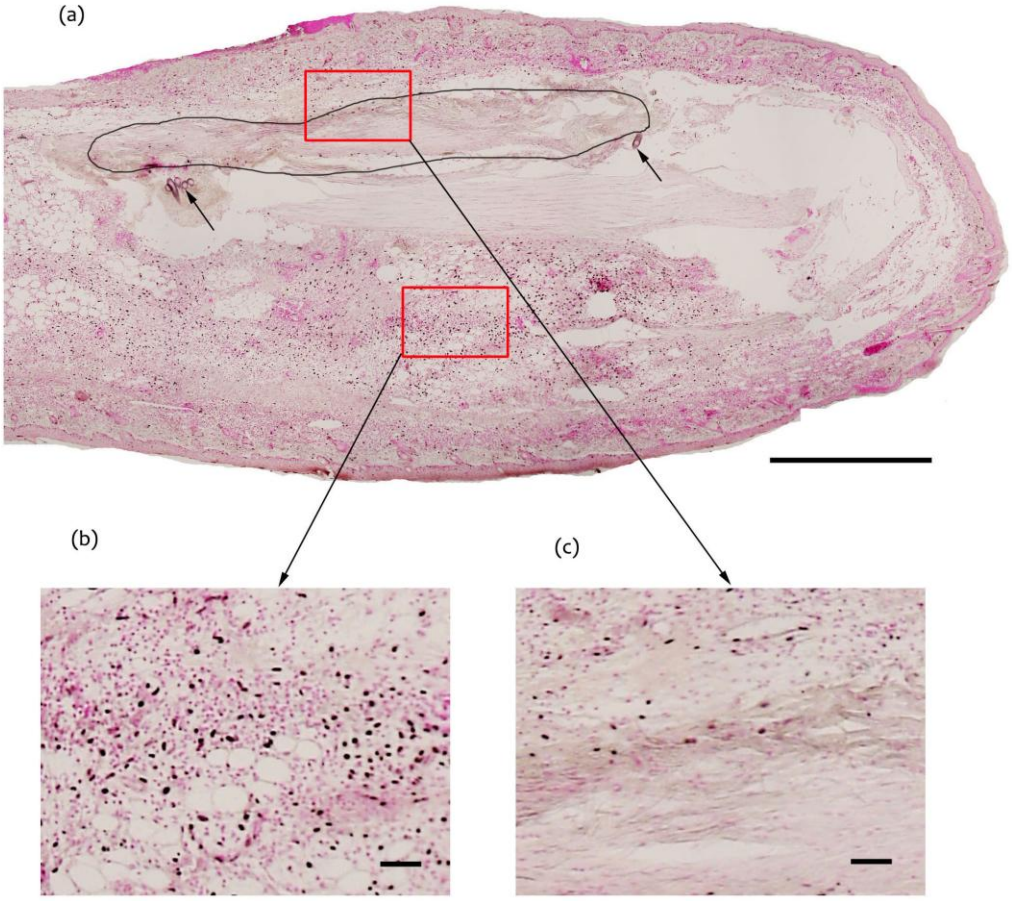

Figure 3.31- (a) Sagittal section of the Achilles tendon and surrounding skin and subcutaneous tissue showing BrdU staining at Day 3. Graft outlined with black line, small arrows indicating the sutures used to secure the graft; Magnification x5, Bar-500 µm (b) The subcutaneous tissue has a large number of BrdU positive cells while (c) graft tendon shows only a small number of BrdU positive cells in the periphery, Magnification x20, Bar-100 µm

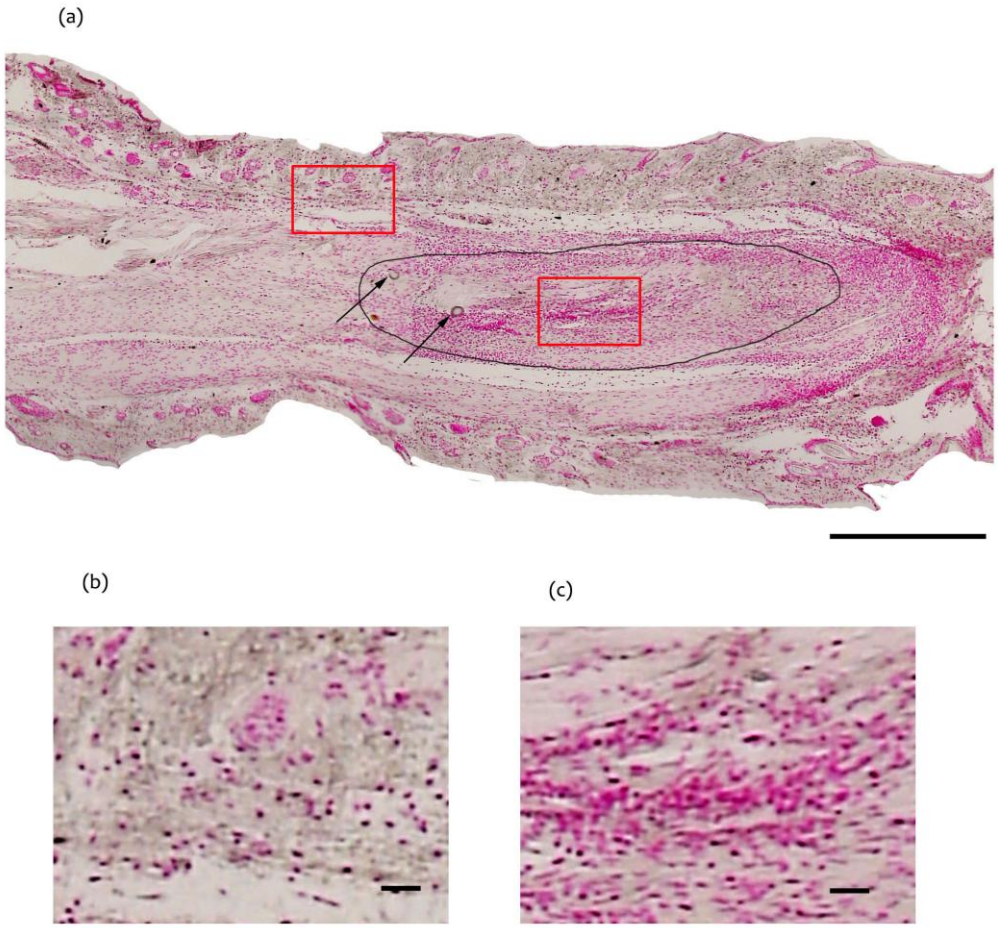

Figure 3.32- (a) Sagittal section of the Achilles tendon and surrounding skin and subcutaneous tissue showing BrdU staining at Day 21. Graft outlined with black line, small arrows indicating the sutures used to secure the graft; Magnification x5, Bar-500 µm.(b) The subcutaneous tissue still has a large number of BrdU positive cells while (c) graft tendon shows an increase in the number of BrdU positive cell;, Magnification x20, Bar-100 µm

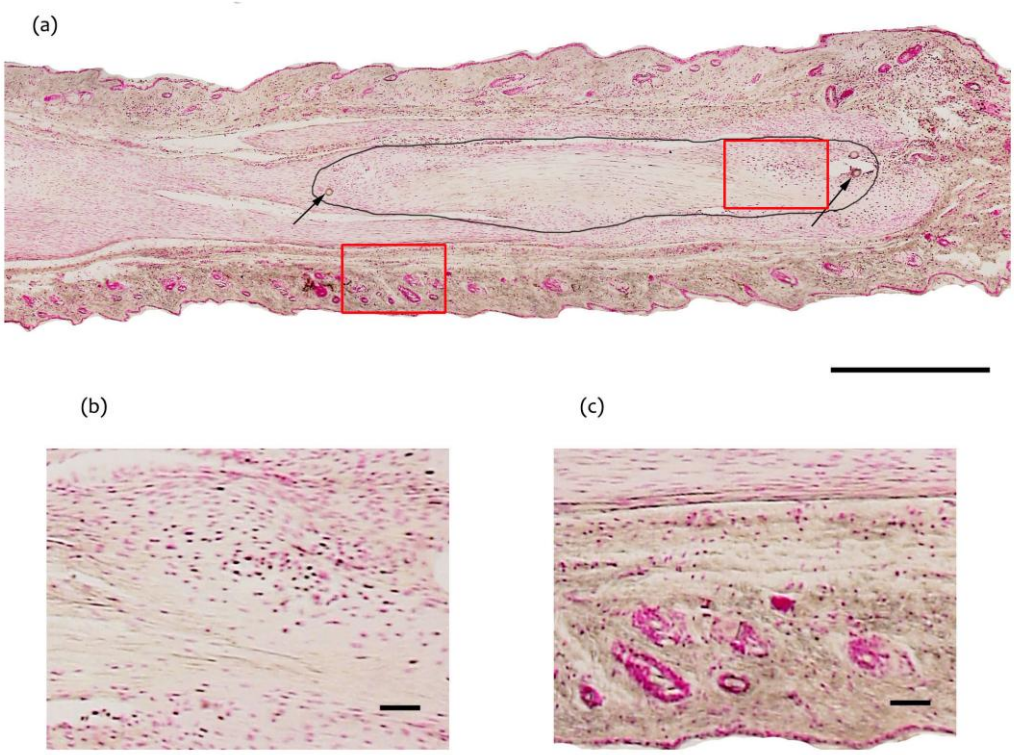

Figure 3.33 - (a) Sagittal section of the Achilles tendon and surrounding skin and subcutaneous tissue showing BrdU staining at Day 90. Graft outlined with black line, small arrows indicating the sutures used to secure the graft; Magnification x5, Bar-500 µm. Proliferative activity remains higher than normal in (b) Graft and host tendon and (c) Subcutaneous tissue, Magnification x20, Bar-100 µm

3.2.5 Collagen synthesis- Hsp47 Immunostain

Collagen synthesis as measured by Hsp 47 expression was increased in the subcutaneous tissues initially at 3 days followed by increased expression in the host tendon and tendon graft at Day 21, reducing to baseline levels at Day 90 (Figure 3.34- Figure 3.37).

Hsp 47 expression was significantly greater in the autografted subcutaneous tissue at Day 3 and Day 90 when compared with syngenic subcutaneous tissue, however syngenic tendon grafts showed marked significantly greater Hsp 47 expression at Day 21 when compared to tendon autograft (1182±80 vs 839 ±77 cells/ mm^2).

At Day 3 Hsp47 positive cells were seen in small numbers in all parts of the leg but there were significantly more cells in the subcutaneous areas than in the tendon tissue. The subcutaneous tissue maintained a similar level of activity at Day 21 but at day 90 this had reduced to a much lower level. At Day 21 the area of the graft showed a massive increase in Hsp47 activity which was obvious in all samples at this time point (Table 3.6).

The host tendon also participated in collagen synthesis and this was more prominent in the areas surrounding the donor graft (Figure 3.36). Though collagen synthesis reduced in all parts of the sample by day 90, the area of the graft continued to show a higher activity than the rest of the tendon. Cell alignment was restored to normal longitudinal orientation (Figure 3.37).

Table 3.6- Hsp47 Stain- Number of cells/mm² and corresponding SEM (n=4 mice/time point, 3 slides/mice)

Hsp47	Control	Day 3	Day 21	Day 90	Control SEM	Day 3 SEM	Day 21 SEM	Day 90 SEM
Syngenic Tendon Graft	0.00	232.97	1182.19	337.24	0.00	23.03	80.02	66.98
Syngenic Host Tendon	59.38	236.98	457.03	139.22	13.44	32.11	65.89	34.38
Syngenic Subcutaneous tissue	181.25	648.44	667.97	291.66	29.06	52.92	51.64	47.19
Autograft Tendon Graft	0.00	347.66	839.84	312.50	0.00	40.00	77.81	27.97
Autograft Host Tendon	59.38	286.41	524.69	179.69	13.44	33.91	54.20	20.66
Autograft Subcutaneous tissue	181.25	830.72	505.16	539.06	29.06	38.59	48.59	53.28

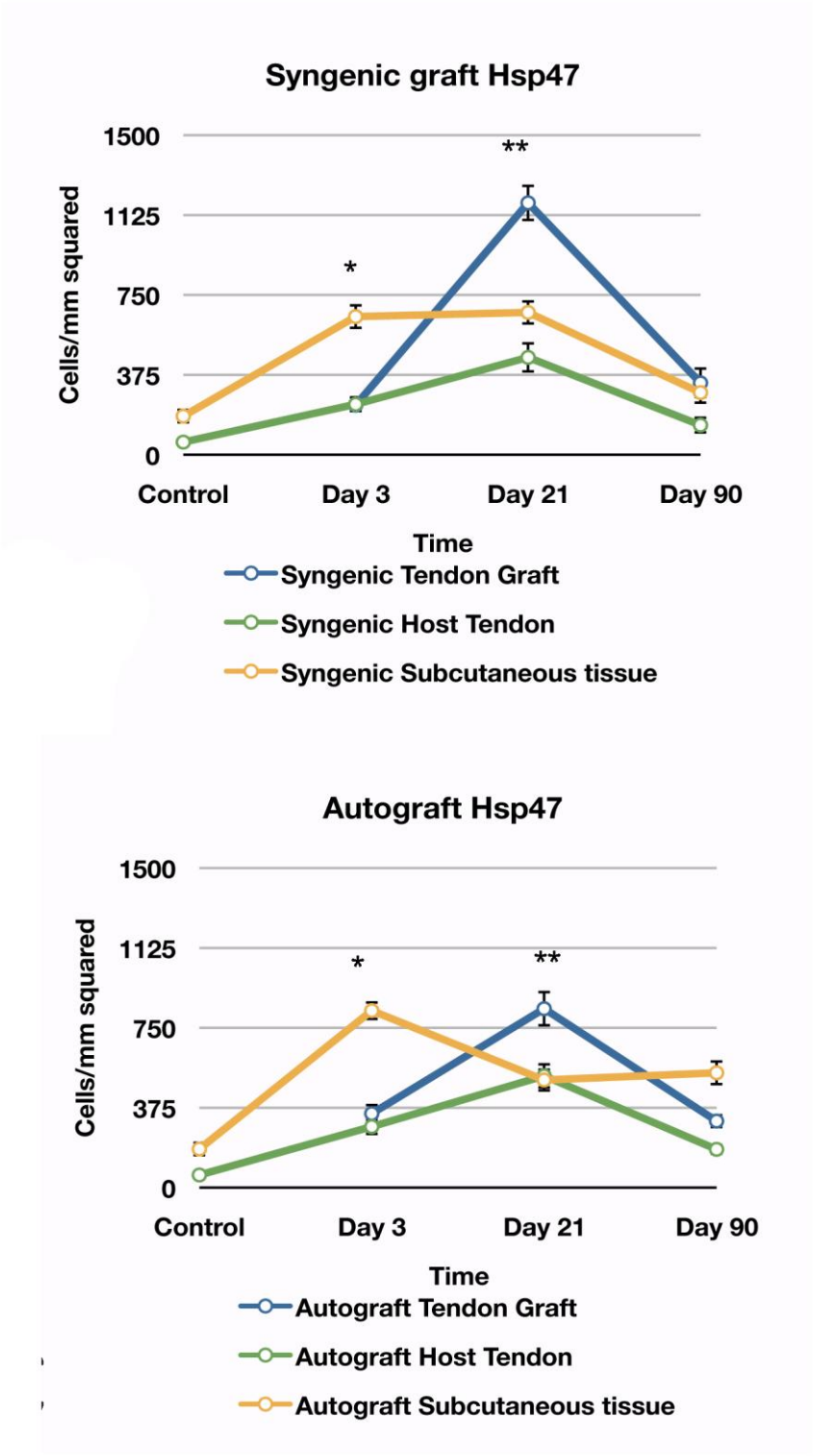

Figure 3.34- Graphical representation of chronological events after syngenic (above) and autologous (Below) grafting with Hsp47 stain. Hsp 47 expression was significantly greater in the autografted subcutaneous tissue at Day 3 and Day 90 when compared with syngenic subcutaneous tissue, however syngenic tendon grafts showed marked significantly greater Hsp 47 expression at Day 21 when compared to tendon autograft (1182±80 vs 839 ±77 cells/ mm2). Significance recorded with * in the graph if p-value was less than 0.05 and ** if p was less than 0.001.

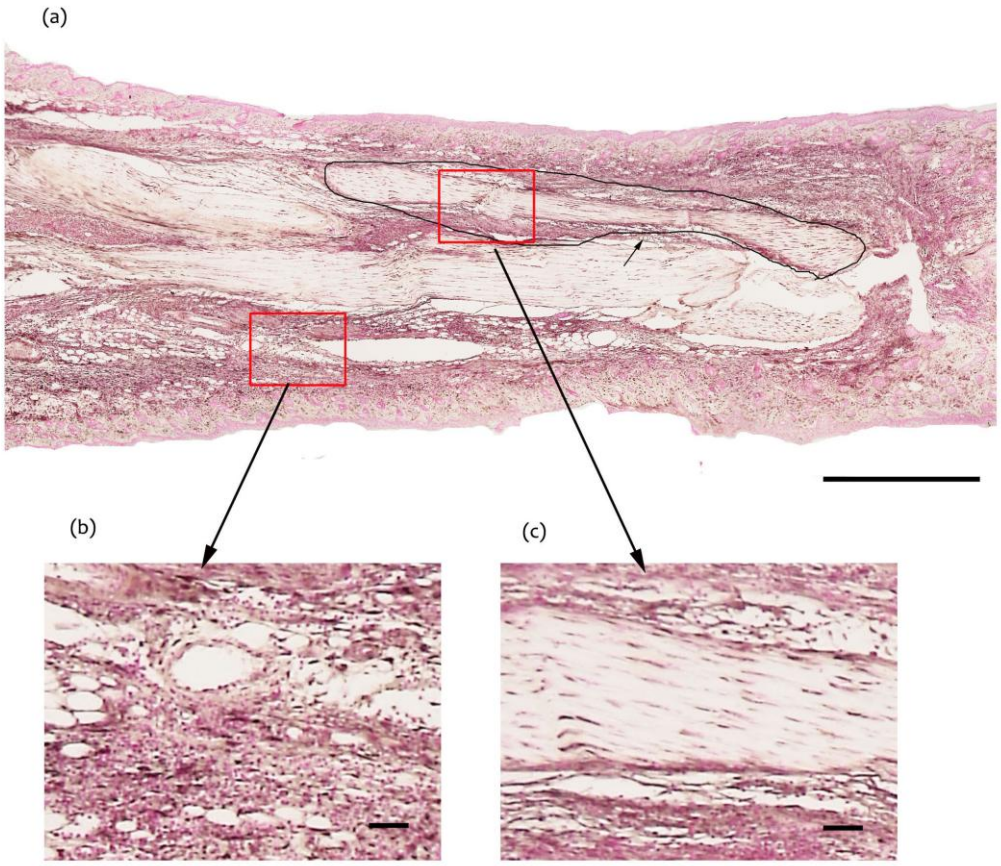

Figure 3.35 - (a) Sagittal section of the Achilles tendon and surrounding skin and subcutaneous tissue showing Hsp47 staining at Day 3 showing collagen synthesis. Graft outlined with black line, small arrows indicating the sutures used to secure the graft; Magnification x5, Bar-500 µm.(b) The subcutaneous tissue showing significant increase in collagen synthesis (DAB staining-Black) while (c) Graft tendon shows a moderate level of activity;, Magnification x20, Bar-100 µm

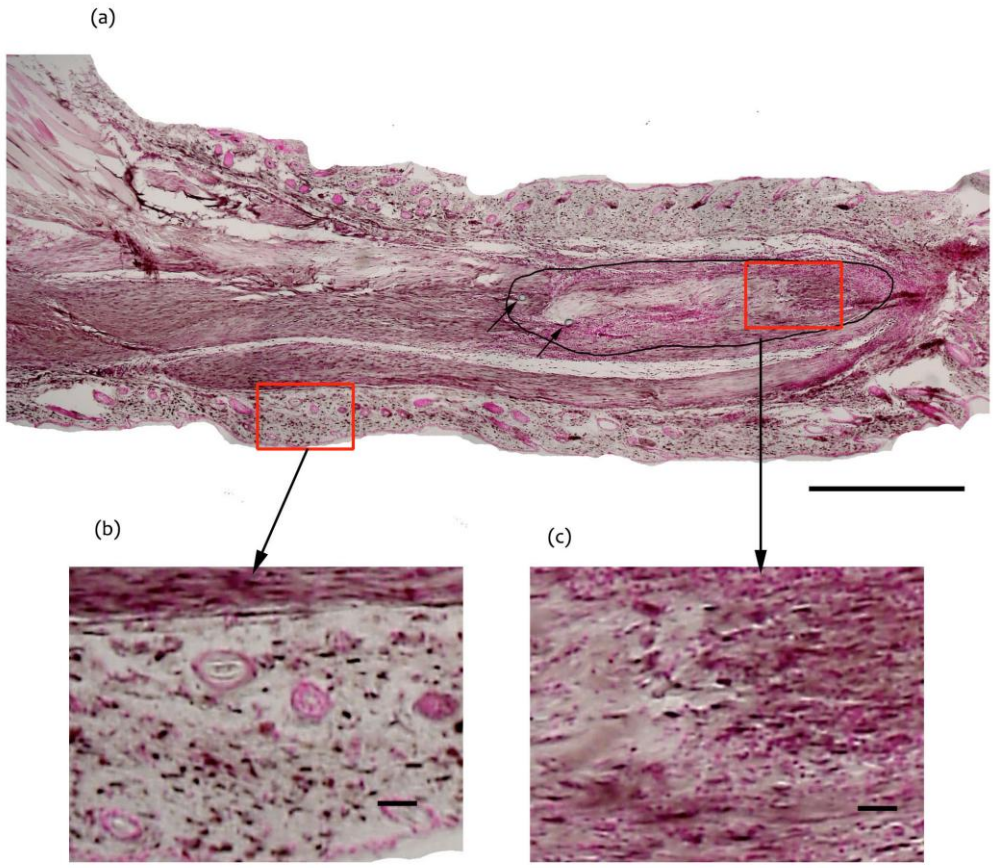

Figure 3.36 - (a) Sagittal section of the Achilles tendon and surrounding skin and subcutaneous tissue showing intense HSP47 staining in all areas at Day 21. Graft outlined with black line, small arrows indicating the sutures used to secure the graft; Magnification x5, Bar-500 µm. (b) The subcutaneous tissue continues to show high levels of collagen synthesis (DAB staining-Black) while (c) Graft tendon shows a marked rise in synthetic activity; Magnification x20, Bar-100 µm

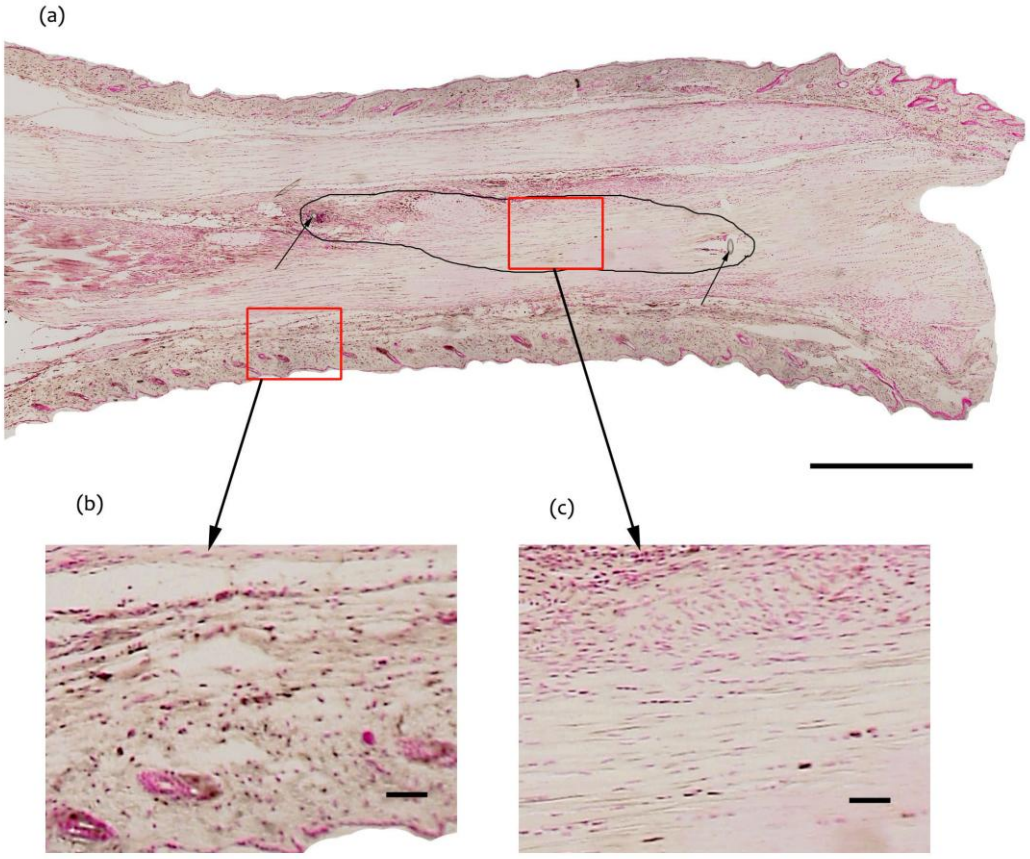

Figure 3.37- (a) Sagittal section of the Achilles tendon and surrounding skin and subcutaneous tissue showing Hsp47 staining at Day 90. Graft outlined with black line, small arrows indicating the sutures used to secure the graft; Magnification x5, Bar-500 µm. (b) Only a small number of cells in subcutaneous tissue and (c) Graft tendon show synthetic activity; Magnification x 20, Bar-100 µm

3.2.6 Cellular Apoptosis- TUNEL Immunostain

Apoptosis as measured by TUNEL expression showed a gradual increase from Day 3 reaching a peak at Day 21 and diminishing by Day 90(Figure 3.38- Figure 4.41). Syngenic grafts showed a far greater expression of TUNEL at Day 21 than autograft tendon (1109± 122 vs. 626 ±81 cells/mm^2) which was significant ($p < 0.001$).

At Day 3 TUNEL positive apoptotic cells were seen in small numbers in all parts of the leg but there were significantly more cells in the subcutaneous areas than in the tendon tissue (Figure 3.39). The subcutaneous tissue maintained a similar level of activity at Day 21 through to Day 90. At day 21 many of the cells in the area of the graft stained positive for TUNEL (Figure 3.40). By day 90 apoptosis has reduced to a very low level in all parts of the host and graft tendon (Figure 3.41). The donor tendon maintained a low level of apoptosis at all time points (Table 3.7).

Table 3.7- TUNEL Stain- Number of cells/mm^2 and corresponding SEM (n=4 mice/time point, 3 slides/mice)

TUNEL	Control	Day 3	Day 21	Day 90	Control SEM	Day 3 SEM	Day 21 SEM	Day 90 SEM
Syngenic Tendon Graft	0.00	82.03	1109.38	126.41	0.00	10.38	122.80	21.42
Syngenic Host Tendon	106.25	48.17	175.78	106.53	11.47	19.66	46.72	20.41
Syngenic Subcutaneous tissue	337.50	516.88	688.75	570.94	37.17	53.72	75.94	66.80
Autograft Tendon Graft	0.00	147.03	626.25	199.22	0.00	23.11	81.25	44.66
Autograft Host Tendon	106.25	92.44	438.75	121.09	11.47	14.45	68.78	29.23
Autograft Subcutaneous tissue	337.50	524.69	658.85	451.72	37.17	64.38	73.42	47.81

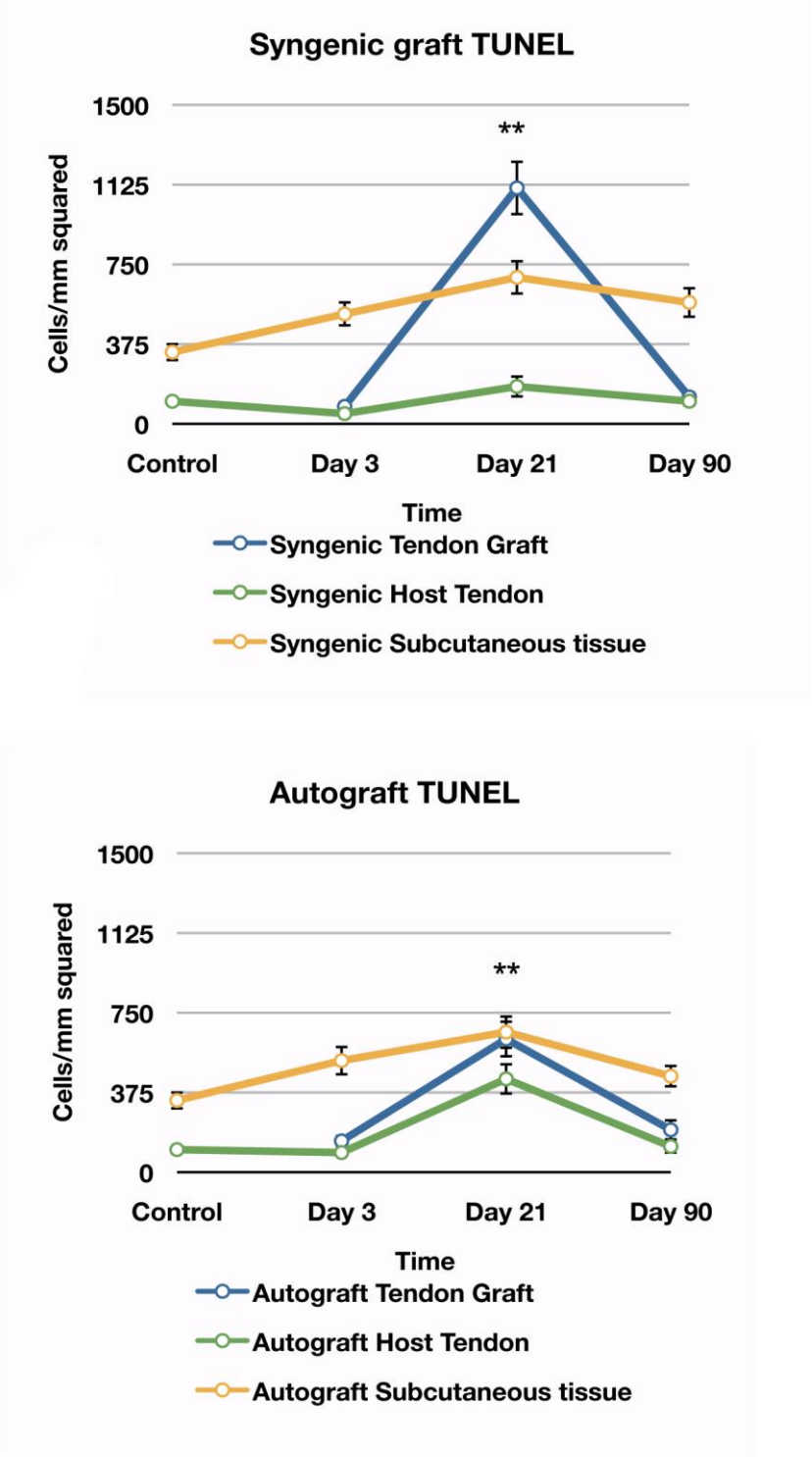

Figure 3.38 – Graphical representation of chronological events after syngenic (top) and autologous (bottom) grafting with TUNEL stain showing apoptosis. TUNEL expression showed a gradual increase from control non injured tissues at Day 3 reaching a peak at Day 21 and diminishing by Day 90. Syngenic grafts showed a far greater expression of TUNEL at Day 21 than autografted tendon (1109± 122 vs 626 ±81 cells/mm2) which was significant ($p < 0.001$).Significance recorded with * in the graph if p-value was less than 0.05 and ** if p was less than 0.001.

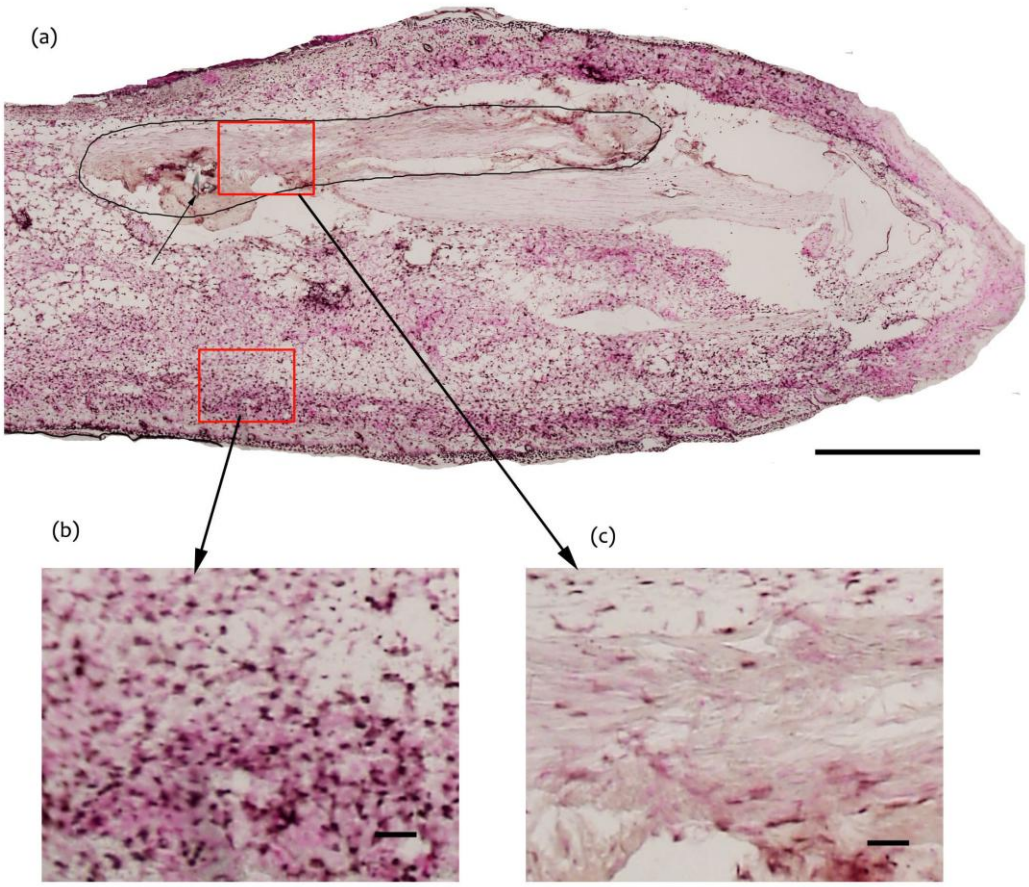

Figure 3.39- (a) Sagittal section of the Achilles tendon and surrounding skin and subcutaneous tissue showing TUNEL staining at Day 3. Graft outlined with black line, small arrows indicating the sutures used to secure the graft; Magnification x5, Bar-500 µm.(b) The subcutaneous tissue has a large number of TUNEL positive cells while (c) Graft tendon shows only a small number of TUNEL positive cells, Magnification x20, Bar-100 µm

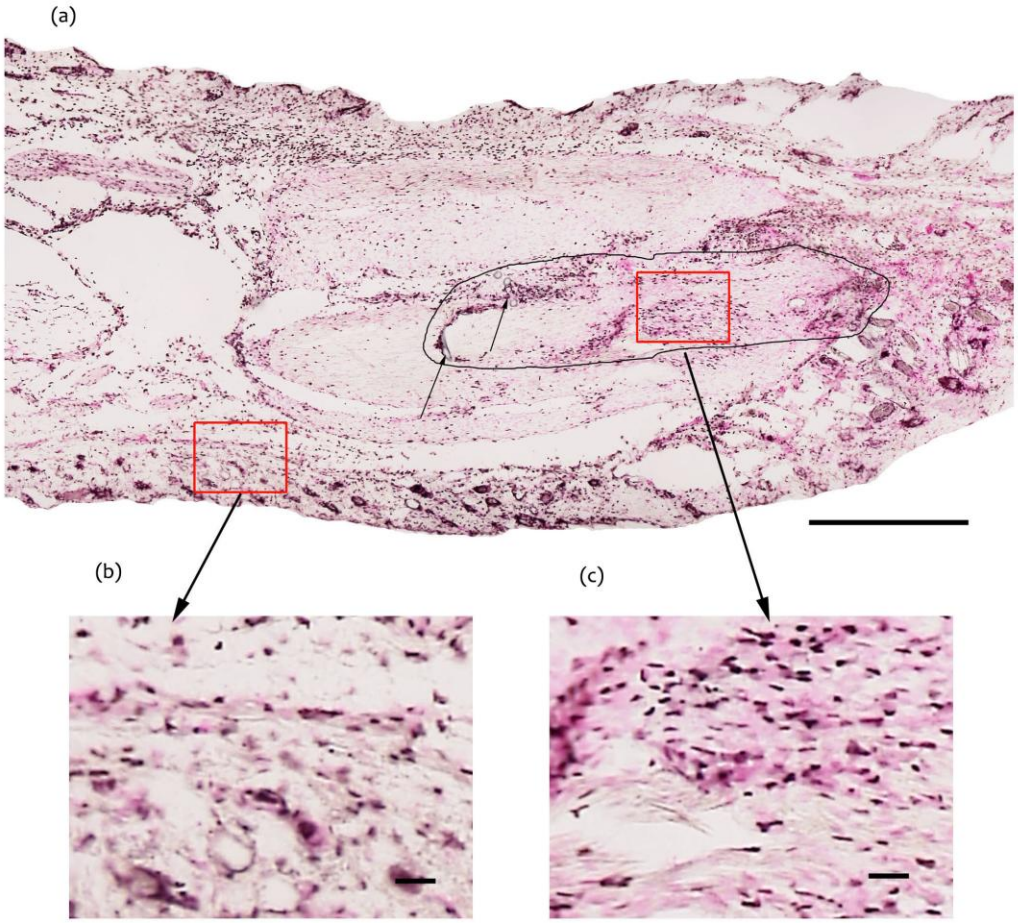

Figure 3.40- (a) Sagittal section of the Achilles tendon and surrounding skin and subcutaneous tissue showing TUNEL staining at Day 21. Graft outlined with black line, small arrows indicating the sutures used to secure the graft; Magnification x5, Bar-500 µm. (b) The subcutaneous tissue still has a large number of TUNEL positive cells while (c) Graft tendon shows a significant rise in the number of apoptotic cells, Magnification x20, Bar-100 µm

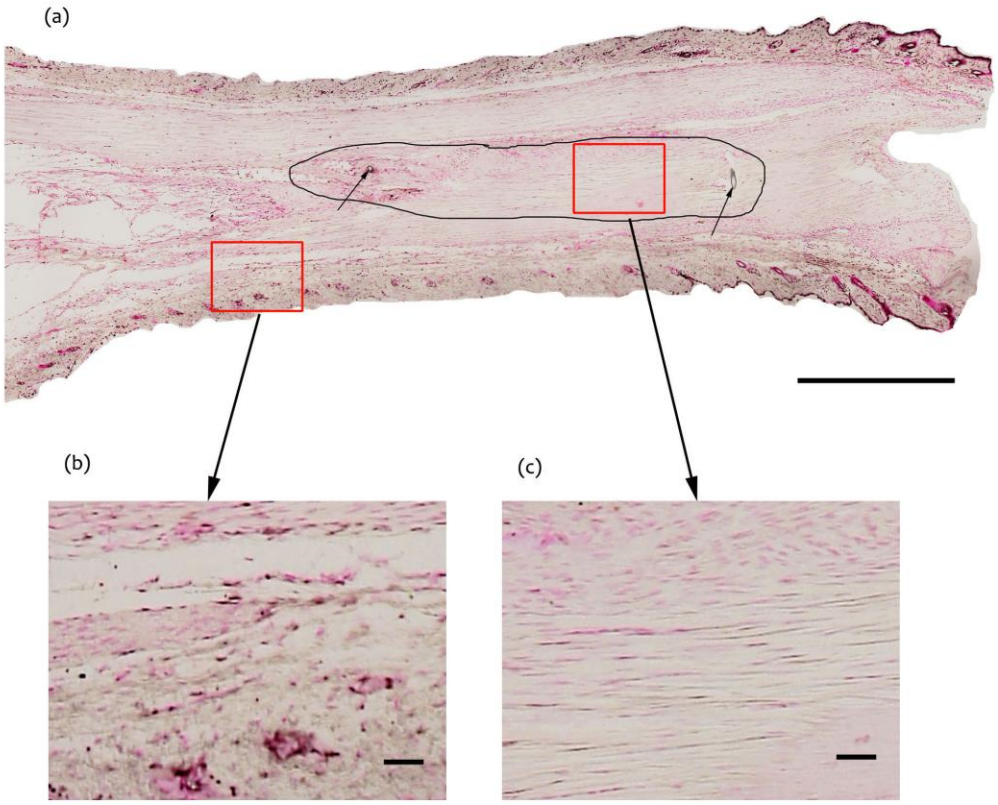

Figure 3.41- (a) Sagittal section of the Achilles tendon and surrounding skin and subcutaneous tissue showing TUNEL staining at Day 90. Graft outlined with black line, small arrows indicating the sutures used to secure the graft; Magnification x5, Bar-500 µm. (b) The subcutaneous tissue and (c) Graft tendon shows a small number of apoptotic cells, Magnification x20, Bar-100 µm

3.2.7 Staining for vascular pericytes-Alpha SMA Immunostaining

Alpha SMA staining highlighted two types of structures- one was associated with lumens and the other was non lumen related individual cellular stains. Lumen related Alpha- SMA staining showed a significant ($p < 0.05$) increase in the vascularity of the subcutaneous tissue at Day 3 (74.21± 7.72 and 53.38±6.7 cells/mm^2 in syngenic and autografts respectively), compared to control unwounded tendons (21.875± 13.6 cells/mm^2). Vascularity remained at high levels at Day 21 (66.4±9.04 in syngenic and 55.98± 5.25 cells/mm^2 in autografts) and at Day 90 (67.7±5.87in syngenic and 37.7± 7.05 cells/mm^2 in autografts) (Figure 3.42- Figure 3.45). Vessel related Alpha SMA staining was absent in the control unwounded tendons and in the tendon substances at Day 3 .Blood vessels were seen in the tendon graft at Day 21 (29.94±11.6 and 14.32±4.88 cells/mm^2 in syngenic grafts and autografts) which reduced in number by Day 90 (1.3±1.3 and 6.51±3.57 cells/mm^2 in syngenic grafts and autografts). A very small number of blood vessels were also seen in the host tendon at day 21 (7.816±3.59 and 7.81±4.5 cells/mm^2 in syngenic grafts and autografts. Non lumen related Alpha SMA staining was present in the subcutaneous tissue at all time points and in the tendon graft at Day 21 and Day 90.

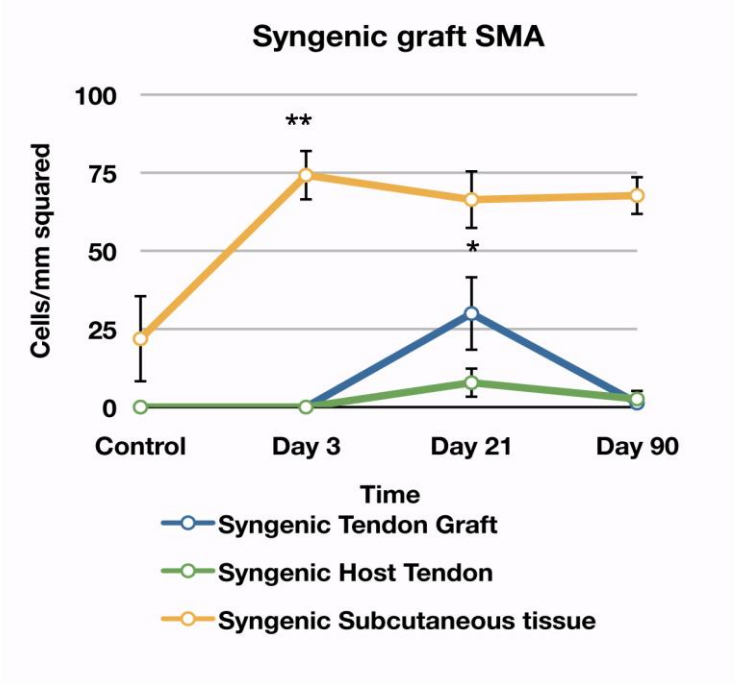

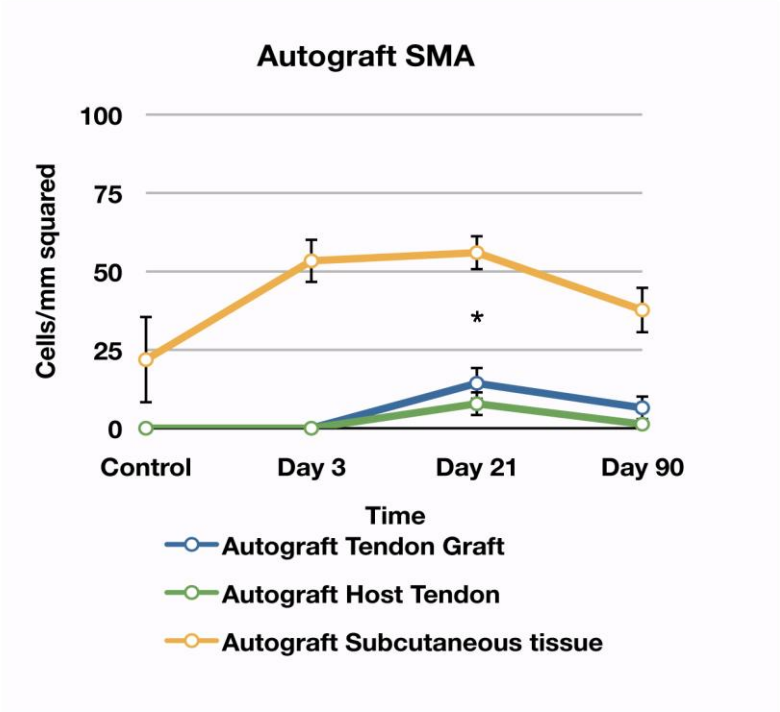

Figure 3.42 - Graphical representation of chronological events after syngenic (top) and autologous (bottom) grafting with Alpha-SMA staining showing vascularisation**.** Alpha- SMA staining showed a significant ($p < 0.05$) increase in the vascularity of the subcutaneous tissue at Day 3 (74.21± 7.72 and 53.38±6.7 cells/mm2 in syngenic and autografts respectively) , compared to control unwounded tendons (21.875± 13.6 cells/mm2). Significance recorded with * in the graph if p-value was less than 0.05 and ** if p was less than 0.001.

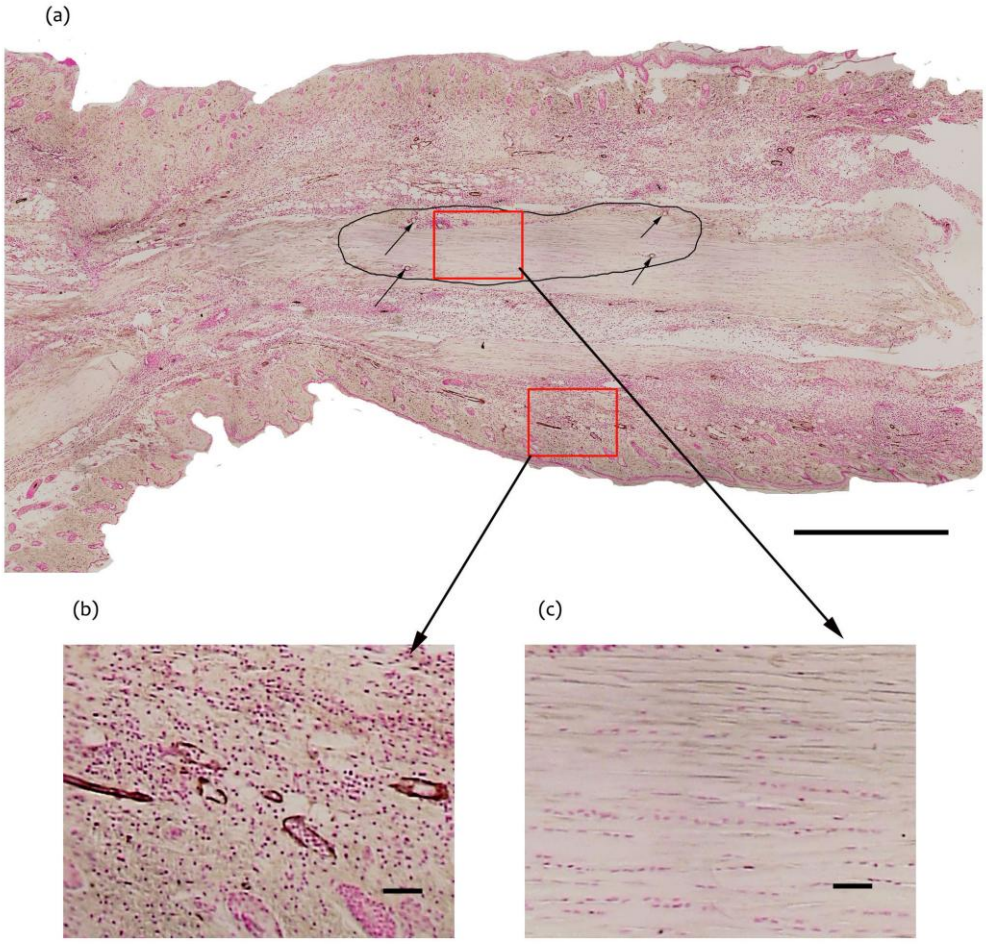

Figure 3.43 - (a) Sagittal section of the Achilles tendon and surrounding skin and subcutaneous tissue showing Alpha SMA Day 3. Graft outlined with black line, small arrows indicating the sutures used to secure the graft; Magnification x5, Bar-500 µm.(b) The subcutaneous tissue has a large number of lumen related Alpha-SMA positive cells indicating angiogenesis associated with inflammatory phase of healing while (c) Graft tendon shows no lumen related Alpha SMA staining, Magnification x20, Bar-100 µm

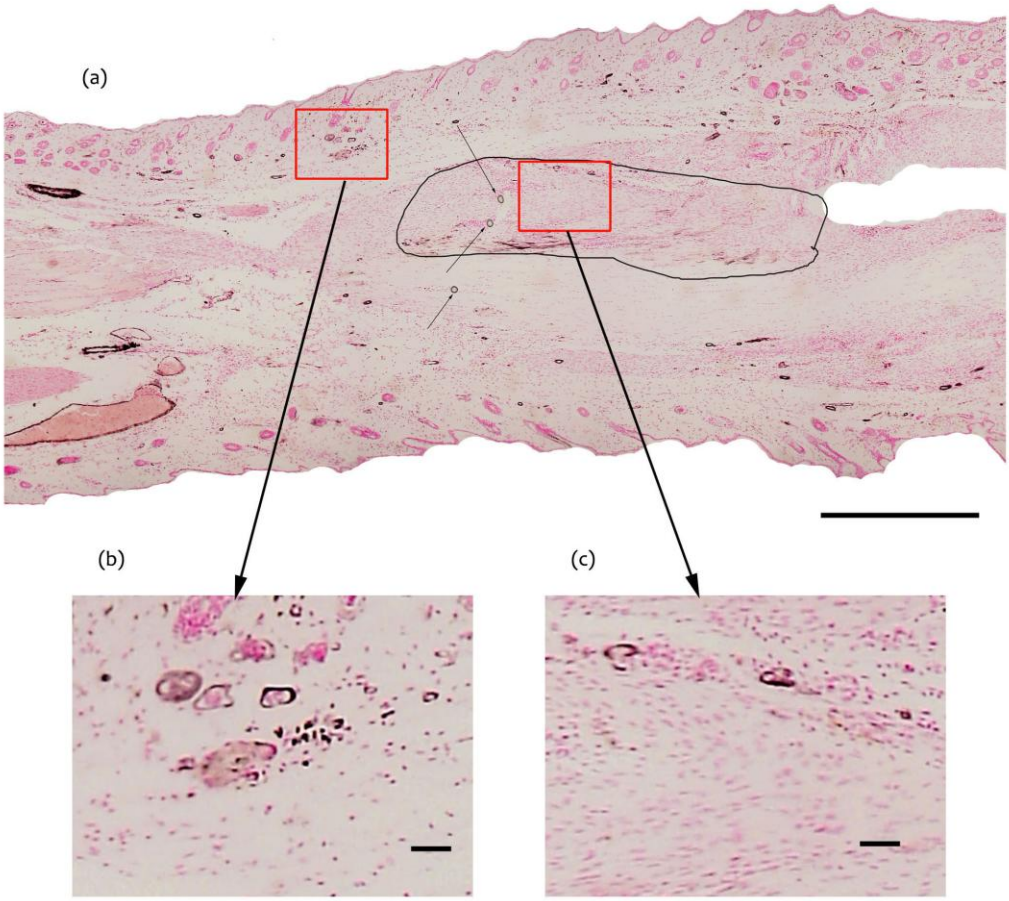

Figure 3.44- (a) Sagittal section of the Achilles tendon and surrounding skin and subcutaneous tissue showing Alpha SMA at Day 21. Graft outlined with black line, small arrows indicating the sutures used to secure the graft; Magnification x5, Bar-500 µm.(b) The subcutaneous tissue still shows a large number of lumen related Alpha-SMA positive cells c) Graft tendon also shows appearance of a number of lumen related Alpha SMA staining, Magnification x20, Bar-100 µm

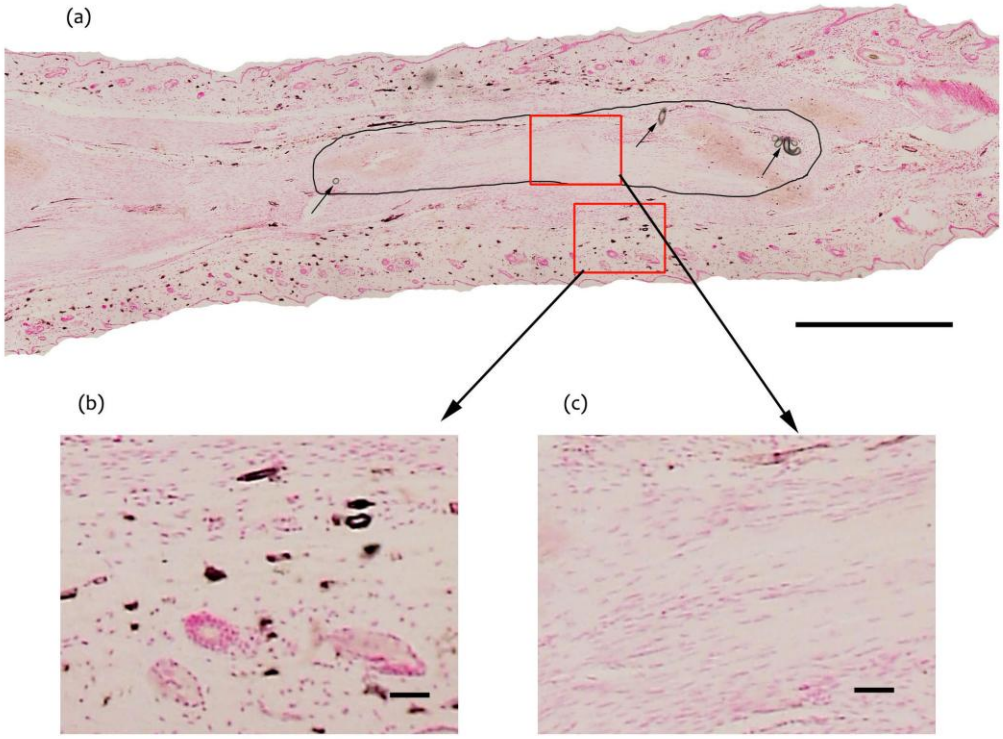

Figure 3.45 - (a) Sagittal section of the Achilles tendon and surrounding skin and subcutaneous tissue showing Alpha SMA at Day 90. Graft outlined with black line, small arrows indicating the sutures used to secure the graft; Magnification x5, Bar-500 µm.(b) The subcutaneous tissue continues to show a number of lumen related Alpha-SMA positive cells c) Graft tendon also shows a small number of lumen related Alpha SMA staining, Magnification x20, Bar-100 µm

3.2.8 Three dimensional cell mapping

In order to achieve a better spatiotemporal orientation of cellular activity three dimensional reconstruction were done from serial section immunohistochemistry (Figure 3.46- 3.48). which showed overlapping of GFP positive cells and HSp47 positive cells further proving that graft cells actively synthesize collagen.

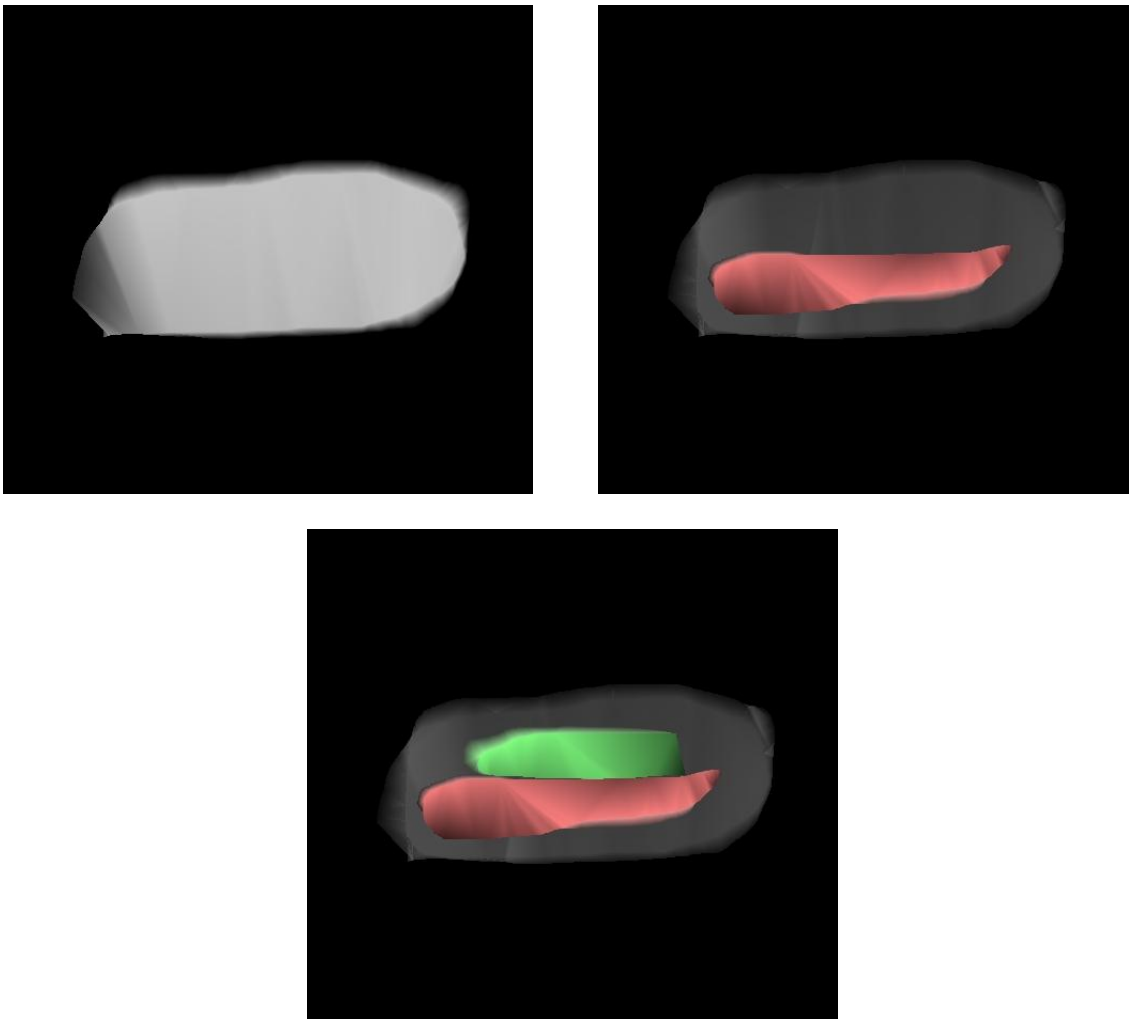

Figure 3.46- Building of three dimensional reconstructions from serial section immunohistochemistry, First the areas are outlined and marled out with a chosen colour. In this case subcutaneous tissue is marked grey, graft-green and host tendon –red. Stained cells are then plotted into the image

3.2.8.1 Inflammatory profile

Three Dimensional Reconstruction of serial sections (Figure 3. 47 a-c) showed that at Day 3 (Figure 3.47a) inflammatory cells (outlined with yellow dots) were abundant in the subcutaneous tissue (outlined in grey). At day 21 (Figure 3.37b) inflammatory cells overlapped the areas outlined by the host (Outlined in red) and the donor tendon (Outlined in green). At Day 90 (Figure 3.37c) minimal inflammatory cells were cells both in tendon and in the subcutaneous tissues.

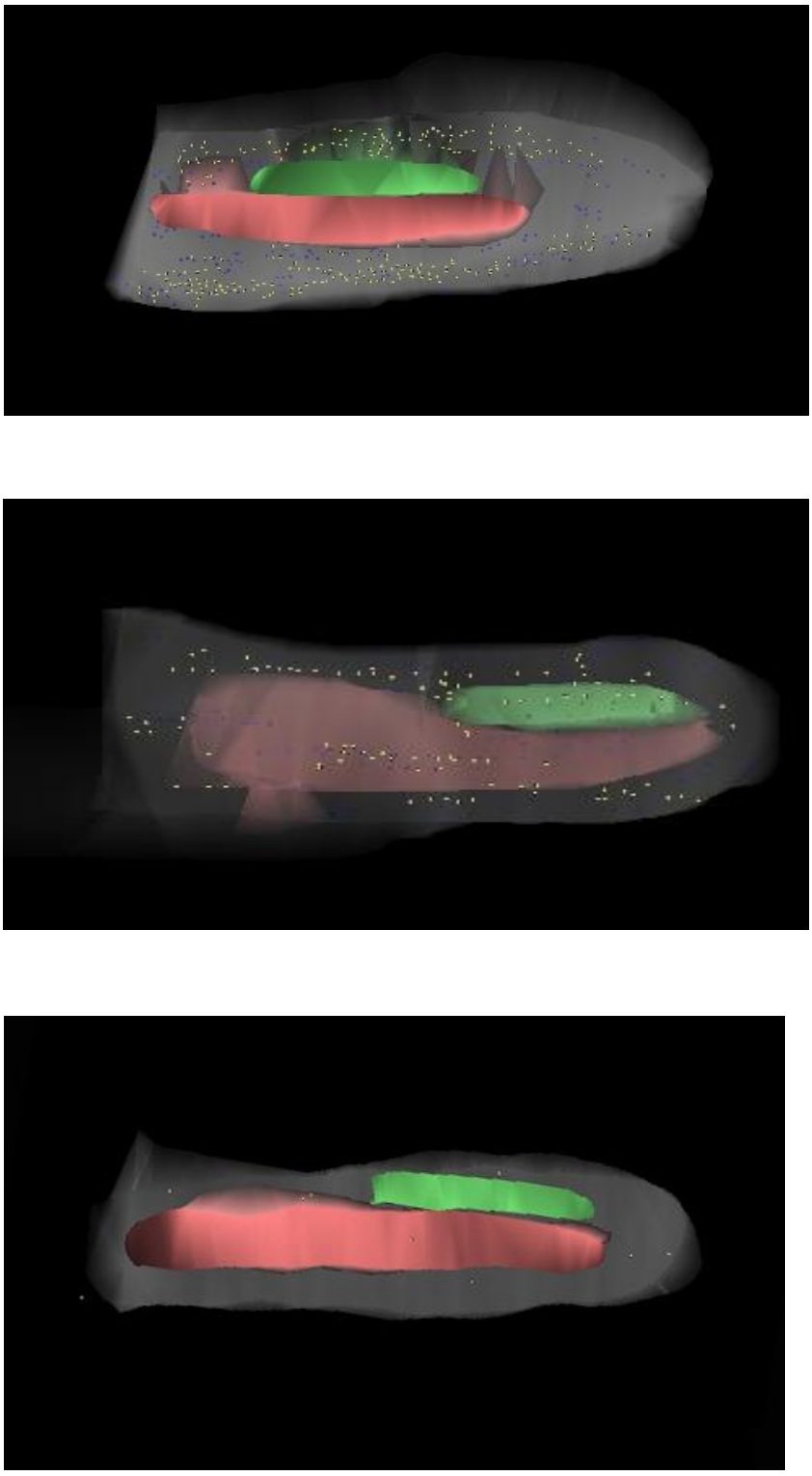

Figure 3.47 -Spatiotemporal distribution of Inflammatory cell -Macrophage (Blue) and CD45 positive cells(Yellow) at day 3(top), day 21(middle) and Day90 (Bottom). Graft Green, Host tendon red, ST-Grey

3.2.8.2 Collagen synthesis

Three Dimensional Reconstruction of serial sections (Figure 3. 48 a-c) showed that at Day 3 (Figure 3.48a) collagen synthesizing cells (outlined with yellow dots) were present in small numbers in the subcutaneous tissue and tendon with no collagen synthesis seen in GFP positive donor tendon cells (outlined with blue dots). At day 21 (Figure 3.38b) Hsp47 positive cells crowded the areas outlined by the host (Outlined in red) and the donor tendon (Outlined in green). Marked overlapping was seen between GFP positive and Hsp47 positive cells. At Day 90 (Figure 3.37c) minimal inflammatory cells were cells both in tendon and in the subcutaneous tissues.

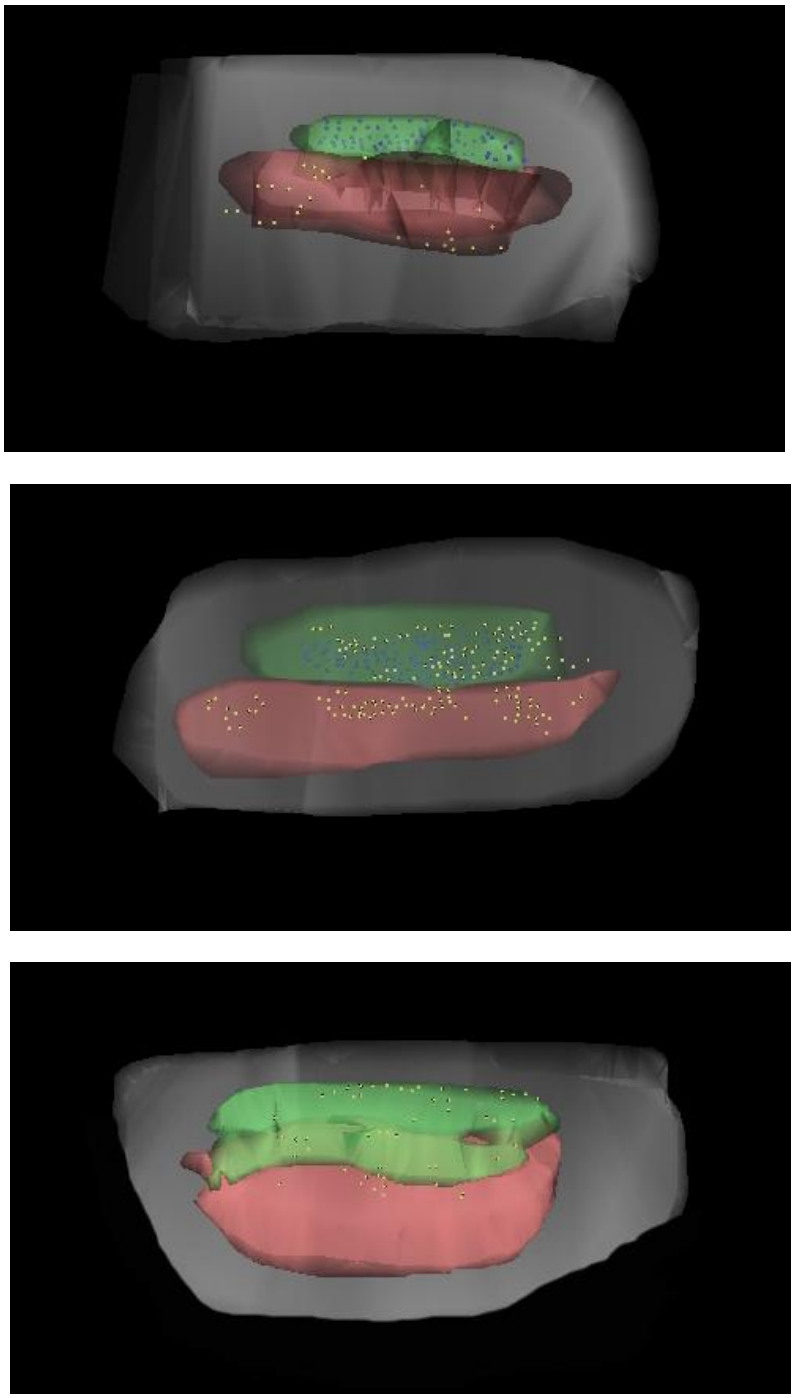

Figure 3.48 -Spatiotemporal distribution of GFP positive cells (Blue) and cells synthesizing collagen (Yellow) at day 0) top, day21 and day90 (Bottom). Graft Green, Host tendon red, ST-Grey

3.2.8.9 Overall summary- tendon grafting

The time points selected of 3 days, 21 days and 90 days related to the phases of wound healing corresponding to the inflammatory phase, peak synthesis phase, and end of remodelling phase as noted in previous tendon wounding experiments. The pattern of the cellular changes following grafting was similar between autografts and syngenic grafts however the amplitude of cellular activity did differ between certain aspects of the healing process. The pattern of inflammation following grafting showed an intense inflammatory reaction in the subcutaneous tissue at Day 3, followed by an increase in inflammatory cells in the host tendon and grafted tendon at Day 21, which gradually diminished but did not reach baseline levels in all tissues at Day 90.

The pattern of cellular proliferation showed a gradual increase in BrdU staining from control levels after grafting that mainly occurred in the subcutaneous tissues, whereas BrdU expression peaked in the host tendon and the tendon graft at Day 21 and gradually diminished at Day 90. Collagen synthesis as measured by Hsp 47 expression was increased in the subcutaneous tissues initially at 3 days followed by increased expression in the host tendon and tendon graft at Day 21, reducing to baseline levels at Day 90. Apoptosis as measured by TUNEL expression showed a gradual increase from control non injured tissues at Day 3 reaching a peak at Day 21 and diminishing by Day 90. Lumen related Alpha- SMA staining showed a significant increase in the vascularity of the subcutaneous tissue at Day 3 compared to control unwounded tendons. Vascularity remained at high levels at Day 21 and at Day 90.

By grafting C57 tendon onto a GFP host there was a marked increase in GFP expression at Day 3 which could be attributed to by host inflammatory cells. It was also evident that the C57 graft became populated by host GFP cells by day 21 with the GFP expression in grafted tendon being greater than that of host tendon. By grafting GFP tendon onto a C57 host, the number of GFP cells increased per unit area by Day 21. However GFP expression rapidly disappeared by Day 90

3.3 Results- Construct testing

3.3.1 Results- Fibrin Construct Grafting

The fibrin- construct disintegrated within 72 hours. GFP stain showed loss of GFP positive cell by Day 3 (Figure 3.50) . The construct was encapsulated within a fibrin clot and the cells lost its oval tendon-fibroblast like appearance and became rounded. The construct and its surrounding subcutaneous tissue became hypercellular indicating an inflammatory infiltrate (Figure 3.49)

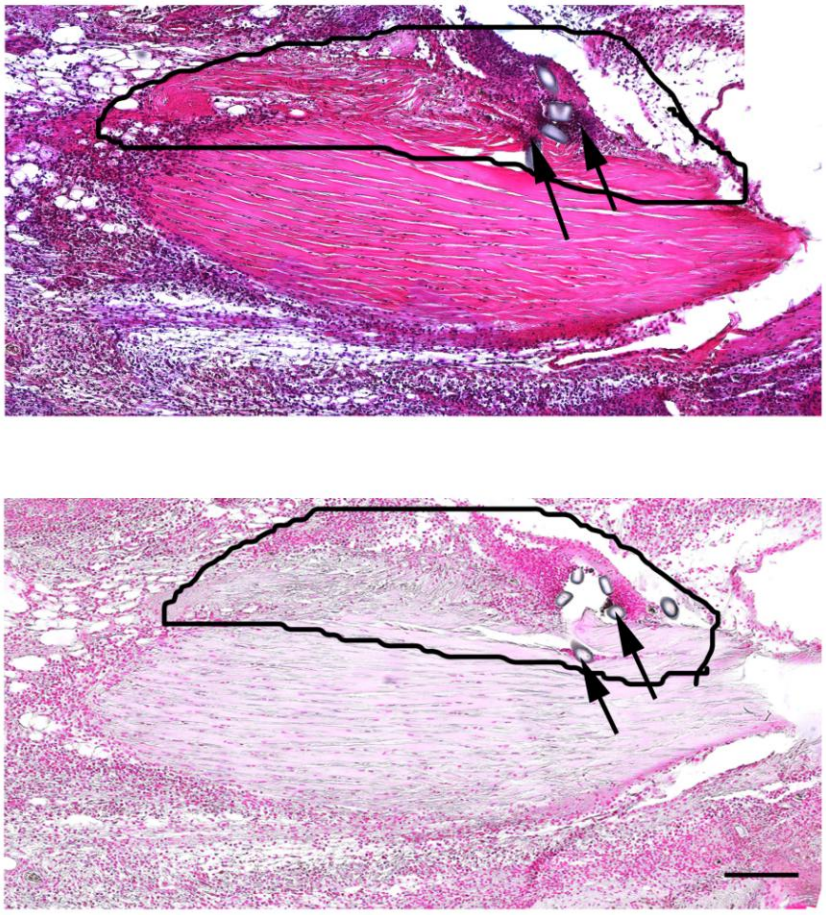

Figure 3.49 - Day 3 of construct grafting-Top H&E stained section and bottom GFP stained section – Construct outlined in black. Arrows indicate sutures used to secure construct. NO GFP positive cells are seen. Magnification.x10; Bar-200 µm

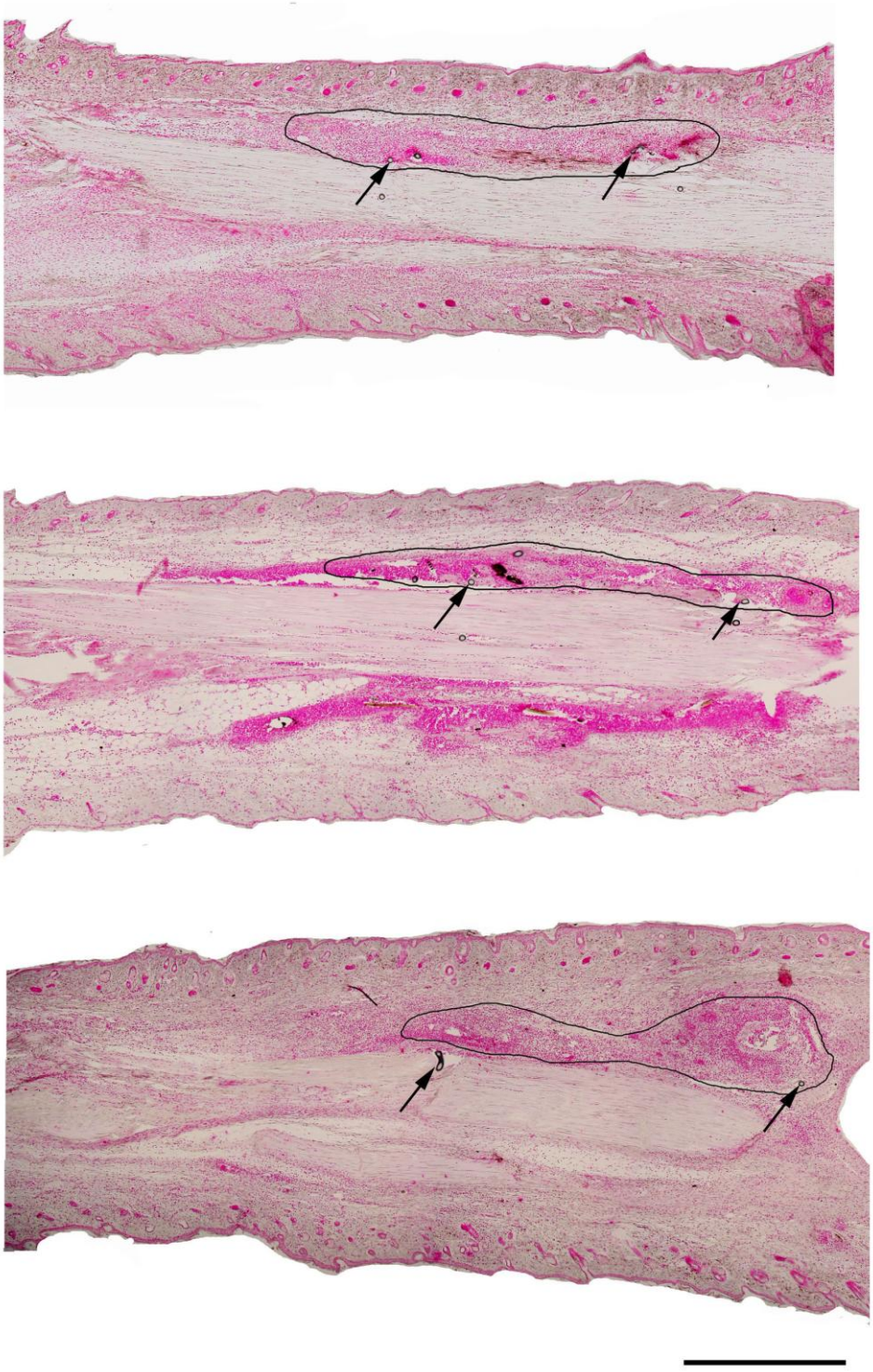

Figure 3.50 -GFP stained construct grafting- Day 0, Day 3 and Day 7 (Top to bottom). Construct appears to have disintegrated very early with loss of GFP stain within 3 days. Construct outline in black, Arrow indicating the securing sutures; Magnification x 5 , Scale Bar-500 µm

3.3.2 PCL Construct testing

The PCL construct melted at 60 degrees and therefore routine wax processing could not be used to study their fate. SEM studies showed that the construct acted as a scaffold and new tendon-like tissue was being laid down around it by Day 21.

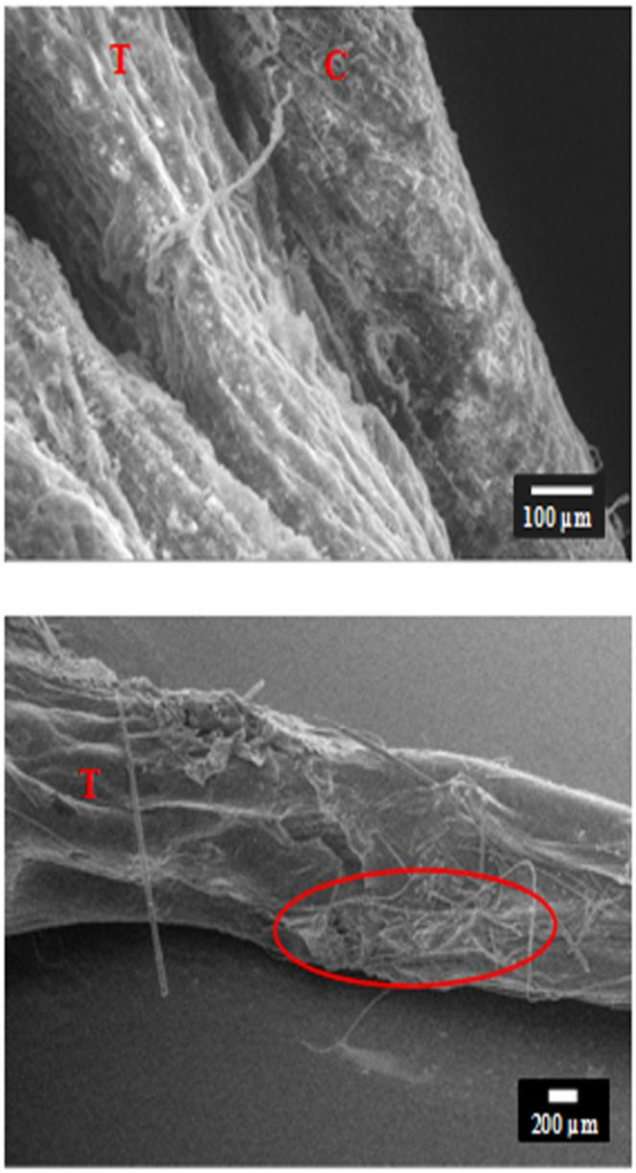

Figure 3.51 - SEM micrographs of a single 3D bundle grafted into the created defect of a mouse Achilles tendon taken at Time Zero (top) and 3 weeks (Bottom) after implantation. Time zero identifies the potential position of the bundle within the tendon (magnification x100), and at 3 weeks potentially new tissue which has encapsulated the bundle can be seen (magnifications x2500). Where C=Construct, T= tendon; Surgery by Nawsheen Alam, SEM by Lucy Bosworth

Chapter Four

Discussion

4.1 Anatomy of the mouse Achilles tendon

Rodent models are commonly used mammalian models for *in vivo* studies due to their availability, size, low cost, ease of handling, and fast reproduction rate. The availability of a large number of genetic species allows for identification of therapeutic targets as the mouse genome is similar to the human genetic map (Mouse Genome sequence consortium, Nature 2002). The small size of mouse tendons and ligaments has so far limited their use for tendon research. This trend is now changing (Chhabra et al., 2003; Hasslund et al., 2008; Mikic et al., 2006; Wong et al., 2009) in order to take advantage of the large number of inbred and outbred strains of mice (Jackson Lab, USA). The availability of the GFP species which offers easy tracking of cells encouraged us to develop a mouse model which will allow us to study cellular events following transplantation of tendon either in the form of a graft or an engineered construct.

Recent studies have used the mouse flexor tendon to study the biology of sutures, flexor tendon healing and adhesion formation (Wong et al., 2006b; Wong et al., 2009). The mouse flexor tendon has also been used to study adhesions after tendon grafting (Hasslund et al., 2008). A larger model would provide a technically reproducible model for the study of tendon and construct grafting. The flexor tendon is an intrasynovial tendon and the majority of the tendon grafts used in clinical practice is extrasynovial in origin. Therefore, the Achilles tendon of the mouse was studied to establish a new model for the study of tendon grafting biology.

A number of similarities were found between the anatomy of the mouse and the human Achilles tendon in terms of its origin, insertion and rotation. In both mice and human the Achilles tendon was formed by the tendons of gastrocnemius and soleus and inserted into the posterior surface of the calcaneum bone. In mouse however, the plantaris tendon was present consistently in all animals and lay on the posterior aspect of the Achilles tendon. The tendon was covered by loose connective tissue, the paratenon. This was particularly obvious anterior to the tendon and created a plane between the Achilles tendon and the deep flexor compartment in which blood vessels

were seen to traverse. In the distal part, the loose areolar tissue widened and contained an area of fatty tissue. In human, a similar area is known as Kaegar's pad of fat (Benjamin et al., 2008; Theobald et al., 2006) and is thought to contribute to reducing the risk of tendon kinking. In loaded Achilles tendon the fat pad slides 60% further into the retrocalcaneal bursa providing lubrication and preventing friction injuries (Ghazzawi et al., 2009). On the posterior aspect, thin fascial extensions were seen passing from the skin into the connective tissue sleeve around the Achilles tendon. This fascial envelope and connections may play an important role in the gliding of the Achilles tendon. It probably represents the microvacuolar system described by Guimberteau (Guimberteau et al., 2010) allowing the tendon to move without any distortion of the skin. Alcian blue staining showed that the fascial envelope is high in proteoglycans and has a loose areolar distribution. The increase in proetoglycans at the region of union of soleus and gastrocnemius may play a role in lubrication of the bundles of adjoining collagen to move over each other as speculated by Vogel (Vogel and Peters, 2005). The tendon proper shows no obvious areas of fibrocartilaginous zones. At the insertion region of the Achilles tendon definite areas of fibrocartilage were seen.

The insertion region of the Achilles tendon has been studied in detail in cadavers (Milz et al., 2002; Rufai et al., 1995). Similar to human Achilles tendon, the mice Achilles tendon was found to be separated from the calcaneum by the retorcalcaneal bursa just above its insertion. The bursa together with its fibrocartilaginous walls is thought to protect the distal most part of the tendon from friction injuries during dorsiflexion of the ankle. Thickening of the epitenon was seen at the concave and convex surface of the tendon, where the tendon was in contact with the surface and changing direction to insert in the bone. The thickening of the epitenon or endotenon have previously been described for wrap- around tendons (Benjamin et al., 1995). Benjamin et al. speculate that the thickening in the epitenon or endotenon may play a role in protecting tendon vasculature.

Alpha-Smooth muscle actin, an isoform of actin that is typical of smooth muscle cells have been demonstrated in the cytoplasm of pericytes, a cell residing in the endothelieal layer of blood vessels. Alpha SMA stain of the Achilles tendon showed that the tendon substance was avascular. Non vessel related alpha SMA positive cells were found in the epitenon of normal Achilles tendon which may represent presence of myofibroblasts. These cells have previously been implicated in remodeling of injured tendon (Weiler et al., 2002). Abundant blood vessels were seen in the loose areolar tissue anterior to the tendon. The relatively larger caliber vessels that appear to be contributing to the smaller vessels passing into the mesotenon is likely to be the posterior tibial vessels. Human cadaveric studies have shown that the Achilles tendon receives blood supply from musculotendinous and osseotendinous junctions(Ahmed et al., 1998; Carr and Norris, 1989) and also receives supply from posterior tibial vessels (Ahmed et al., 1998) through the mesotenon. A second large caliber vascular bundle was seen closely related to the tendon but did not give off any direct branches to the tendon. This group of large caliber vessels could represent the saphenous vascular bundle. Serial cross sections showed a uniform number of blood vessels in the mesotenon at all levels which is in keeping with previous reports by Ahmed et al. (Ahmed et al., 1998). This is in contrast to intrasynovial flexor tendon which has been shown to receive segmental blood supply (Peacock, 1959; Zhang et al., 1990).

4.2 Biology of tendon grafting

The practice of tendon grafting continues to be a useful technique for the reconstruction of damaged segments of tendon and for the reconstruction of ligaments. The biology of tendon graft integration bears some similarities to healing of injured tendons but also follows a cellular repopulation phenomenon particular to grafted tissue.

Our study of syngenic GFP tendon grafting showed that no graft cell was detected at day 90. Kubo and co-workers performed confocal studies of GFP positive grafts that have yielded results similar to our study (Iwata et al., 2008; Kobayashi et al., 2005) while a recent study by the same group suggested that graft cells disappear by day 7 (Tachiiri et al., 2010). The disparity between the time lines was not explained but variation in surgical technique may have contributed to the earlier disappearance of the graft cells.

It is also possible that some of the graft cells persist but fail to express GFP. Insitu hybridization study of sex mismatched tendon grafting reported a delayed repopulation by recipient cells between 12 and 30 weeks (Thorfinn et al., 2009). Thorfinn used tendons reseeded with cells which had been expanded *in vitro*, therefore may be less immunogenic and may not respond to loss of mechanical integrity in a manner similar to intrinsic tendon cells. Reseeding may also have led to a residual acellular area in the tendon core due to lack of cell penetration which may also have contributed to the delay in cellular repopulation. Tendon grafting studies of mice flexor tendon have shown that acellular freeze dried allografts are repopulated by 42 days (Hasslund et al., 2008). The control autografts in Hussland's study showed chronological events similar to our study with hypercellularity at day 28 but cellular repopulation could not be identified in the autografts. Sex mismatched syngenic studies are needed to clarify this point of interest.

The benefit of our DAB based immunohistological study was that it allowed us to see the cellular events in relation to the complete architecture of the leg and draw

conclusions regarding the spatiotemporal orientation of cells. The position of the graft could be identified with some ease by the GFP stain and the presence of the proximal and distal suture up to Day 21. After this time point only the position of the two sutures allowed for the continued verification of the area of the graft. Our study was different from the above studies in terms of the design as we used a patch/ onlay graft while the above studies used either a tendon to bony insertion (Iwata et al., 2008; Kobayashi et al., 2005) or end to end repair (Hasslund et al., 2008). As Achilles tendon is a weight bearing tendon, removal and replacement of a complete segment without immobilisation of the whole leg, may have impaired mice ambulation leading to poor health. On the other hand an onlay graft offered a broader insight of cellular events as cell traffic was both from side to side and from the stumps. One of the limitations of the model could be that using a patch graft excluded the role of direct mechanical forces on the early remodelling of the graft. Previous studies have shown that creating a window in extensor tendon led to hypertrophy of the rest of the tendon until the window is filled with fibrillar collagen and incorporated in the tendon (Matthew et al., 1987). The authors speculated that the nonlesional part of the tendon responded to the added stress by the formation of more collagen as well as the lesional part. In our study it is likely that the grafted tendon segment was not involved in load transmission in the early part of healing. At Day 3 the tendon graft appeared to be separated from the rest of the tendon by a fibrin clot. Around Day 21 the graft appeared to be incorporated inside the tendon with significant rise in collagen synthetic activity both in the graft and the host tendon. The boundary of the graft was indistinct. The collagen synthetic activity at Day 21 may represent the redistribution of load throughout the tendon in keeping with Matthew's findings of the appearance of small fibrils in the non-lesion area between 10-30 days.

At Day 21 the graft was hypercellular and had both abundant rounded and oval cells which may represent inflammatory and tendon cells respectively. Positive GFP staining suggested that graft cells were viable until Day 21. High level of Hsp47 activity in the area of the graft at Day 21 also indicates that cells are very active atleast until this stage of healing. The early results are similar to histological reports by Mason and Shearon

(Mason and Shearon, 1932) and Potenza (Potenza, 1964) who showed that the graft remained viable throughout the healing period. In our study, the disappearance of GFP positive cells from the GFP syngenic grafts and the number of apoptotic cells in the graft at Day 21 suggests that the cells of the graft have a finite life after transplantation. The matrix turnover of the graft was not studied and therefore cannot be commented upon. But Hsp 47 activity in and around the graft at Day 21 suggest deposition of new matrix by cells in the area of the graft. Therefore we suggest that the graft cells are both viable and metabolically active in the early phase of healing.

The mechanism of disappearance of graft cells is not yet known. It is possible that loss of intercellular communication leads to inability of the tendon graft to respond to stress (McNeilly et al., 1996) which then undergo a process of apoptosis (Egerbacher et al., 2008; Kawabata et al., 2009). Apoptosis was more marked in syngenic grafts than autologous grafts and this may be due to either immunogenicity of the GFP grafts or a disparity of size compared to autologous grafts which were perfect fits in their host environment as they were replaced orthotopically. Immunogenic reaction between GFP and their syngenic counterpart has rarely been reported. Matsuo reported rejection of full thickness dorsal skin graft between GFP and C57BL/6 mice, which was then avoided by using tail skin (Matsuo et al., 2007). The biological processes observed in both syngenic and autologous grafts were parallel in terms of timing. Moreover no signs of rejection were seen either clinically or macroscopically all of which provides argument against an immunogenic response to the syngenic graft.

An interesting and unexplained phenomenon in the graft cells was observed at Day 21. The GFP stain in GFP positive syngenic graft was more intense compared to day 3 and the cells appeared to be crowding together. The GFP in mammalian cells is distributed across cytoplasm and nucleus. One explanation may be that the initiation of apoptosis which is marked by cell condensation increases the intensity of the GFP signal. It may also be possible that redistribution of mechanical load leads to graft cells trying to realign themselves in the line of stress. There may also be a movement of cells away from the sutures though this was not obvious. The sutures were put in the long axis of

the tendon and therefore acellular zones occurring due to the gripping component of the suture was avoided (Wong et al., 2010). Alternatively the matrix may have been degrading causing the cells to crowd together.

The function of cells of the graft is not clear. In our study the very high level of Hsp47 activity of the tendon cells of the graft at Day 21 suggests that cells of the grafted tendon are very active and participates in neo tendon formation. Collagen synthesis peaked at Day 21 which is in keeping with the traditional phases of healing. Though the graft cells disappear after this stage, their role in the early phase of healing appears to be of significance for the remodelling of tendon. An earlier peak of synthetic activity at day 3 and day 7 post grafting has been reported for GFP chimeric rat tendon grafting models (Kajikawa et al., 2008; Tachiiri et al., 2010). There may be an interspecies variability between mice and rat or the GFP cells in the rat model may be more immunogenic. The difference in the study designs may account for the difference in time frames with our study. In our study we applied a patch graft to a partial window model and therefore mechanical forces involved in the remodelling process were very different from other tendon grafting experiments and may not be comparable.

Three dimensional reconstruction of serial histological sections showed overlapping of collagen synthetic activity with the GFP positive graft cells. This suggests that graft cells are not quiescent and have an active role in healing. This may explain why cellular autografts appear to have more strength than acellular allografts (Romanini et al., 2010; Scheffler et al., 2008). In sheep model of Anterior Cruciate Ligament Reconstruction recellularization and revascularization was significantly delayed in the allograft at 6 and 12 weeks of healing, while significantly lower structural and mechanical properties were found at 52 weeks (Scheffler et al., 2008).Chong reported contradicting results and showed no difference existed between the tensile strength of normal and acellularised tendons (Chong et al., 2009). Less adhesion formation was reported as an added advantage in acellular tendon grafts (Hasslund et al., 2008). The debate may continue as evidence on both sides continues to mount. Our study provides evidence in favour of cellular grafts and it is possible that if cells can be encouraged to start synthesizing

collagen at a higher rate and at an earlier time point, such as by the use of mechanical, electrical or factorial stimulation, construct and graft remodelling may be expedited.

Apoptosis has been shown to be a part o f the healing process of wounded tendons. Lui (Lui et al., 2007) reported that TUNEL positive cells peaked at 28 days following tendon wounding while Wong (Wong et al., 2009) reported a peak at 84 days in a mice tendon adhesion model. A recent study reports a much earlier peak in apoptosis in the healing tendons at day 3, followed about 10 days later by the peak proliferation period (Wu et al., 2010).Wu also found that apoptosis was inhibited between 2 and 4 weeks. It appears that apoptosis plays a significantly greater role in tendon graft healing compared to healing of wounded tendons. In our study TUNEL positive cells were present in the tendons at day 3, increased significantly by day 21 and continued to be present at day 90. Apoptotic cells were present both at the area of the donor tendon and in the host tendon as well as surrounding peritendinous areas. Apoptosis therefore appears to be an integral part of cellular repopulation in tendon graft healing. Apoptosis may be triggered by loss of mechanical integrity and the need for realignment by the tendon cells. Apoptosis has been shown to be induced both by mechanical loading of intact tendon (Scott et al., 2005) or by the lack of it (Egerbacher et al., 2008). Egerbacher et al. suggest that loss of homeostatic tension causes an alteration in cell-matrix interactions leading to an in increase in apoptosis. In our study a slightly higher level of apoptosis was seen in syngenic grafts compared to autologous grafts where size and shape mismatch was minimum. The subcutaneous tissue and peritendinous area showed very high level of apoptotic activity from Day 3. The large number of inflammatory cells present in the subcutaneous tissue probably undergoes apoptosis leading to the high TUNEL activity in this area (Brown et al., 1997). Some of the apoptotic activity in the tendon at Day 21 can also be contributed to the death of invading inflammatory cells (Homburg and Roos, 1996).

Several studies have reported a close association between apoptosis and cell proliferation (Lui et al., 2007; Wu et al., 2010). Lui reported that as well as TUNEL positive cells, the level of PCNA positive fibroblast like cells remained high at day 28

indicating a high level of cellular proliferation. They speculate that this association may be suggestive of an attempt of the cells to repair DNA during apoptosis and that cells undergo abortive events in the early mitotic phases, therefore staining positive for both TUNEL and PCNA. The results of this study are comparable to our finding of apoptotic and proliferative cells in tendon graft healing, both of which peaked at Day 21. The number of BrdU positive cells in the tendon tissue peaked at Day 21, while the number of BrdU positive cells was high in the subcutaneous tissue from Day 3 to Day 90, peaking at Day 21. At Day 3 most of the BrdU positive cells in the subcutaneous tissue are likely to be inflammatory in nature. In the early period the hypercellular subcutaneous tissue has marked positive staining for inflammatory markers-CD45, Ly6G and F4/80 which respectively represent pan leukocyte, neutrophils and macrophages. At Day 3 the number of CD45 and Ly6G positive cells are higher than the F4/80 stained cells. Only a very small number of inflammatory cells are seen in the tendon substance at this time. But by Day 21 there is a significant rise in the number of neutrophils and macrophages in the tendon substance and this is more marked in the area of the graft. Both CD45 and Ly6G positive cells are significantly greater in the syngenic graft compared to autografts which may be either due to early rejection of the syngenic graft, which could not be completely ruled out or experimental conditions such as size mismatch. The short interval between harvesting the syngenic graft and placing it in the host tendon compared to no time gap between harvesting and securing the autologous graft may also have contributed to the higher inflammatory response.

At Day 21 the inner tendon core appeared relatively hypocellular compared to its surrounding tendon tissue. The difference in the level of inflammatory cells between the outer and inner tendon has previously been noted in Anterior Cruciate Ligament reconstruction (Kawamura et al., 2005). It appears that the tendon core lags behind the outer tendon in terms of inflammation and remodelling. The role of the inflammatory cells inside the tendon substance is not obvious. But the presence of these cells in the synthetic phase of healing may be of significance. The reported increase in ED2 positive mature tissue macrophages at the later stages of healing suggest that these cells may have a role in graft healing. In our study their presence coincided with a high synthetic

activity in the graft area at day 21 which is also indicative of a reparative role. F4/80 positive macrophages were greater in autografts suggesting greater coordinated healing and earlier remodelling of tissues. A possible explanation may be that the inflammatory cells release cytokines and growth factors that stimulate apoptosis while also releasing factors to stimulate matrix synthesis. Macrophages have been shown to produce cytokines that can contribute to healing by induction of angiogenesis, fibroblast proliferation, and extracellular matrix synthesis and degradation (Nathan, 1987). Studies of macrophage depletion following Anterior Cruciate Ligament reconstruction have shown improved morphologic and biomechanical properties at the healing of tendon-bone interface (Hays et al., 2008) while also showing significant reduction in cellular proliferation(Godbout et al., 2010). The exact role of various inflammatory cells and their interaction should be investigated further.

The intense inflammatory reaction in the subcutaneous tissue at Day 3 is accompanied by a marked increase in the number of blood vessels which is in keeping with the normal events of the inflammatory phase of wound healing (Wong et al., 2009). At Day 21 the previously avascular tendon graft and host tendon show positive staining for lumen associated alpha-SMA indicating that the graft is vascularised and this is maintained even at Day 90. This suggest vascularisation is accompaniment of graft healing which is in keeping with previous reports (Gelberman et al., 1992a). The blood vessels have been shown to be associated with bone marrow derived cells (Zantop et al., 2006) and are likely to be responsible for the influx of inflammatory cells in the tendon at Day 21.

Our study showed that cells of tendon graft undergo cellular repopulation and this is associated with an influx of inflammatory cells, apoptosis, proliferation, and collagen synthesis. Cellular events in the tendon lagged behind events in the subcutaneous tissue and only reached comparable levels around Day 21. We suggest that earlier repopulation may influence graft healing positively and healing time may be accelerated by targeted manipulation of graft cells. This hypothesis would be tested in future investigations. Our study also indicates that cellular grafts and constructs are likely to

provide earlier remodelling due to the active participation of the graft cells leading to earlier biomechanical recovery and future work will also focus in this area.

4.3 Application of the model for testing of novel tendon constructs and suggestions for future work

In 1999, the U.S. National Committee on Biomechanics proposed that *in vitro* development of tissue engineered constructs should be tested *in vivo* to determine what signals cells experience *in vivo* as they interact (Butler et al., 2000). *In vitro* mechanical testing and cell culture assays provide key information to the improvement and tuning of the construct. However, experimental testing in an appropriate animal model remains an essential step to identify the response of the construct to the biological environment.

If a construct contains implanted cells the viability and mobility of the implanted cells is of primary consideration. Outcomes of the implanted cells may include, quiescence, proliferation, apoptosis and ischemic death (Carpenter and Hankenson, 2004). If the construct is acellular the fundamental question is that of cellular repopulation and biological integration.

We successfully used the mouse Achilles tendon model for *in vivo* testing of two very different engineered constructs. The small nature of these constructs which are at early stages of their development meant that the mouse Achilles was a perfect model for testing these constructs. The cellular fibrin construct was developed from the tail tendon of GFP mouse and the viability of the cells could be followed in time using GFP immunohistochemistry. Unfortunately the fibrin graft disintegrated early in the experiments and by day 3 no GFP cells could be seen. The benefit of *in vivo* testing is that it allows for identification of such problems early in tissue engineering and leads to revisiting of the in *vitro* stages. In this case several theories were considered. Tension has been shown to be essential for the formation of the fibripositor positive fibrin construct (Kapacee et al., 2008). It may be possible that when the constructs are divided from their pinned attachments, the loss of tension leads to rapid disintegration

of the delicate construct. It may also be possible that the fibrin based construct lacked an enveloping cell layer around the construct. The *in vivo* environment may have recognised this as a fibrinous material and caused an early degradation. If the cells in the construct can be manipulated to resist the initial invasion of the inflammatory cells, the fibripositor positive cells may get enough time to adapt to their new environment. Further *in vitro* experiments of the construct are currently in progress which may be followed by *in vivo* testing.

The second construct was chosen to test if the model would allow us to identify seeding of acellular scaffolds and the timeline of events. The advantage of the electrospun Polycaprolactone (PCL) construct is that it has tendon- like longitudinally oriented fibers which are very light weight with a large surface area, allowing a greater degree of cell attachment to occur. Polycaprolactone (PCL) is a biocompatible and bioresorbable
polyester that has a slower degradation rate than other bioresorbable polymers, which may allow seeded cells time to generate and organise Extracellular Matrix (Bosworth et al., 2008). Unfortunately the small number of animals and the low melting point of the construct did not allow us to carry out histological investigations. The harvested tendons were investigated with Scanning Electron Microscopy (SEM) and in situ, the architecture of the PCL construct appeared to have some similarities to normal tendon. At Day 21 there appeared to be potentially new tissue surrounding the scaffold indicating incorporation of the construct. Cellular seeding could not be determined. Further *in vitro* manipulation of the PCL construct is in progress and future *in vivo* experiments will be carried out using low melting point wax processed histology, immunohistochemistry and SEM.

The investigations carried out to test a cell-based and an acellular construct yielded only preliminary results. But the study proved that the mouse Achilles tendon model could be successfully used to carry out *in vivo* construct testing. It also showed that *in vitro* development of engineered tissue or biomaterial should run alongside testing in an

appropriate animal model as this allows for problems to be detected early and changes to be made in study design from the early stages.

The Mouse Achilles tendon offers an economic and reproducible model for the study of tendon injuries. The availability of GFP species with cell tracking facilities allowed for the development of a versatile tendon grafting model which can also be used to test biomaterials.

Tendon graft cells remain viable and metabolically active in the early phases of graft integration. The cells of the graft appear to undergo a process of apoptosis and are completely replaced by host cells in the later phase. The interaction between cell activity and cell death plays a significant role in the remodeling and reorganization of the tendon. We suggest that cellular grafts may offer advantages over acellular grafts in terms of earlier remodeling leading to a shorter recovery period.

Early results of an engineered cell-based fibrin construct did not provide sufficient persistence, while acellular constructs showed some potential as a viable scaffold material. The Mouse Achilles tendon proved to be an appropriate model for the *in vivo* testing of tendon constructs.

Chapter Five

Bibliography

Abrahamsson SO, Gelberman RH, Amiel D, Winterton P, Harwood F. 1995. Autogenous flexor tendon grafts: fibroblast activity and matrix remodeling in dogs. J Orthop Res 13(1):58-66.

Ahmed IM, Lagopoulos M, McConnell P, Soames RW, Sefton GK. 1998. Blood supply of the Achilles tendon. J Orthop Res 16(5):591-596.

Amiel D, Harwood FL, Gelberman RH, Chu CR, Seiler JG, 3rd, Abrahamsson S. 1995. Autogenous intrasynovial and extrasynovial tendon grafts: an experimental study of pro alpha 1(I) collagen mRNA expression in dogs. J Orthop Res 13(3):459-463.

Amiel D, Kleiner JB, Akeson WH. 1986a. The natural history of the anterior cruciate ligament autograft of patellar tendon origin. Am J Sports Med 14(6):449-462.

Amiel D, Kleiner JB, Roux RD, Harwood FL, Akeson WH. 1986b. The phenomenon of "ligamentization": anterior cruciate ligament reconstruction with autogenous patellar tendon. J Orthop Res 4(2):162-172.

Ark JW, Gelberman RH, Abrahamsson SO, Seiler JG, 3rd, Amiel D. 1994. Cellular survival and proliferation in autogenous flexor tendon grafts. J Hand Surg Am 19(2):249-258.

Arnoczky SP, Tarvin GB, Marshall JL. 1982. Anterior cruciate ligament replacement using patellar tendon. An evaluation of graft revascularization in the dog. J Bone Joint Surg Am 64(2):217-224.

Ashley FL, McConnell DV, Polak T, Stone RS, Marmor L. 1964. An Evaluation of the Healing Process in Avian Digital Flexor Tendons and Grafts Following the Application of an Artificial Tendon Sheath. Plast Reconstr Surg 33:411-421.

Badylak S, Arnoczky S, Plouhar P, Haut R, Mendenhall V, Clarke R, Horvath C. 1999. Naturally occurring extracellular matrix as a scaffold for musculoskeletal repair. Clin Orthop Relat Res(367 Suppl):S333-343.

Badylak SF, Tullius R, Kokini K, Shelbourne KD, Klootwyk T, Voytik SL, Kraine MR, Simmons C. 1995. The use of xenogeneic small intestinal submucosa as a

biomaterial for Achilles tendon repair in a dog model. J Biomed Mater Res 29(8):977-985.

Banes AJ, Donlon K, Link GW, Gillespie Y, Bevin AG, Peterson HD, Bynum D, Watts S, Dahners L. 1988. Cell populations of tendon: a simplified method for isolation of synovial cells and internal fibroblasts: confirmation of origin and biologic properties. J Orthop Res 6(1):83-94.

Bedi A, Kawamura S, Ying L, Rodeo SA. 2009. Differences in tendon graft healing between the intra-articular and extra-articular ends of a bone tunnel. HSS J 5(1):51-57.

Benjamin M, Kaiser E, Milz S. 2008. Structure-function relationships in tendons: a review. J Anat 212(3):211-228.

Benjamin M, Qin S, Ralphs JR. 1995. Fibrocartilage associated with human tendons and their pulleys. J Anat 187 (Pt 3):625-633.

Benjamin M, Ralphs JR. 1998. Fibrocartilage in tendons and ligaments--an adaptation to compressive load. J Anat 193 (Pt 4):481-494.

Bi Y, Ehirchiou D, Kilts TM, Inkson CA, Embree MC, Sonoyama W, Li L, Leet AI, Seo BM, Zhang L, Shi S, Young MF. 2007. Identification of tendon stem/progenitor cells and the role of the extracellular matrix in their niche. Nat Med 13(10):1219-1227.

Birk DE, Mayne R. 1997. Localization of collagen types I, III and V during tendon development. Changes in collagen types I and III are correlated with changes in fibril diameter. Eur J Cell Biol 72(4):352-361.

Birk DE, Trelstad RL. 1986. Extracellular compartments in tendon morphogenesis: collagen fibril, bundle, and macroaggregate formation. J Cell Biol 103(1):231-240.

Bosworth L, Clegg P, Downes S. 2008. Electrospun nanofibres of polycaprolactone, and their use for tendon regeneration. Int J Nano and Biomaterials Vol. 1(3):263–279.

Broughton G, 2nd, Janis JE, Attinger CE. 2006. Wound healing: an overview. Plast Reconstr Surg 117(7 Suppl):1e-S-32e-S.

Brown DL, Kao WW, Greenhalgh DG. 1997. Apoptosis down-regulates inflammation under the advancing epithelial wound edge: delayed patterns in diabetes and improvement with topical growth factors. Surgery 121(4):372-380.

Butler DL, Goldstein SA, Guilak F. 2000. Functional tissue engineering: the role of biomechanics. J Biomech Eng 122(6):570-575.

Butler DL, Juncosa-Melvin N, Boivin GP, Galloway MT, Shearn JT, Gooch C, Awad H. 2008. Functional tissue engineering for tendon repair: A multidisciplinary strategy using mesenchymal stem cells, bioscaffolds, and mechanical stimulation. J Orthop Res 26(1):1-9.

Butler DL, Juncosa N, Dressler MR. 2004. Functional efficacy of tendon repair processes. Annu Rev Biomed Eng 6:303-329.

Canty EG, Lu Y, Meadows RS, Shaw MK, Holmes DF, Kadler KE. 2004. Coalignment of plasma membrane channels and protrusions (fibripositors) specifies the parallelism of tendon. J Cell Biol 165(4):553-563.

Canty EG, Starborg T, Lu Y, Humphries SM, Holmes DF, Meadows RS, Huffman A, O'Toole ET, Kadler KE. 2006. Actin filaments are required for fibripositor-mediated collagen fibril alignment in tendon. J Biol Chem 281(50):38592-38598.

Cao Y, Liu Y, Liu W, Shan Q, Buonocore SD, Cui L. 2002. Bridging tendon defects using autologous tenocyte engineered tendon in a hen model. Plast Reconstr Surg 110(5):1280-1289.

Carpenter JE, Hankenson KD. 2004. Animal models of tendon and ligament injuries for tissue engineering applications. Biomaterials 25(9):1715-1722.

Carr AJ, Norris SH. 1989. The blood supply of the calcaneal tendon. J Bone Joint Surg Br 71(1):100-101.

Chaplin DM. 1973. The vascular anatomy within normal tendons, divided tendons, free tendon grafts and pedicle tendon grafts in rabbits. A microradioangiographic study. J Bone Joint Surg Br 55(2):369-389.

Chhabra A, Tsou D, Clark RT, Gaschen V, Hunziker EB, Mikic B. 2003. GDF-5 deficiency in mice delays Achilles tendon healing. J Orthop Res 21(5):826-835.

Chong AK, Riboh J, Smith RL, Lindsey DP, Pham HM, Chang J. 2009. Flexor tendon tissue engineering: acellularized and reseeded tendon constructs. Plast Reconstr Surg 123(6):1759-1766.

Comley AS, Krishnan J. 1999. Donor site morbidity after quadriceps tendon harvest for rotator cuff repair. Aust N Z J Surg 69(11):808-810.

Dejardin LM, Arnoczky SP, Ewers BJ, Haut RC, Clarke RB. 2001. Tissue-engineered rotator cuff tendon using porcine small intestine submucosa. Histologic and mechanical evaluation in dogs. Am J Sports Med 29(2):175-184.

Derwin KA, Badylak SF, Steinmann SP, Iannotti JP. 2004. Extracellular matrix scaffold devices for rotator cuff repair. J Shoulder Elbow Surg 19(3):467-476.

Egerbacher M, Arnoczky SP, Caballero O, Lavagnino M, Gardner KL. 2008. Loss of homeostatic tension induces apoptosis in tendon cells: an in vitro study. Clin Orthop Relat Res 466(7):1562-1568.

Ertel AN. 1989. Flexor tendon ruptures in rheumatoid arthritis. Hand Clin 5(2):177-190.

Fenwick SA, Hazleman BL, Riley GP. 2002. The vasculature and its role in the damaged and healing tendon. Arthritis Res 4(4):252-260.

Flynn JE, Wilson JT, Child CG, Graham JH. 1960. Heterogenous and autogenous-tendon transplants. An experimental study of preserved bovine-tendon transplants in dogs and autogenous-tendon transplants in dogs. J Bone Joint Surg Am 42-A:91-110.

Freilich AM, Chhabra AB. 2007. Secondary flexor tendon reconstruction, a review. J Hand Surg Am 32(9):1436-1442.

Furie RA, Chartash EK. 1988. Tendon rupture in systemic lupus erythematosus. Semin Arthritis Rheum 18(2):127-133.

Gelberman RH, Chu CR, Williams CS, Seiler JG, 3rd, Amiel D. 1992a. Angiogenesis in healing autogenous flexor-tendon grafts. J Bone Joint Surg Am 74(8):1207-1216.

Gelberman RH, Manske PR, Vande Berg JS, Lesker PA, Akeson WH. 1984. Flexor tendon repair in vitro: a comparative histologic study of the rabbit, chicken, dog, and monkey. J Orthop Res 2(1):39-48.

Gelberman RH, Seiler JG, 3rd, Rosenberg AE, Heyman P, Amiel D. 1992b. Intercalary flexor tendon grafts. A morphological study of intrasynovial and extrasynovial donor tendons. Scand J Plast Reconstr Surg Hand Surg 26(3):257-264.

Ghazzawi A, Theobald P, Pugh N, Byrne C, Nokes L. 2009. Quantifying the motion of Kager's fat pad. J Orthop Res 27(11):1457-1460.

Gigante A, Specchia N, Rapali S, Ventura A, de Palma L. 1996. Fibrillogenesis in tendon healing: an experimental study. Boll Soc Ital Biol Sper 72(7-8):203-210.

Godbout C, Bilodeau R, Van Rooijen N, Bouchard P, Frenette J. 2010. Transient neutropenia increases macrophage accumulation and cell proliferation but does not improve repair following intratendinous rupture of Achilles tendon. J Orthop Res 28(8):1084-1091.

Graf J, Schneider U, Niethard FU. 1990. [Microcirculation of the Achilles tendon and significance of the paratenon. A study with the plastination method]. Handchir Mikrochir Plast Chir 22(3):163-166.

Grant WP, Sullivan R, Sonenshine DE, Adam M, Slusser JH, Carson KA, Vinik AI. 1997. Electron microscopic investigation of the effects of diabetes mellitus on the Achilles tendon. J Foot Ankle Surg 36(4):272-278; discussion 330.

Guimberteau JC, Delage JP, McGrouther DA, Wong JK. 2010. The microvacuolar system: how connective tissue sliding works. J Hand Surg Eur Vol 35(8):614-622.

Gungormus C, Kolankaya D. 2008. Characterization of type I, III and V collagens in high-density cultured tenocytes by triple-immunofluorescence technique. Cytotechnology 58(3):145-152.

Hagberg L, Heinegard D, Ohlsson K. 1992. The contents of macromolecule solutes in flexor tendon sheath fluid and their relation to synovial fluid. A quantitative analysis. J Hand Surg Br 17(2):167-171.

Hanly JG, Urowitz MB. 1986. Tendon rupture in systemic lupus erythematosus. Ann Rheum Dis 45(4):349.

Hasslund S, Jacobson JA, Dadali T, Basile P, Ulrich-Vinther M, Soballe K, Schwarz EM, O'Keefe RJ, Mitten DJ, Awad HA. 2008. Adhesions in a murine flexor tendon graft model: autograft versus allograft reconstruction. J Orthop Res 26(6):824-833.

Hays PL, Kawamura S, Deng XH, Dagher E, Mithoefer K, Ying L, Rodeo SA. 2008. The role of macrophages in early healing of a tendon graft in a bone tunnel. J Bone Joint Surg Am 90(3):565-579.

Heinemeier KM, Olesen JL, Haddad F, Langberg H, Kjaer M, Baldwin KM, Schjerling P. 2007. Expression of collagen and related growth factors in rat tendon and skeletal muscle in response to specific contraction types. J Physiol 582(Pt 3):1303-1316.

Hess GW. 2010. Achilles tendon rupture: a review of etiology, population, anatomy, risk factors, and injury prevention. Foot Ankle Spec 3(1):29-32.

Holmes I. 1971. Variations in tendon cell morphology with animal, site and age. J Anat 108(Pt 2):305-309.

Homburg CH, Roos D. 1996. Apoptosis of neutrophils. Curr Opin Hematol 3(1):94-99.

Hu G, Gura T, Sabsay B, Sauk J, Dixit SN, Veis A. 1995. Endoplasmic reticulum protein Hsp47 binds specifically to the N-terminal globular domain of the amino-propeptide of the procollagen I alpha 1 (I)-chain. J Cell Biochem 59(3):350-367.

Iannotti JP, Codsi MJ, Kwon YW, Derwin K, Ciccone J, Brems JJ. 2006. Porcine small intestine submucosa augmentation of surgical repair of chronic two-tendon rotator cuff tears. A randomized, controlled trial. J Bone Joint Surg Am 88(6):1238-1244.

Ikawa M, Kominami K, Yoshimura Y, Tanaka K, Nishimune Y, Okabe M. 1995. A rapid and non-invasive selection of transgenic embryos before implantation using green fluorescent protein (GFP). FEBS Lett 375(1-2):125-128.

Ippolito E, Natali PG, Postacchini F, Accinni L, De Martino C. 1980. Morphological, immunochemical, and biochemical study of rabbit achilles tendon at various ages. J Bone Joint Surg Am 62(4):583-598.

Iwata Y, Morihara T, Tachiiri H, Kajikawa Y, Yoshida A, Arai Y, Tokunaga D, Sakamoto H, Matsuda K, Kurokawa M, Kawata M, Kubo T. 2008. Behavior of host and graft cells in the early remodeling process of rotator cuff defects in a transgenic animal model. J Shoulder Elbow Surg 17(1 Suppl):101S-107S.

Iwuagwu FC, McGrouther DA. 1998. Early cellular response in tendon injury: the effect of loading. Plast Reconstr Surg 102(6):2064-2071.

Kajikawa Y, Morihara T, Sakamoto H, Matsuda K, Oshima Y, Yoshida A, Nagae M, Arai Y, Kawata M, Kubo T. 2008. Platelet-rich plasma enhances the initial mobilization of circulation-derived cells for tendon healing. J Cell Physiol 215(3):837-845.

Kajikawa Y, Morihara T, Watanabe N, Sakamoto H, Matsuda K, Kobayashi M, Oshima Y, Yoshida A, Kawata M, Kubo T. 2007. GFP chimeric models exhibited a biphasic pattern of mesenchymal cell invasion in tendon healing. J Cell Physiol 210(3):684-691.

Kannus P. 2000. Structure of the tendon connective tissue. Scand J Med Sci Sports 10(6):312-320.

Kapacee Z, Richardson SH, Lu Y, Starborg T, Holmes DF, Baar K, Kadler KE. 2008. Tension is required for fibripositor formation. Matrix Biol 27(4):371-375.

Karaoglu S, M BF, Woo SL, Fu YC, Liang R, Abramowitch SD. 2008. Use of a bioscaffold to improve healing of a patellar tendon defect after graft harvest for ACL reconstruction: A study in rabbits. J Orthop Res 26(2):255-263.

Kawabata H, Katsura T, Kondo E, Kitamura N, Miyatake S, Tanabe Y, Setoguchi T, Komiya S, Yasuda K. 2009. Stress deprivation from the patellar tendon induces apoptosis of fibroblasts in vivo with activation of mitogen-activated protein kinases. J Biomech 42(15):2611-2615.

Kawamura S, Ying L, Kim HJ, Dynybil C, Rodeo SA. 2005. Macrophages accumulate in the early phase of tendon-bone healing. J Orthop Res 23(6):1425-1432.

Kealey GP. 1997. Disease transmission by means of allograft. J Burn Care Rehabil 18(1 Pt 2):S10-11.

Khan U, Edwards JC, McGrouther DA. 1996. Patterns of cellular activation after tendon injury. J Hand Surg Br 21(6):813-820.

Kleiner JB, Amiel D, Harwood FL, Akeson WH. 1989. Early histologic, metabolic, and vascular assessment of anterior cruciate ligament autografts. J Orthop Res 7(2):235-242.

Kobayashi M, Watanabe N, Oshima Y, Kajikawa Y, Kawata M, Kubo T. 2005. The fate of host and graft cells in early healing of bone tunnel after tendon graft. Am J Sports Med 33(12):1892-1897.

Kryger GS, Chong AK, Costa M, Pham H, Bates SJ, Chang J. 2007. A comparison of tenocytes and mesenchymal stem cells for use in flexor tendon tissue engineering. J Hand Surg Am 32(5):597-605.

Lee CH, Huang GS, Chao KH, Wu SS, Chen Q. 2005. Differential pretensions of a flexor tendon graft for anterior cruciate ligament reconstruction: a biomechanical comparison in a porcine knee model. Arthroscopy 21(5):540-546.

Lim JK, Hui J, Li L, Thambyah A, Goh J, Lee EH. 2004. Enhancement of tendon graft osteointegration using mesenchymal stem cells in a rabbit model of anterior cruciate ligament reconstruction. Arthroscopy 20(9):899-910.

Liu SH, Kabo JM, Osti L. 1995. Biomechanics of two types of bone-tendon-bone graft for ACL reconstruction. J Bone Joint Surg Br 77(2):232-235.

Liu W, Chen B, Deng D, Xu F, Cui L, Cao Y. 2006. Repair of tendon defect with dermal fibroblast engineered tendon in a porcine model. Tissue Eng 12(4):775-788.

Lui PP, Cheuk YC, Hung LK, Fu SC, Chan KM. 2007. Increased apoptosis at the late stage of tendon healing. Wound Repair Regen 15(5):702-707.

Lundborg G, Holm S, Myrhage R. 1980. The role of the synovial fluid and tendon sheath for flexor tendon nutrition. An experimental tracer study on diffusional pathways in dogs. Scand J Plast Reconstr Surg 14(1):99-107.

Maeda M, Nakamura T, Fukui A, Koizumi M, Yamauchi T, Tamai S, Nagano-Tatsumi K, Haga S, Hashimoto K, Yamamoto H. 1999. The role of serum imbibition for skin grafts. Plast Reconstr Surg 104(7):2100-2107.

Maffulli N, Leadbetter WB. 2005. Free gracilis tendon graft in neglected tears of the achilles tendon. Clin J Sport Med 15(2):56-61.

Manske PR, Lesker PA. 1984. Histologic evidence of intrinsic flexor tendon repair in various experimental animals. An in vitro study. Clin Orthop Relat Res(182):297-304.

Marsolais D, Cote CH, Frenette J. 2001. Neutrophils and macrophages accumulate sequentially following Achilles tendon injury. J Orthop Res 19(6):1203-1209.

Mason ML, Shearon CG. 1932. The process of tendon repair: An experimental study of tendon suture and tendon graft. Arch Surg 25:615.

Mastrokalos DS, Springer J, Siebold R, Paessler HH. 2005. Donor site morbidity and return to the preinjury activity level after anterior cruciate ligament reconstruction using ipsilateral and contralateral patellar tendon autograft: a retrospective, nonrandomized study. Am J Sports Med 33(1):85-93.

Matsuo S, Kurisaki A, Sugino H, Hashimoto I, Nakanishi H. 2007. Analysis of skin graft survival using green fluorescent protein transgenic mice. J Med Invest 54(3-4):267-275.

Matthew C, Moore MJ, Campbell L. 1987. A quantitative ultrastructural study of collagen fibril formation in the healing extensor digitorum longus tendon of the rat. J Hand Surg Br 12(3):313-320.

Matthews P, Richards H. 1975. The repair reaction of flexor tendon within the digital sheath. Hand 7(1):27-29.

Mayer L. 1916. The physiological method of tendon transplantation. I. Historical; Anatomy and Physiology of Tendons. Surgery, Gynaecology and Obstetrics 22:183-197.

McNeilly CM, Banes AJ, Benjamin M, Ralphs JR. 1996. Tendon cells in vivo form a three dimensional network of cell processes linked by gap junctions. J Anat 189 (Pt 3):593-600.

Mikic B, Bierwert L, Tsou D. 2006. Achilles tendon characterization in GDF-7 deficient mice. J Orthop Res 24(4):831-841.

Milano G, Mulas PD, Ziranu F, Piras S, Manunta A, Fabbriciani C. 2006. Comparison between different femoral fixation devices for ACL reconstruction with

doubled hamstring tendon graft: a biomechanical analysis. Arthroscopy 22(6):660-668.

Milz S, Rufai A, Buettner A, Putz R, Ralphs JR, Benjamin M. 2002. Three-dimensional reconstructions of the Achilles tendon insertion in man. J Anat 200(Pt 2):145-152.

Moore MJ, De Beaux A. 1987. A quantitative ultrastructural study of rat tendon from birth to maturity. J Anat 153:163-169.

Moore T, Anderson B, Seiler JG, 3rd. 2010. Flexor tendon reconstruction. J Hand Surg Am 35(6):1025-1030.

Murphy KD, Mushkudiani IA, Kao D, Levesque AY, Hawkins HK, Gould LJ. 2008. Successful incorporation of tissue-engineered porcine small-intestinal submucosa as substitute flexor tendon graft is mediated by elevated TGF-beta1 expression in the rabbit. J Hand Surg Am 33(7):1168-1178.

Nathan CF. 1987. Secretory products of macrophages. J Clin Invest 79(2):319-326.

Nisbet NW. 1960. Anatomy of the calcaneal tendon of the rabbit. J Bone Joint Surg Br 42-B:360-366.

Nyyssonen T, Luthje P, Kroger H. 2008. The increasing incidence and difference in sex distribution of Achilles tendon rupture in Finland in 1987-1999. Scand J Surg 97(3):272-275.

O'Ceallaigh S, Herrick SE, Bennett WR, Bluff JE, Ferguson MW, McGrouther DA. 2007. Perivascular cells in a skin graft are rapidly repopulated by host cells. J Plast Reconstr Aesthet Surg 60(8):864-875.

O'Ceallaigh S, Herrick SE, Bluff JE, McGrouther DA, Ferguson MW. 2006. Quantification of total and perfused blood vessels in murine skin autografts using a fluorescent double-labeling technique. Plast Reconstr Surg 117(1):140-151.

Oryan A, Shoushtari AH. 2008. Histology and ultrastructure of the developing superficial digital flexor tendon in rabbits. Anat Histol Embryol 37(2):134-140.

Ouyang HW, Goh JC, Lee EH. 2004. Use of bone marrow stromal cells for tendon graft-to-bone healing: histological and immunohistochemical studies in a rabbit model. Am J Sports Med 32(2):321-327.

Peacock EE, Jr. 1959. A study of circulation in normal
tendons and healing grafts. Ann Surg 149:415.

Pickersgill CH, Marr CM, Reid SW. 2001. Repeatability of diagnostic ultrasonography in the assessment of the equine superficial digital flexor tendon. Equine Vet J 33(1):33-37.

Potenza AD. 1962. Tendon healing within the flexor digital sheath in the dog. J Bone Joint Surg Am 44-A:49-64.

Potenza AD. 1964. The Healing of Autogenous Tendon Grafts within the Flexor Digital Sheath in Dogs. J Bone Joint Surg Am 46:1462-1484.

Romanini E, D'Angelo F, De Masi S, Adriani E, Magaletti M, Lacorte E, Laricchiuta P, Sagliocca L, Morciano C, Mele A. 2010. Graft selection in arthroscopic anterior cruciate ligament reconstruction. J Orthop Traumatol 11(4):211-219.

Rowe RW. 1985. The structure of rat tail tendon. Connect Tissue Res 14(1):9-20.

Rufai A, Ralphs JR, Benjamin M. 1995. Structure and histopathology of the insertional region of the human Achilles tendon. J Orthop Res 13(4):585-593.

Scheffler SU, Schmidt T, Gangey I, Dustmann M, Unterhauser F, Weiler A. 2008. Fresh-frozen free-tendon allografts versus autografts in anterior cruciate ligament reconstruction: delayed remodeling and inferior mechanical function during long-term healing in sheep. Arthroscopy 24(4):448-458.

Schnoor M, Cullen P, Lorkowski J, Stolle K, Robenek H, Troyer D, Rauterberg J, Lorkowski S. 2008. Production of type VI collagen by human macrophages: a new dimension in macrophage functional heterogeneity. J Immunol 180(8):5707-5719.

Sckell A, Leunig M, Fraitzl CR, Ganz R, Ballmer FT. 1999. The connective-tissue envelope in revascularisation of patellar tendon grafts. J Bone Joint Surg Br 81(5):915-920.

Scott A, Khan KM, Heer J, Cook JL, Lian O, Duronio V. 2005. High strain mechanical loading rapidly induces tendon apoptosis: an ex vivo rat tibialis anterior model. Br J Sports Med 39(5):e25.

Seida JC, LeBlanc C, Schouten JR, Mousavi SS, Hartling L, Vandermeer B, Tjosvold L, Sheps DM. 2010. Systematic review: nonoperative and operative treatments for rotator cuff tears. Ann Intern Med 153(4):246-255.

Seiler JG, 3rd, Chu C, Abrahamsson SO, Gelberman RH. 1993a. The fate of autogenous tendon grafts. Iowa Orthop J 13:56-62.

Seiler JG, 3rd, Chu CR, Amiel D, Woo SL, Gelberman RH. 1997. The Marshall R. Urist Young Investigator Award. Autogenous flexor tendon grafts. Biologic mechanisms for incorporation. Clin Orthop Relat Res(345):239-247.

Seiler JG, 3rd, Gelberman RH, Williams CS, Woo SL, Dickersin GR, Sofranko R, Chu CR, Rosenberg AE. 1993b. Autogenous flexor-tendon grafts. A biomechanical and morphological study in dogs. J Bone Joint Surg Am 75(7):1004-1014.

Sharma P, Maffulli N. 2006. Biology of tendon injury: healing, modeling and remodeling. J Musculoskelet Neuronal Interact 6(2):181-190.

Shin RH, Zhao C, Zobitz ME, Amadio PC, An KN. 2008. Mechanical properties of intrasynovial and extrasynovial tendon fascicles. Clin Biomech (Bristol, Avon) 23(2):236-241.

Shino K, Horibe S. 1991. Experimental ligament reconstruction by allogeneic tendon graft in a canine model. Acta Orthop Belg 57 Suppl 2:44-53.

Singer DI, Morrison WA, Gumley GJ, O'Brien BM, Mitchell GM, Barton RM, Frykman GK. 1989. Comparative study of vascularized and nonvascularized tendon grafts for reconstruction of flexor tendons in zone 2: an experimental study in primates. J Hand Surg Am 14(1):55-63.

Sivakumar B, Akhavani MA, Winlove CP, Taylor PC, Paleolog EM, Kang N. 2008. Synovial hypoxia as a cause of tendon rupture in rheumatoid arthritis. J Hand Surg Am 33(1):49-58.

Strickland JW. 1983. Management of acute flexor tendon injuries. Orthop Clin North Am 14(4):827-849.

Sun M, Kingham PJ, Reid AJ, Armstrong SJ, Terenghi G, Downes S. 2010. In vitro and in vivo testing of novel ultrathin PCL and PCL/PLA blend films as peripheral nerve conduit. J Biomed Mater Res A 93(4):1470-1481.

Tachiiri H, Morihara T, Iwata Y, Yoshida A, Kajikawa Y, Kida Y, Matsuda K, Fujiwara H, Kurokawa M, Kawata M, Kubo T. 2010. Characteristics of donor and host cells in the early remodeling process after transplant of Achilles tendon with and without live cells for the treatment of rotator cuff defect--what is the ideal graft for the treatment of massive rotator cuff defects? J Shoulder Elbow Surg 19(6):891-898.

Takahashi T, Kasashima Y, Ueno Y. 2004. Association between race history and risk of superficial digital flexor tendon injury in Thoroughbred racehorses. J Am Vet Med Assoc 225(1):90-93.

Taras JS, Gray RM, Culp RW. 1994. Complications of flexor tendon injuries. Hand Clin 10(1):93-109.

Teli M, Chiodini F, Sottocasa R, Villa T. 2005. Influence of the diameters of tendon graft and bone tunnel in hamstring ACL reconstruction. A bovine model. Chir Organi Mov 90(3):281-285.

Theobald P, Bydder G, Dent C, Nokes L, Pugh N, Benjamin M. 2006. The functional anatomy of Kager's fat pad in relation to retrocalcaneal problems and other hindfoot disorders. J Anat 208(1):91-97.

Thorfinn J, Saber S, Angelidis IK, Ki SH, Zhang AY, Chong AK, Pham HM, Lee GK, Chang J. 2009. Flexor tendon tissue engineering: temporal distribution of donor tenocytes versus recipient cells. Plast Reconstr Surg 124(6):2019-2026.

Towler DA, Gelberman RH. 2006. The alchemy of tendon repair: a primer for the (S)mad scientist. J Clin Invest 116(4):863-866.

Victor J, Bellemans J, Witvrouw E, Govaers K, Fabry G. 1997. Graft selection in anterior cruciate ligament reconstruction--prospective analysis of patellar tendon autografts compared with allografts. Int Orthop 21(2):93-97.

Vogel KG, Peters JA. 2005. Histochemistry defines a proteoglycan-rich layer in bovine flexor tendon subjected to bending. J Musculoskelet Neuronal Interact 5(1):64-69.

Weiler A, Unterhauser FN, Bail HJ, Huning M, Haas NP. 2002. Alpha-smooth muscle actin is expressed by fibroblastic cells of the ovine anterior cruciate ligament and its free tendon graft during remodeling. J Orthop Res 20(2):310-317.

Williams IF, McCullagh KG, Silver IA. 1984. The distribution of types I and III collagen and fibronectin in the healing equine tendon. Connect Tissue Res 12(3-4):211-227.

Wong J, Bennett W, Ferguson MW, McGrouther DA. 2006a. Microscopic and histological examination of the mouse hindpaw digit and flexor tendon arrangement with 3D reconstruction. J Anat 209(4):533-545.

Wong JK, Alyouha S, Kadler KE, Ferguson MW, McGrouther DA. 2010. The cell biology of suturing tendons. Matrix Biol 29(6):525-536.

Wong JK, Cerovac S, Ferguson MW, McGrouther DA. 2006b. The cellular effect of a single interrupted suture on tendon. J Hand Surg Br 31(4):358-367.

Wong JK, Lui YH, Kapacee Z, Kadler KE, Ferguson MW, McGrouther DA. 2009. The cellular biology of flexor tendon adhesion formation: an old problem in a new paradigm. Am J Pathol 175(5):1938-1951.

Wu JL, Yeh TT, Shen HC, Cheng CK, Lee CH. 2009. Mechanical comparison of biodegradable femoral fixation devices for hamstring tendon graft--a biomechanical study in a porcine model. Clin Biomech (Bristol, Avon) 24(5):435-440.

Wu YF, Chen CH, Cao Y, Avanessian B, Wang XT, Tang JB. 2010. Molecular events of cellular apoptosis and proliferation in the early tendon healing period. J Hand Surg Am 35(1):2-10.

Yasuda K, Tomita F, Yamazaki S, Minami A, Tohyama H. 2004. The effect of growth factors on biomechanical properties of the bone-patellar tendon-bone graft after anterior cruciate ligament reconstruction: a canine model study. Am J Sports Med 32(4):870-880.

Zantop T, Gilbert TW, Yoder MC, Badylak SF. 2006. Extracellular matrix scaffolds are repopulated by bone marrow-derived cells in a mouse model of achilles tendon reconstruction. J Orthop Res 24(6):1299-1309.

Zavahir F, McGrouther DA, Misra A, Smith K, Brown RA, Mudera V. 2001. A study of the cellular response to orientated fibronectin material in healing extensor rat tendon. J Mater Sci Mater Med 12(10-12):1005-1011.

Zavazava N, Kabelitz D. 2000. Alloreactivity and apoptosis in graft rejection and transplantation tolerance. J Leukoc Biol 68(2):167-174.

Zhang ZZ, Zhong SZ, Sun B, Ho GT. 1990. Blood supply of the flexor digital tendon in the hand and its clinical significance. Surg Radiol Anat 12(2):113-117.

Appendix

Zinc Fixation

Preparation of Zinc fixative (Beckstead J.H., 1994)

For 500ml of zinc fixative solution 1.322g of Tris HCl and 0.194g of Tris base was added to 500mls of distilled water (100mM Tris.Hcl pH 7.4) and stirred continuously until the salts had dissolved. Following dissolution, under continuous stirring, 0.25 g of Calcium acetate (0.05% Calcium acetate) is added to the solution, followed by 2.5g of Zinc acetate (0.5% Zinc acetate) then followed by 2.5g of Zinc Chloride (0.5% Zinc chloride). Once all the salt had dissolved the fixative is stored at 4°C until use. The final pH should be 6.5-7.5

For mice who underwent suture wounding and proximal suture immobilization mice samples were placed into zinc fixative and stored at 4°C for 48 hours then transferred to 50% IMS solution prior to tissue processing.

Decalcification

Preparation of EDTA decalcification solution

For 2 litres of 20% EDTA solution add to 1000 ml of 40% EDTA liquid to 850 mls of dH20 in a fume cupboard and stir continuously. Add slowly approx 150-160 mls of concentrated HCL under pH guidance to adjust pH to 7-7.4. This procedure should be performed with protective eye wear in a fume cupboard.

The method of EDTA decalcification was used to demineralise the bone so that paraffin processing and whole digit sectioning could be performed. This solution was used to decalcify individual digits for a total of 15 days with solution changes every 5 days. Radiographs of the samples were performed on the 15^{th} day to ensure complete decalcification using a dental x-ray machine (Faxitron, UK.) with power settings at 45kVp and 5 second exposure.

Tissue Processor Program-Paraffin wax processing

Following fixation samples were placed into an automated tissue processor (Tissue Tek Vacuum Infiltration Processor) following a program intended for skin samples which best preserved tendon architecture. This protocol was selected from a number of programs tested which gave the least brittleness in the tendon on sectioning. The pressure/vacuum cycles (p/v cycles) are fixed throughout processing. The wax impregnated tissue was then embedded in paraffin wax blocks.

Process	Solution	Time (Hr: Min)	Temperature (°C)	P/V cycle (On/Off)
	50% IMS	0:45	-	On
	70% IMS	0:45	-	On
	90% IMS	1:00	-	On
	100% IMS	0:30	-	On
	100%IMS	0:30	-	On
	100%IMS	1:00	-	On
	50:50 IMS/Toluene	0:30	-	On
	100% Toluene	0:30	-	On
	100% Toluene	0:30	-	On
	100% Toluene	1:00	50	On
	1st wax	0:30	60	On
	2nd wax	0:30	60	On
	3rd wax	0:30	60	On
	4th wax	1:00	60	On

Buffers

PBS(0.1M)

1 L PBS concentrate (1M Sigma Aldrich)

60gm NaCl

10L ddH_2O

PBS-Tween

1 L PBS concentrate (1M Sigma Aldrich)

60gm NaCl

10L ddH_2O

10ml Tween

Tris buffer

12.1 gm TRIS Base

1M HCl

900ml dH_2O

General staining

Harris' Haematoxylin Solution

To make approximately 500mls of haematoxylin dissolve 4 g haematoxylin monohydrate in 40ml IMS. Place 760 mls of distilled water into a one litre heat proof flask and heat until approximately 60°C then add 80 g of aluminium potassium sulfate dodecahydrate (Sigma). Heat to 70°C and add alcohol solution. Heat to 75°C and add 0.8g sodium iodate which should result in solution looking like port. Remove from heat and place into an ice/water bath and cool for 30 minutes. Add 32 ml of glacial acetic acid and stir at room temperature overnight. Filter dissolved solution through Whatman paper, bottle and store.

1% Eosin Y

To make 500 ml of Eosin Y add 5 g of eosin Y to 500ml of distilled water and stir until dissolved. Bottle and store.

Nuclear fast red

To make 500mls of nuclear fast red solution dissolve 25 g of aluminium sufate in 500mls of dH20. Then add 0.5 g of nuclear fast red and dissolve over a hot plate at 40°C. Filter and add a crystal of thymol. Bottle and store

Miller's Stain

Brought from BDH

Alcian Blue pH 2.5

3% Glacial Acetic Acid
Acetic Acid- 3ml
Distilled water 100 ml

Alcian Blue solution

3% Glacial Acetic Acid 100 ml
Alcian Blue 8Gx 1gm
Mix and adjust pH to 2.5 using acetic acid. Filter, add a thymol crystal and store at room temperature

Picric Acid (1%)

5 ml Picric Acid
500 ml 70% IMS

The Picric Acid (Hopkins and Williams Ltd, Essex, UK) was dissolved in the 70% IMS in the fume hood and stored at room temperature.

Biebrich Scarlet

0.5 gm biebrich scarlet
5 gm glacial acetic acid
495 ddH_2O

The glacial acetic acid was mixed with the ddH_2O to make 1% acetic acid solution. The biebrich scarlet (Gurr, BDH Laboratory supplies) was then added and dissolved with stirring. The stain was stored at room temperature.

PMA/PTA (50%/50%)

12.5 gm phosphomolybdic acid
12.5 gm phosphotungstic acid
500 ml ddH_2O
The phosphomolybdic acid (BDH laboratory supplies) and the phosphotungstic acid (BDH laboratory supplies) were separately dissolved in 250 ml of ddH2O. The two solutions were mixed thoroughly and stored at room temperature.

Fast Green

12,5 gm Fast Green
12.5 ml glacial acetic acid
487.5 ml ddH_2O

A 2.5 % Glacial acetic acid solution was prepared by combining the glacial acetic acid and the ddH_2O. The Fast Green (Gurr, BDH laboratory supplies) was added and dissolved with stirring. The stain was stored at room temperature.

0.5 % acidified Potassium Permanganate

2.5 gm Potassium Permanganate
15 ml sulphuric acid
485 ml dH_2O

Toluidine Blue Stock solution

1 gm Toluidine Blue
100 ml 70% alcohol

Van Gieson Counter Stain

50 ml saturated Picric acid solution
9ml 1% aqueous acid fuchsin solution
50 ml dH_2O

Postoperative Analgesia

Subcutaneous Buprenorphine 0.05 mg/kg (Vetergesic-Reckitt Benckiser Healthcare UK Limited)
0.25 ml of stock solution diluted in 4.75 ml of saline (In additive free vacutainer)
Will stay active for two weeks 30 gm mice-0.2 ml for 0.1 mg/kg and 0.1 ml for 0.05 ml/kg

Poly(ε-caprolactone) 3D electrospun bundles – *in vivo* study

3D bundles were fabricated by electrospinning a 10 % w/v PCL (Mw 80,000) in acetone solution with parameters; voltage 20 kV, flow-rate 0.05 ml/min and distance to collector 15 cm. A purpose-made mandrel of aluminium with diameter 120 mm and edge thickness of 3 mm (Fine Mandrel – FM) was mounted on a non-conductive Tufnol rod. Fibres were spun onto the edge of the mandrel rotating at a speed of 500 RPM for 15 minutes, as this was sufficient time for complete coverage of the mandrel edge. The mat of fibres deposited on the mandrel edge was removed as a single long strip and cut every 3 cm along its length into smaller
sheets. Each sheet of fibres was then submerged in distilled water and manually twisted to form a three-dimensional bundle that was left to dry on the open bench.

Sterilisation of electrospun samples

To minimise the risk of infection all electrospun samples, including random and aligned 2D fibrous mats, and 3D bundles and plaits were sterilised prior to use. Sterilisation through increasing concentrations of ethanol (VWR) was conducted in the class II microbiological safety cabinet (University of Manchester). Ethanol concentrations used included; 50, 70, 90 and 100 % v/v ethanol (diluted as necessary with distilled water). Samples were sterilised overnight for each concentration. Following sterilisation with 100%ethanol, samples were washed twice in PBS.

Presentations and Posters from the Thesis

Oral

1) Oral presentation at British Association of Plastics Reconstructive and Aesthetic Surgeon summer meeting (BAPRAS) –July 2009

2) Oral presentation at the European Hand Congress of June 2008 (FESSH/ EFHST)

3) Oral presentation at University of Manchester Graduate Research Symposium July 2009

4) RCSENG Donor's annual meeting of the Shropshire Freemasons- February 2009

5) University of Manchester Dermatological Sciences Winter meeting 2009

Poster

1) Royal college of Surgeons of England Research Evening, May 2009

2) University of Manchester Faculty of Medicine Graduate Symposium, January 2009

3) Poster Presentation at TERMIS (Tissue Engineering and Regenerative Medicine International Society September 2007)

Abbreviations

ABC	Avidin Biotin Complex
Alpha- SMA	Alpha smooth muscle actin
BMT	Bone marrow transplant
BrdU	5-Bromo-2-deoxyuridine
C57/BLJ	C57 black mice species
CD	Cluster Differentiation
CD 45	Pan leukocytic marker
CD 3	Activated T cell marker
ECM	Extracellular matrix
ECR	Extensor Carpi Radialis
Hsp47	Heat Shock Protein 47
GDF	Growth differentiation factor
GFP	Green fluorescent protein
GFPBMT	Green Fluorescent Protein Bone Marrow Transplant
H&E	Haematoxylin and eosin Y
LacZ	Beta galactosidase reporter gene
MSC	Mesenchymal Stem Cell
PBS	Phosphate buffered saline
SEM	Scanning Electron Microscope
SIS-ECM	Small Intestinal Submucosa-Extracellular matrix
SLE	Systemic Lupus Erythematosus
TGFβ 1	Transforming growth factor 1
TGFβ 3	Transforming growth factor 3
TUNEL	Terminal-deoxynucleotidyl Transferase Biotin dUTP End labelling

Glossary

Syngeneic	Genetically identical members of the same species
Transgenic	A transgenic animal is one that carries a foreign gene that has been deliberately inserted into its genome.
Autograft	Tissue transplanted from one part of the body to another in the same individual.
Allograft	Cell/Tissue/ Organ sourced from a genetically non-identical member of the same species
Xenograft	Transplantation of living cells, tissues or organs from one species to another
Isograft	A subset of allografts in which organs or tissues are transplanted from a donor to a genetically identical recipient (such as an identical twin)